STRUCTURAL REPAIR OF PRESTRESSED CONCRETE BRIDGE GIRDERS

by

Jarret Lee Kasan

Bachelor of Science, University of Pittsburgh, 2007

Submitted to the Graduate Faculty of the

Swanson School of Engineering in partial fulfillment

of the requirements for the degree of

Master of Science

University of Pittsburgh

2009

UNIVERSITY OF PITTSBURGH

SWANSON SCHOOL OF ENGINEERING

This thesis was presented

by

Jarret Lee Kasan

It was defended on

January 22, 2009

and approved by

Dr. Piervincenzo Rizzo, Assistant Professor,
Department of Civil and Environmental Engineering

Dr. John F. Oyler, Adjunct Associate Professor,
Department of Civil and Environmental Engineering

Dr. Kent A Harries, Assistant Professor,
William Kepler Whiteford Faculty Fellow,
Department of Civil and Environmental Engineering
Thesis Advisor

STRUCTURAL REPAIR OF PRESTRESSED CONCRETE BRIDGE GIRDERS

Jarret Lee Kasan, M.S.

University of Pittsburgh, 2009

It is common practice that aging and structurally damaged prestressed concrete bridge members are taken out of service and replaced. This, however, is not an efficient use of materials and resources since the member can often be repaired *in situ*. There are numerous repair techniques proposed by entrepreneurial and academic institutions which restore prestressed concrete girder flexural strength and save both material and economic resources. Of course, not all repair methods are applicable in every situation and thus each must be assessed based on girder geometry and the objectives of the repair scenario. This document focuses on the practical application of prestressed concrete bridge girder repair methods.

In this document, repair methods are presented for three prototype prestressed concrete highway bridge girder shapes: adjacent boxes (AB), spread boxes (SB), and AASHTO-type I-girders (IB), having four different damage levels. A total of 22 prototype repair designs are presented. Although not applicable to all structure types or all damage levels, the repair techniques covered include the use of carbon fiber reinforced polymer (CFRP) strips, CFRP fabric, near-surface mounted (NSM) CFRP, prestressed CFRP, post-tensioned CFRP, strand splicing and external steel post-tensioning. It is the author's contention that each potential structural repair scenario should be assessed independently to determine which repair approach is best suited to the unique conditions of a specific project. Therefore, no broad classifications have been presented directly linking damage level (or a range of damage) to specific repair types.

Nonetheless, it is concluded that when 25% of the strands in a girder no longer contribute to its capacity, girder replacement is a more appropriate solution.

Guidance with respect to inspection and assessment of damage to prestressed concrete highway bridge girders and the selection of a repair method is presented. These methods are described through 22 detailed design examples. Based on these examples, review of existing projects and other available data, a detailed review of selection and performance criteria for prestressed concrete repair methods is provided.

TABLE OF CONTENTS

ACKNOWLEDGEMENTS XIV

NOTATION XVI

1.0 INTRODUCTION 1

1.1 INTRODUCTION 1

1.2 SCOPE AND OBJECTIVE OF THESIS 2

1.3 OUTLINE OF THESIS 3

1.4 DISCLAIMER 3

2.0 LITERATURE REVIEW 4

2.1 THE NCHRP 12-21 PROJECT 4

2.2 TRADITIONAL REPAIR TECHNIQUES 11

2.2.1 Strand Splicing 11

2.2.2 Post Tensioning 13

2.2.3 Corrosion Mitigation 14

2.3 EXTERNAL NON PT CFRP RETROFIT 15

2.4 EXTERNAL PT CFRP RETROFIT 16

2.4.1 CFRP Anchorage 19

2.4.2 Commercially-Available PCFRP System 21

2.5 NSM CFRP REPAIRS 22

2.6 EXPECTED DAMAGE 23
3.0 INVENTORY CONDITION ASSESSMENT 36
3.1 BRIDGE INVENTORY REVIEWED 36
3.2 SOURCES OF DAMAGE TO PRESTRESSED CONCRETE GIRDERS.. 38
3.3 TYPES OF DAMAGE TO PRESTRESSED CONCRETE BRIDGE GIRDERS 41
4.0 PROTOTYPE PRESTRESSED GIRDER SELECTION 53
4.1 DAMAGE CLASSIFICATION 53
4.2 REPAIR EXAMPLE SELECTION 55
5.0 PROTOTYPE REPAIR DESIGNS 61
5.1.1 Materials 61
5.1.2 Assumptions and Simplifications 62
5.1.3 XTRACT Program 63
5.1.4 Girder Damage 64
5.1.5 Bridge Loading 65
5.2 NON PRESTRESSED PREFORM CFRP STRIP REPAIRS 66
5.2.1 Design Example AB 4-0-0 66
5.2.2 Further Examples 74
5.3 NON PRESTRESSED CFRP FABRIC REPAIR 74
5.4 NSM CFRP REPAIRS 75
5.4.1 NSM Strip Size Optimization 76
5.5 PRESTRESSED CFRP STRIP REPAIR 77
5.6 BONDED POST-TENSIONED CFRP REPAIR 78

5.6.1 Anchorage of CFRP 79
5.7 STRAND SPLICE REPAIR 80
5.8 EXTERNAL STEEL POST-TENSIONING 81
5.9 PRELOAD TECHNIQUE 83
6.0 CONCLUSIONS, DISCUSSION AND RECOMMENDATIONS 111
6.1 DISCUSSION 113
6.1.1 Damage Assessment and Damaged Girder Rating 113
6.1.2 Repair Type Selection 114
6.1.3 Repair Technique Applicability 115
6.1.4 Girder Shape 117
6.1.5 Ductility 117
6.2 FUTURE WORK 118
6.2.1 Strand 'Redevelopment Length' 118
6.2.2 Best Practices Document 118
APPENDIX A 120
BIBLIOGRAPHY 137

LIST OF TABLES

Table 2-1 Repair Selection Criteria (Shanafelt and Horn 1980)..... 25

Table 2-2 Comparison of Various Beam-End Numerical Ratings and Overall Ratings (Tabatabi et al. 2004). 26

Table 3-1 Summary of statewide and District 11 prestressed bridge inventory. 43

Table 3-2 Bridges Selected for further investigation of inspection records. 44

Table 3-3 Sources of Observed Damage. 45

Table 3-4 Types of Observed Damage. 46

Table 4-1 Proposed damage classifications. 57

Table 4-2 Repair Examples..... 57

Table 5-1 Prototype girder material and geometric properties. 85

Table 5-2 CFRP material and geometric properties (Sika 2008a and 2008c). 85

Table 5-3 Post-tensioning steel material and geometric properties (Williams 2008)..... 86

Table 5-4 Target and repaired flexural capacities for repair designs..... 87

Table 5-5 AB loading with AASHTO-prescribed distribution factor g = 0.285. 88

Table 5-6 AB loading with distribution factor g = 0.5. 88

Table 5-7 SB loading. 89

Table 5-8 IB loading. 89

Table 5-9 Non-prestressed perform CFRP strip repair results. 90

Table 5-10 CFRP fabric repair results. 91

Table 5-11 NSM CFRP repair results. 92

Table 5-12 NSM size optimization. 93

Table 5-13 Prestressed CFRP repair results. 94

Table 5-14 Post-tensioned CFRP repair results. 95

Table 6-1 Repair Selection Criteria. 119

LIST OF FIGURES

Figure 2-1 External post-tensioned repair methods (Shanafelt and Horn 1980). 27

Figure 2-2 Splice 3: Steel jacket repair method (Shanafelt and Horn 1980). 28

Figure 2-3 Commercially available 'turnbuckle' style strand splice repair method (PCI). 28

Figure 2-4 Strand splicing methods (Shanafelt and Horn 1980). 29

Figure 2-5 Combination of repair methods (Splice 5) (Shanafelt and Horn 1980). 30

Figure 2-6 Specimen cross sections tested by Wight et al. (2001). 30

Figure 2-7 Moment –displacement plots for beams tested by Wight et al. (2001). 31

Figure 2-8 Proposed direct prestressing system (Wight et al. 2001). 31

Figure 2-9 Proposed indirect prestressing system (Casadei et al. 2006). 32

Figure 2-10 Proposed deflection controlled indirect prestressing system (Yu et al. 2008a). 32

Figure 2-11 Nonmetallic anchoring systems (Kim et al. 2008a). 33

Figure 2-12 Sika CarboStress system (SIKA). 34

Figure 2-13 Schematic of externally bonded and NSM CFRP techniques. 35

Figure 3-1 Loss of section of AASHTO girder due to vehicle impact (Harries; not taken in PA). 47

Figure 3-2 Scraping due to minor vehicle impact 47

Figure 3-3 Impact damage to I beam (PennDOT). 47

Figure 3-4 Exposed and ruptured strand due to vehicle impact (Lake View Drive Bridge; Harries 2006). 48
Figure 3-5 Vehicle impact due to collision. 48
Figure 3-6 Evidence of water on soffits of adjacent box girders. 48
Figure 3-7 Water from unanticipated sources. 49
Figure 3-8 Damage to strands caused by relocating barrier supports (PennDOT). 49
Figure 3-9 Girder with insufficient cover and inconsistent strand spacing 49
Figure 3-10 Damage due to extreme events-beyond the scope of the present study. 50
Figure 3-11 Continuum of corrosion damage (Naito et al. 2006; Harries 2006). 51
Figure 3-12 Representative shear distress (Lake View Drive EXTERIOR test girder; Harries 2006). 52
Figure 3-13 Representative flexural distress (Lake View Drive INTERIOR test girder; Harries 2006). 52
Figure 4-1 Prototype AB girder cross section. 58
Figure 4-2 Prototype SB girder cross section. 58
Figure 4-3 Prototype IB girder cross section. 59
Figure 4-4 Flow charts illustrating viable retrofit techniques based on level of damage. 60
Figure 5-1 Example of analysis identification. 96
Figure 5-2 Preformed CFRP strip repairs. 97
Figure 5-3 Preformed CFRP strip repaired AB moment-curvature plot. 98
Figure 5-4 Preformed CFRP strip repaired SB moment-curvature plot. 98
Figure 5-5 Suggested strip location for AB 4-0-0. 99
Figure 5-6 Flexural behavior of prestressed girders (Collins and Mitchell 1997). 99

Figure 5-7 CFRP fabric repairs. 100
Figure 5-8 CFRP fabric repair moment-curvature plot. 100
Figure 5-9 NSM repairs. 101
Figure 5-10 NSM repair moment-curvature plot. 101
Figure 5-11 Prestressed CFRP repaired AB. 102
Figure 5-12 Prestressed CFRP repaired SB. 102
Figure 5-13 Prestressed CFRP repaired IB. 103
Figure 5-14 Prestressed CFRP repaired AB moment-curvature plot. 103
Figure 5-15 Prestressed CFRP repaired SB moment-curvature plot. 104
Figure 5-16 Prestressed CFRP repaired IB moment-curvature plot. 104
Figure 5-17 Post-tensioned CFRP repaired AB. 105
Figure 5-18 Post-tensioned CFRP repaired SB. 105
Figure 5-19 Post-tensioned CFRP repaired IB. 106
Figure 5-20 Post-tensioned CFRP repaired AB moment-curvature plot. 106
Figure 5-21 Post-tensioned CFRP repaired SB moment-curvature plot. 107
Figure 5-22 Post-tensioned CFRP repaired IB moment-curvature plot. 107
Figure 5-23 External post-tensioned steel repaired IB 6-2-1 drawing. 108
Figure 5-24 External post-tensioned steel repaired IB 10-2-1 drawing. 108
Figure 5-25 External post-tensioned steel repaired IB moment-curvature plot. 109
Figure 5-26 Bolster examples. 110

ACKNOWLEDGEMENTS

I am pleased and excited to note my gratitude to Dr. Kent A. Harries. His encouragement, motivation and guidance have been vital in developing this document in its present form. Also, his insight has been valuable in developing my skills and understanding of structural design concepts and he should be credited for such. I must thank him for the time he has spent with me on this project and motivating me to perform at my best.

Equally significant, I would like to thank Dr. Piervincenzo Rizzo and Dr. John F. Oyler for serving on my committee. The encouragement and insights provided by Dr. Rizzo are greatly appreciated. Additionally, the motivation Dr. Oyler provided since my time as an undergraduate student as well as our technical discussions have been invaluable and instrumental in shaping my interest in structural engineering.

I would also like to thank my peers Ms. Jen Kacin, Mr. Chad Ford, Mr. Michael Hartranft, Mr. Michael Sachs, Mr. Matthew Lee, Mr. Michael Task and Mr. Can Aktas for their help and support.

Jonathan Moses, T.C. Wilkinson, Lou Ruzzi, Rao Chaluvadi, all of PennDOT District 11-0 and David White, of Sika North America, are thanked for their roles in providing important materials and direction necessary for completion of this document.

Finally, special thanks go to my parents, Eli and Linda, siblings, Melissa, Eli and Kevin and Sam for all of their love, support and encouragement over the years. Without them, I would be lost. Thank you for everything.

NOTATION

The following abbreviations and notation are used in this work.

Abbreviations

AASHO	American Association of State Highway Officials
AASHTO	American Association of State Highway and Transportation Officials
AB	Adjacent Box Beam
ACI	American Concrete Institute
CFRP	Carbon Fiber Reinforced Polymer
CFCC	Carbon Fiber Composite Cables
FRP	Fiber Reinforced Polymer
IB	I-Beam (or AASHTO Girder)
NCHRP	National Cooperative Highway Research Program
NSM	Near-surface mounted (FRP)
PCFRP	Prestressed carbon fiber reinforced polymer
SB	Spread Box Beam (or Multi Box Beam)

Notation

A_f	FRP cross sectional area
A_p	Prestressed reinforcement area in the tension zone

b	width of compression face of member
C_E	environmental reduction factor
c	distance from extreme concrete compression fiber to the neutral axis
cg strands	center of gravity of strands, measured from bottom of member
d_f	effective depth of FRP flexural reinforcement
d_p	distance from the extreme concrete compression fiber to centroid of prestressed reinforcement
E_c	modulus of elasticity of concrete
E_f	tensile modulus of elasticity of FRP
E_{ps}	tensile modulus of elasticity of prestressing steel, taken as 28500 ksi
e	eccentricity of prestressing steel with respect to centroidal axis of member
f_c'	specified compressive strength of concrete
$f_c'_{DECK}$	specified compressive strength of concrete in the deck
f_{fe}	effective stress in FRP; stress level attained at section failure
f_{fu}	design ultimate tensile strength of FRP
f_{fu}*	ultimate tensile strength of the FRP material as reported by the manufacturer
f_{ps}	stress in prestressed reinforcement at nominal strength
f_{pu}	specified tensile strength of prestressing tendons
K_{splice}	stiffness of strand splice
$L_{exposed}$	exposed length of prestressing strand
L_{tr}	transfer length of prestressing strand
I	moment of inertia of section
M	moment due to eccentric prestressing force in strands

M_{DECK}	moment on girder due to deck
M_{DW}	moment on girder due to wearing surface
M_{EXTmax}	maximum external moment applied to structure for preload technique
M_{HS20}	moment on girder due to an HS20 truck
M_{HS25}	moment on girder due to an HS25 truck
M_{JB}	moment on girder due to Jersey barrier
M_{LANE}	moment on girder due to AASHTO (2007) lane load
M_n	nominal flexural strength of girder
M_{nf}	contribution of FRP to nominal flexural strength of girder
M_{np}	contribution of prestressing steel to nominal flexural strength of girder
M_{SW}	moment on girder due to its self-weight
M_{TAN}	moment on girder due to AASHTO (2007) tandem load
M_u	design ultimate flexural strength of girder
n	number of plies of FRP reinforcement
P_e	effective force in prestressing reinforcement (after all losses)
r	radius of gyration of a section
S	section modulus
t_f	nominal thickness of one ply of FRP reinforcement
y_b	distance from extreme bottom fiber to the section centroid
y_t	distance from top fiber to the section centroid
α	empirical constant to determine an equivalent rectangular stress distribution in concrete
β_1	ratio of depth of equivalent rectangular stress block to depth of neutral axis

Δ_{splice} change in length or 'shortening' of strand splice

ε_{bi} strain level in concrete substrate at time of FRP installation (tension is positive)

ε_c strain level in concrete

ε_c' maximum strain of unconfined concrete corresponding to f'_c; may be taken as 0.002

ε_{cu} ultimate axial strain of unconfined concrete

ε_{fd} debonding strain of externally bonded FRP reinforcement

ε_{fd}^* debonding strain of externally bonded PT FRP reinforcement

ε_{fe} effective strain level in FRP reinforcement attained at failure

ε_{fu} design rupture strain of FRP reinforcement

ε_{fu}^* ultimate rupture strain of FRP reinforcement

ε_{pe} effective strain in prestressing steel after losses

ε_{pi} initial strain level in prestressed steel reinforcement

ε_{pnet} net strain in flexural prestressing steel at limit state after prestress force is discounted (i.e.: excluding strains due to effective prestress force after losses)

ε_{ps} strain in prestressed reinforcement at nominal strength

ε_{pt} strain induced in FRP reinforcement by PT

ψ_f FRP strength reduction factor

This thesis reports all values in US units (inch-pound) throughout. The following "hard" conversion factors have been used:

1 inch = 25.4 mm

1 kip = 4.448 kN

1 ksi = 6.895 MPa

Reinforcing bar sizes are reported using the designation given in the appropriate reference. A bar designated using a "#" sign (e.g.: #4) refers to the standard inch-pound designation used in the United States where the number refers to the bar diameter in eighths of an inch.

1.0 INTRODUCTION

1.1 INTRODUCTION

The demands on transportation infrastructure, in particular bridges, have increased significantly in recent years. This can be seen in the increase in traffic volume and design loadings (AASHTO 1960 and 2007). Additional demands associated with degradation of bridge infrastructure coupled with the rise in fuel and material costs have made structural repair and retrofitting a more attractive solution to fix aging, damaged and failing structures. Prestressed concrete girders represent a relatively new portion of the bridge inventory – the oldest of these structures is only now approaching 50 years old. Therefore repair of prestressed concrete bridge elements has not received as much attention as repair of other, older structural forms. As the prestressed concrete bridge inventory 'comes of age', the repair of this structural form is an area which needs further investigation. It has been shown that repair of prestressed concrete bridge girders is possible, but not very common (Feldman et al. 1996). Often the decision to replace the bridge or the repair method chosen is not appropriate for the level of damage present resulting in inefficient and improper repair actions (Shanafelt and Horn 1980). It is proposed that with more education and familiarity with field applications of appropriate repair technology, the more often repair actions will be selected over bridge replacement, ultimately conserving resources. Presently, it is not uncommon that if a girder cannot be superficially repaired (by either painting or patching

techniques) it is replaced. Nonetheless, there are numerous repair techniques proposed by entrepreneurial and academic institutions which restore girder strength and save both material and economic resources. It is with this latter paradigm in mind that the decision to repair or replace damaged prestressed concrete bridge members should be viewed. This thesis focuses on the practical application of prestressed concrete bridge girder repair methods.

1.2 SCOPE AND OBJECTIVE OF THESIS

It is the goal of this thesis to provide illustration of practical structural repair solutions for damaged prestressed concrete bridge girders with the emphasis on restoration of strength. This thesis focuses on state-of-the-art techniques for the *structural* repair of these members (rather than aesthetic repairs, which are addressed only briefly). Common repair techniques include steel jacketing, strand splicing, external post-tensioning and post-tensioned and non post-tensioned carbon fiber reinforced polymer (CFRP) applications. Viability and limitations of each repair method are discussed for three common prestressed girder types: Spread box (SB), Adjacent box (AB) and ASSHTO-type I-beams (IB) with the focus being on CFRP repairs. Representative prototype repairs are presented with complete calculations, from which a discussion of the applicability, advantages and disadvantages of each methodology is developed. While limited in scope, the parameters necessary to make the 'repair or replace' decision are proposed.

1.3 OUTLINE OF THESIS

Chapter 2 of this thesis provides the necessary background information regarding prestressed concrete member repair and rehabilitation techniques. Chapter 3 reviews the prestressed concrete bridge inventory of Pennsylvania, establishing both need and a scope for the remaining Chapters. Representative structures are chosen from those reviewed in Chapter 3 and are described in Chapter 4. Chapter 5 describes prototype repair designs which include CFRP repairs, strand splicing and steel post tensioning repairs. Finally, Chapter 6 summarizes the work presented in this document, suggests a repair selection matrix and provides recommendations and future research opportunities.

1.4 DISCLAIMER

This document presents engineering design examples; use of the results and or reliance on the material presented is the sole responsibility of the reader. The contents of this document are not intended to be a standard of any kind and are not intended for use as a reference in specifications, contracts, regulations, statutes, or any other legal document. The opinions and interpretations expressed are those of the author and other duly referenced sources. The designs presented have not been implemented nor have they been sealed by a professional engineer.

2.0 LITERATURE REVIEW

This literature review provides the necessary background to illustrate repair, retrofit and rehabilitation techniques for prestressed concrete bridge girders. The importance of NCHRP Project 12-21 (Shanafelt and Horn 1980) should be noted. This document is considered seminal and identifies the state-of-the-art and state-of-practice as of its publication. A significant amount of work has been performed using the findings of NCHRP 12-21 as the primary reference – thus the results of NCHRP 12-21 are summarized here and considered representative of pre-1980s treatment of this subject. The state-of-the-art portion of the present review considers technology developed since the completion of the NCHRP 12-21 project in 1985. The following sections discuss repair techniques based on NCHRP 12-21, external and internal post-tensioned and non post-tensioned CFRP repair systems, anchorage systems for CFRP and expected damage guidelines.

2.1 THE NCHRP 12-21 PROJECT

NCHRP *Report 226* (Shanafelt and Horn 1980) focused on providing guidance for the assessment, inspection and repair of damaged prestressed concrete bridge girders. Suggestions were given for standardized inspection including proper techniques, tools and forms. The authors

emphasized the need to separate the damage assessment tasks (inspection) from the engineering assessment tasks (load rating, etc.).

Often the decision to replace or the repair method chosen is not appropriate for the level of damage present resulting in inefficient and improper repair actions. A damage classification system, allowing users to quantify the damage present was proposed. Shanafelt and Horn classified damage into one of three categories:

Minor damage is defined as concrete with shallow spalls, nicks and cracks, scrapes and some efflorescence, rust or water stains. Damage at this level does not affect member capacity. Repairs are for aesthetic or preventative purposes.

Moderate damage includes larger cracks and sufficient spalling or loss of concrete to expose strands. Moderate damage does not affect member capacity. Repairs are intended to prevent further deterioration.

Severe damage is any damage requiring structural repairs. Typical damage at this level includes significant cracking and spalling, corrosion and exposed and broken strands.

Minor and moderate damage can be repaired via patching and painting techniques. Since minor and moderate damage do not require structural repairs, emphasis was placed on severe damage.

In *Report 226*, eleven different repair methods were developed for the severe damage condition and are discussed in detail; none however was demonstrated or tested. Each repair technique was evaluated to provide an overview of the processes and advantages and limitations of the method. Guidelines were proposed based on service load capacity, ultimate load capacity, overload capacity, fatigue life, durability, cost, user inconvenience and speed of repairs, aesthetics and range of applicability. Evaluation of the repair techniques based on these

parameters was conducted using a value-engineering process. Areas to be considered for future research were identified, particularly associated with the proposed splice repairs. Some of the repair techniques presented needed to be tested and evaluated for strength and fatigue loading.

Repair methods considered in *Report 226* were external post-tensioning, metal sleeve splicing (to avoid confusion, this method will be referred to as 'steel jacketing' in the present work), strand splicing, a combination of these methods, and replacement.

External post-tensioning is affected using steel rods, strands or bars anchored by corbels or brackets (typically referred to as 'bolsters') which are cast or mounted onto the girder; typically on the girder's side (although occasionally on the soffit). The steel rods, strands or bars are then tensioned by jacking against the bolster or preload (which will be discussed later). Examples of this method are shown in Figure 2-1. Splice 1 (*Report 226* designation) used Grade 40 reinforcing bars, Splice 2 used Grade 60 steel rods encased in PVC conduits as a corrosion resisting measure, and Splice 4 used a corbel that was continuous over the entire length of the girder for corrosion protection of six post-tensioned 270 ksi strands. Post-tensioning force in the case of Splice 1 is nominal and is induced by preload only. Today, Splice 2 details would generally be accomplished using high strength (150 ksi) post-tensioning bars (such as Williams or Dwyidag products). In this case post-tensioning force may be induced by jacking or preload or a combination of both. For Splice 4, post-tensioning force will typically be induced by jacking. An advantage of Splice 4 is that it can also be designed as a 'harped' system, affecting greater efficiency, particularly with respect to restoring excessive vertical deflection of the girder. In this case both bolsters and deviators must be attached to the beam.

Design of external post-tensioned repair systems is relatively straight forward using a simple plane sections analysis (recognizing that the post-tensioning bar is unbonded). The

attachment/interface of the bolsters, however, requires significant attention. These elements are 'disturbed regions' subject to large concentrated compression forces. Additionally, sufficient shear capacity along the interface between the bolster and existing beam must be provided to transfer the post-tensioning force. Effective shear transfer often requires the bolsters themselves to be post-tensioned (transversely) to the girder to affect adequate 'friction' forces along the interface. Finally, the design of the bolsters and interface must consider the moments induced by the eccentric post-tensioning forces.

Steel jacketing is the use of steel plates to encase the girder to restore girder strength. With this repair technique, post-tensioning force can only be introduced by preloading. Splice 3, shown in Figure 2-2, employs a steel jacket. Generally, this method of repair will also require shear heads, studs or through bars to affect shear transfer between the steel jacket and substrate beam. Steel jacketing is felt to be a very cumbersome technique. In most applications, field welds will be necessary to 'close' the jacket (since the jacket cannot be 'slipped over' end of beam in most applications). Additionally, the jacket will need to be grouted in order to make up for dimensional discrepancies along the beam length. Neither of these details is addressed in *Report 226*.

Strand splices are designed to reconnect severed strands. Methods of reintroducing prestress force into the spliced strand are preloading, strand heating and torquing the splice; the latter is most common, essentially making the splice a turnbuckle of sorts. Strand heating is a method whereby the strand is heated, the strand splice is secured to the strand and as the strand is allowed to cool, it shrinks, thus introducing tension back into the strand. Strand heating of conventional high-strength prestressing strand is not believed to be a terribly rational method of affecting any reasonable prestrain: either a) a long length of strand must be heated; or b) a short

length of strand must be heated to a high temperature. The former is impractical in a bridge girder and the latter will affect the material properties of the strand. Strand heating is not recommended.

Commercially available strand splices have couplers connected to reverse threaded anchors; as the coupler is turned, both anchors are drawn toward each other, inducing a prestress in the attached strand (see Figure 2-3). Schematic examples of strand splices are shown in Figure 2-4. Splice 6 utilizes strand chucks to splice the strands and strand heating to induce tension (recall that the methods reported in *Report 226* were not tested in relation to this work). Splice 7 uses a strand splice that has a nut in the middle which is tightened to reconnect and introduce tension into the strand. Splice 8 uses a round steel bar which connects to a steel transfer plate and then to the strands to reconnect the strands.

Repair techniques may be combined. Combination of repair techniques will allow the user to employ the advantages of each repair. For example, Splice 5, shown in Figure 2-5, uses post-tensioning in conjunction with steel jacketing to restore girder strength. The post-tensioning addresses girder serviceability while the steel jacket reinforces the girder's ultimate capacity.

Most repairs proposed in *Report 226* make use of preloading during girder repair. Preload is the temporary application of a vertical load to the girder during the repair. The preload is provided by either vertical jacking or a loaded vehicle. If the damage has caused a loss of concrete without severing strands, preloading during concrete restoration can restore the strength of the girder without adding prestress. Because preloading may be used to restore partial or full prestress to the repaired area, it effectively reduces tension in the repaired area during live load applications. It is for this reason that preloading is suggested for most repairs, particularly those

including patching. Care should be taken when preloading a structure so as to not overload the structure or cause damage from excessive localized stresses from the preloading force.

It must be noted that Shanafelt and Horn, in *Report 226*, addressed relatively small prestressed elements having only 16 strands. In this case, the preload required to affect the post-tensioning force is relatively small. In this case the structural system is similar in scale to a parking garage. As elements become larger – as for a bridge – the level of preload required becomes very large and not practical to apply. The effectiveness of considering preload is improved with reduced dead-to-live load ratios; however these are not typical in concrete structures.

NCHRP *Report 226* provides the selection matrix, shown in Table 2-1, for selecting repair methods for prestressed girders. Guidelines presented for each repair method are as follows. The 'number of strands' that may be spliced must be placed in context. The prototype girders considered in this study only had 16 strands.

External Post-tensioning: replacing the loss of more than 6-8 strands may be difficult, but this method can be used to restore strength and durability to damaged girders and add strength to existing bridges.

Strand Splicing: this method is good for repair of a few strands but is limited by the geometry of the strand splice and concrete cover.

Steel Jacketing: this method was successfully used to replace the loss of 6 strands, but is not very common.

The second phase of the NCHRP 12-21 project and the focus of NCHRP *Report 280* (Shanafelt and Horn 1985) was to provide a practical user's manual for the evaluation and repair of damaged prestressed concrete bridge members. Significantly, some of the the repair methods

presented in the earlier *Report 226* were load tested and suggestions for their implementation are given. It is important to note that the girders were never loaded to their ultimate capacity. All tests were conducted on a single girder with artificial damage and one of the repair techniques for each test. Therefore, in order to test all repair methods, the girder was not loaded to failure. Ten different load tests were conducted on a single I-girder to measure the behavior of each repair:

1. Load girder up to 75% of the calculated ultimate load capacity;
2. Add concrete corbels and post-tension high-strength bars and load;
3. Disconnect high-strength bars and load (same as load test 1 but girder is now cracked);
4. Break out specified concrete to sever 4 strands (25% of the total 16 strands) and load;
5. Splice 4 strands with single strand splice and patch and load;
6. Reconnect post-tension high-strength bars (same test as test 5 but with external PT);
7. Disconnect bars, break out concrete and sever the four strands spliced in test 5 and load;
8. Patch the girder and tension the external bars;
9. Disconnect bars, break out patch, sever 2 more strands for a total of 6 and splice them with a steel jacket and load; and
10. Load the steel jacketed girder to 100% of the calculated ultimate moment capacity.

While the tests of each repair technique generally demonstrated a sound response, the fact that a) there was no control specimen with which to compare results; and b) the repairs were sequential and thus the degree of damage was necessarily incremented between tests affected the ability to draw conclusions from this test program. Although a significant amount of test data is provided, few conclusions are or can be drawn.

2.2 TRADITIONAL REPAIR TECHNIQUES

The techniques described in NCHRP 12-21 have provided many repair methods which restore strength and serviceability to prestressed concrete girders. The resulting *Reports 226* and *280* provided a background to a significant amount of research testing the viability of each repair method. This section provides a review of literature available since the publication of the NCHRP 12-21 reports. The techniques discussed below are strand splicing, external steel post-tensioning, and beam coatings; these are considered to be traditional repair methods.

2.2.1 Strand Splicing

In repairing a few damaged strands, strand splicing provides an efficient, quick and simple solution. Strand splices reconnect broken strands and allow the strand to be re-tensioned. However, interactions between spliced strands and girder behavior where multiple strand splices are used should be explored. Strand splice tensioning based on the torque wrench method (i.e.: applying a specified torque to a strand splice coupler) was found to be unsatisfactory due to a variation in friction stresses along the splice and thus a variation of stress induced into the strand (Labia et al. 1996). The 'turn of the nut' method which uses the displacement between strand chucks or splice ends and material properties to calculate stress was found to be more easily accomplished and reliable (Labia et al. 1996 and Olson et al. 1992). This method is analogous to the method of assuring appropriate prestress in a strand as it is jacked: by elongation of the strand. Testing has shown that strand splices can restore original girder strength (Labia et al. 1996).

In some instances, the size of the strand splices has been found to be problematic. Beam geometries and the amount of concrete cover limit the use of strand splices. Often, strands are too closely spaced or concrete cover is too small to accommodate the strand splice. Additionally, turnbuckle strand splices have a much larger axial and flexural stiffness than the strands themselves. This affects girder behavior, particularly if the splice repair is not symmetric in the girder cross section. Olson et al. (1992) report a strand splice-repaired test girder that failed in tension at less than 82% of the original girder capacity. Possible reasons cited for the tension failure include: a) increased strand damage during the fatigue program: the stress ranges may have been magnified on the undamaged side of the girder; b) the turnbuckle splices may have worked as anchors on the damaged side of the girder; or c) a combination of the two factors. Premature failure of test girders using the strand splices is cause for concern.

It is important that the strength of the strand splices be assured. Zobel and Jirsa (1998) studied the performance of various strand splice repairs. All splices gave a minimum strength of 85% of the nominal strength of the strand. From this study, strand splices are recommended: a) when ultimate flexural strength of the girder with the remaining undamaged strands is greater than the factored design moment, repair by internal strand splices could be used to reduce the range of stress imposed on the other strands; and b) if fatigue is not a major concern, internal splice methods could be used to restore ultimate flexural strength to a damaged girder. In any case, repairing more than 10-15% of the total number of strands within a single girder is not recommended (Zobel and Jirsa 1998).

There is a single known commercially available strand splice available today. The ‘Grabb-it Splice’ utilizes a reverse threaded coupler. This splice has two factors negatively affecting its use: a) the prestress force that may be developed is limited to 39.5 kips which is

slightly greater than f_{pu} for 0.5 in. strand (Law Engineering 1990). It is believed that the splice strength should be: a) at least 15% greater than the strand strength to minimize the possibility of splice failure (Labia et al. 1996); and b) the splice diameter of 1.625 in. potentially affects concrete cover and strand spacing requirements. In any event, the latter issue requires such splices to be staggered along the length of a member (Grabb-it technical literature 2008).

2.2.2 Post Tensioning

Post tensioning can be used to help restore prestress as well as girder strength. This allows the design to be customized to restore strength and serviceability, as desired. For example, in the adjacent box (AB) beam bridge examined in Preston et al. (1987), the original strand pattern was determined to meet a particular concrete stress requirement. Therefore, it was important for the repair to restore bottom fiber prestress in a manner consistent with the original design intent. The post tensioned repair utilized four post tensioned 0.5 in. diameter, epoxy coated, low-relaxation strands installed 2 in. below the beam soffit, each tensioned and anchored at 21.5 kips. The total depth of the repair was 3 in. Some issues arose when seating the post-tensioning strands as the losses were greater than expected and thus the induced tensile force needed to be increased to account for these losses. Nonetheless, full ultimate capacity of the girder was restored as well as some of the lost prestressing force.

The same concept can be used with CFRP instead of steel as the post tensioning material. El-Hacha and Elbadry (2006) examined the use of post tensioned 7-wire CFRP cables (CFCC) for strengthening of concrete beams. The experiment showed comparable results to steel post-tensioned repairs. The post-tensioning force created a stiffer beam and thus a stiffer load-deflection response.

2.2.3 Corrosion Mitigation

When considering repair of corroded strand, it is important to consider the source of corrosion. For example, corrosion initiated because of cracks in the beam requires repair of the cracks to arrest further corrosion. Prestressing strand is more susceptible to corrosion than lower grades of steel, therefore prestressed concrete beams are susceptible to corrosion, especially at beam ends. Since prestressed strands are anchored in the beam ends, strand corrosion in this area can be detrimental to girder strength. Tabatabi et al. (2004) focused on the repair of the beam end region (within the last two feet of the beam). A protective coating was put on some beam ends before the experimental accelerated corrosion program began to see how this would affect strand corrosion rates. Beam ends were then subjected to wet/dry cycles of salt-water sprays together with an impressed electric current to accelerate the corrosion process. After an initial exposure of six months, all but one of the untreated beam ends was protected using CFRP wrapping or painted with a protective coating. The corrosion process was then allowed to continue for an additional year. It was concluded that surface treatments and coatings are effective in the short term, but not in the long term unless the coating is applied prior to chloride contamination. As expected, a patch repair having no initial protection performed the worst. Table 2-2 compares beam end ratings and displays the most effective mitigation measure. Studies have shown that FRP composite wraps are effective at mitigating future corrosion damage (Tabatabi et al. 2004 and Klaiber et al. 2004). Generally speaking, cathodic protection is also effective, but is not commonly used due to high maintenance costs and method complexity (Broomfield and Tinnea 1992 and Tabatabi et al. 2004).

2.3 EXTERNAL NON PT CFRP RETROFIT

Carbon fiber reinforced polymer (CFRP) strips bonded to prestressed concrete girders can increase flexural capacity of the girder. The use of externally mounted CFRP strips to restore flexural capacity of damaged girders is well documented (Scheibel et al. 2001, Tumialan et al. 2001, Klaiber et al. 2003, Green et al. 2004, Reed and Peterman 2004, Wipf et al. 2004, Reed and Peterman 2005 and Reed et al. 2007). In most cases, repairs performed as expected and designed. Green et al. (2004) investigated the behaviors of four different CFRP systems: two wet lay-up procedures from different manufacturers, a fabric pre-impregnated with resin (prepreg), and a spray layed-up application. For the various repairs, the experimentally observed and theoretical capacities achieved were in the range of 91-108% and 96-114%, respectively, of the unrepaired, undamaged control girder. Beam deflections, however, were found to be reduced in the range of 20 to 23% (Klaiber et al. 2003 and Green et al. 2004, respectively). Often, to reduce the chance of early debonding, transverse U-wrapped CFRP strips were used to help 'hold' the CFRP and underlying concrete patch in place (Scheibel et al. 2001, Tumialan et al. 2001, Klaiber et al. 2003, Green et al. 2004, Reed and Peterman 2004, Wipf et al. 2004 and Reed and Peterman 2005). Additional confinement of the concrete patch is helpful to mitigate the possibility of a 'pop out' failure of the patch where the newly placed patch material breaks away from the girder.

The results reported by Wight et al. (2001) are used here to illustrate the effects of non-PT CFRP retrofit of prestressed concrete beams. Figure 2-6 shows the cross section of the test specimens used by Wight et al. One specimen was not strengthened with CFRP (to serve as a control), one was strengthened with non post-tensioned CFRP sheets and the remaining two used post-tensioned CFRP sheets. Each strengthened member was strengthened with 5 layers of CFRP sheets (where each subsequent layer was 7.87in. (200 mm) shorter than the preceding layer and

centered on the tension face of the specimen) for a total of 0.47in^2 (300 mm^2) of CFRP at midspan. Figure 2-7 summarizes the experimentally observed load-deflection behavior. As seen in Figure 2-7, there is a 20% increase in mid-span moment capacity for the beam strengthened with CFRP as compared to the control beam.

2.4 EXTERNAL PT CFRP RETROFIT

A parallel can be drawn between prestressed and non prestressed CFRP retrofits and prestressed and conventionally reinforced concrete beams. Prestressing the steel precompresses the concrete in the tension zone of the girder. As the beam is loaded, it must first 'undo' the compressive stress induced by the strands resulting in a more durable (fully-prestressed members do not crack under service loads) and stiffer concrete member. Prestressing is the optimized use of both materials since concrete is best in compression and steel performs well in tension. The benefits of stressing CFRP strips prior to application are similar to that of using a prestressed strand in a concrete beam. The four main advantages of using a stressed CFRP repair are (Nordin and Taljsten 2006): a) better utilization of the strengthening material; b) smaller and better distributed cracks in concrete; c) unloading (stress relief) of the steel reinforcement; and d) higher steel yielding loads. Conventionally used CFRP materials have about 1.5 times the tensile stress capacity of 270 ksi steel prestressing strand and a Young's modulus about 75% of that of steel, meaning they can reach a higher strain. Stressing the CFRP for the repair reintroduces prestressing force back into the beam allowing for redistribution and a decrease of stresses in the strands and concrete (Kim et al. 2008b). Thus when reloaded, the stress levels in the existing (remaining) strands will be reduced as compared to the unrepaired beam. In other words,

prestressed CFRP systems create an active load-carrying mechanism which ensures that part of the dead load is carried by the CFRP sheets whereas non prestressed CFRP strips can only support loads applied after installation of the CFRP on the structure (Wight et al. 2001, El-Hacha et al. 2003, Kim et al. 2008a and Kim et al. 2008c). Loading that follows prestressed CFRP placement will result in greater CFRP strains meaning that: a) the material is used in the most efficient manner; and b) the CFRP strip is engaged, resulting in an increase in flexural capacity.

There are three approaches to prestressing or post-tensioning (the terms are used inconsistently in the literature) CFRP. The following terminology is adopted to clarify the types of prestressed CFRP systems (PCFRP):

***Prestressed CFRP*:** The CFRP is drawn into tension using external reaction hardware and is applied to the concrete substrate while under stress. The stress in maintained using the external reaction until the bonding adhesive is cured. The reacting stress is released and the 'prestress' is transferred to the substrate concrete. This method of prestressing is potentially susceptible to large losses at stress transfer and long term losses due to creep of the adhesive system. Additionally, details (such as FRP U-wraps) must be provided to mitigate debonding at the termination of the CFRP strips. Prestressed CFRP systems are analogous to prestressed concrete systems where the stress is transferred by bond to the structural member.

***Unbonded post-tensioned CFRP*:** The CFRP is drawn into tension using the member being repaired to provide the reaction. The stress is transferred to the member by mechanical anchorage. Typically a hydraulic or mechanical stressing system will be used to apply the tension after which it will be 'locked off' at the stressing anchorage. This method of post-tensioning is susceptible to losses during the 'locking off' procedure. Depending on the anchorage method, long term losses due to creep in the anchorage is a consideration. Such

systems must be designed with sufficient clearance between the CFRP and substrate concrete to mitigate the potential for fretting. Unbonded post-tensioned systems are analogous to conventional unbonded post tensioning systems.

***Bonded post-tensioned CFRP*:** The CFRP is stressed and anchored in the same fashion as unbonded systems. Following anchorage, the CFRP is bonded to the concrete substrate resulting in a composite system with respect to loads applied following CFRP anchorage. Since the adhesive system is not under stress due to the post-tension force, adhesive creep is not as significant a consideration with this system. The bonding of the CFRP may also help to mitigate creep losses associated with the anchorage. Bonded post-tensioned systems are analogous to conventional bonded post tensioning systems.

Another advantage of using PCFRP systems is the restoration of service level displacements or performance of the structure. PCFRP systems have a confining effect on concrete (and, significantly, any patch material) because they place the concrete into compression. Therefore, a delay in the onset of cracking and a reduction of crack widths (only in bonded systems) has been found when this technique is used (Wight et al. 2001, El-Hacha et al. 2003, Kim et al. 2008a, Kim et al. 2008c and Yu et al. 2008b).

Wight et al. (2001) demonstrated the difference between prestressed and non-prestressed CFRP applications. The unstrengthened specimens and retrofit details used are shown in Figure 2-6 and the experimentally observed load-deflection curves are shown in Figure 2-7. It can be seen that mid-span moment capacity for the bonded PCFRP is greater than both the unstrengthened control and non-prestressed CFRP strengthened beams (this curve in Figure 2-7 is described as ‘Strengthened with Prestressed FRP’). Flexural capacity of the bonded PCFRP repair was 35 to 40% higher than that of the control specimen. Additionally, the bonded PT

repair displayed a cracking load 150% greater than that of the control specimen. The increase in cracking load is attributed to the addition of prestress-induced compressive force back into the member which makes the beam stiffer than before the repair.

There are significant challenges associated with prestressing CFRP strips. The most obvious is the means by which the strip is prestressed. One solution proposes post tensioning the CFRP strip against the girder end, as seen in Figure 2-8 (Wight et al. 2001 and El-Hacha et al. 2003). This method proposes that the strips are permanently anchored at one end of the beam (commonly called the 'dead end') while jacking forces are introduced at the other, movable end (called the 'jacking end'). Steel rollers are connected to each end of the strip to allow for anchorage. Rollers attached to the jacking end are connected to steel prestressing strands which are connected to a hydraulic ram (jack). The movable end rollers are jacked to the desired extended position and permanently anchored. Alternative prestressing techniques include using indirect methods where the sheets are stressed in a jacking or prestressing frame independent of the beam. Prestressing force is induced by either jacking the sheet against a frame thus increasing its length (Casadei et al. 2006) or by deflection controlled loading (Yu et al. 2008a) as seen in Figures 2-9 and 2-10, respectively. After prestressing by either method, the frame is moved to the girder to allow the strip to be bonded. Once bonded, the prestress force is removed from the frame and transferred (by bond) to the girder.

2.4.1 CFRP Anchorage

In prestressed CFRP applications, the prestressing force in the CFRP strip must transfer into the girder through the bonding agent (adhesive). Due to the high strains at the bond interface, strip debonding is a major concern. It is essential that the entire force be transferred into the beam via

the adhesive layer or the repair will not behave as designed and fail prematurely. Additionally, most suitable high performance epoxy adhesives exhibit significant creep and are therefore unsuitable for maintaining a large prestress force without additional anchorage. If mechanical anchors are left in place, the system is a post-tensioned CFRP system (which can be bonded or unbonded). Permanent anchors can be used to resist the prestressing force and reduce the chance of early debonding and peeling failures (Wight et al. 2001, El-Hacha et al. 2003, Kim et al. 2008a and Yu et al. 2008b). The anchors at the ends of the CFRP strips reduce the shear deformation that occurs within the adhesive layer associated with the prestress force minimizing the possibility of premature failure (El-Hacha et al. 2003). It is noted that the ability of a system to transfer shear, regardless of anchorage or adhesive used, is limited by the shear capacity of the concrete substrate. ACI 440 (2008) recommends that the shear stress transferred is limited to 200 psi in any event.

El-Hacha et al. (2003) tested three different metallic anchors including a round bar, elliptical bar and a flat plate anchor. The results indicated that a flat plate anchor was the most efficient anchor and reinforcement of the anchor zone with CFRP U-wrap resulted in greater failure loads. When the CFRP U-wrap was used in conjunction with the anchorage, failure occurred away from the anchor zone. Although these results seem promising, there are concerns about galvanic corrosion of the anchor when steel and CFRP strips are in direct contact. Mitigation of galvanic corrosion is conventionally addressed by providing an insulating layer, often E-glass (Cadei et al. 2004). This layer is softer than the CFRP and therefore affects the efficiency of the stress transfer.

U-wrapped CFRP strips have been employed as an alternative to metallic anchorage systems (Kim et al. 2008a, Kim et al. 2008b and Yu et al. 2008b). Many nonmetallic mechanical

anchoring systems for the CFRP U-wraps have been explored including (Kim et al. 2008a and Kim et al. 2008b): a) CFRP U-wrap; b) mechanical anchorage; c) prestressed CFRP U-wrap with mechanical anchorage; and d) CFRP wrap anchored systems (see Figure 2-11). Test results indicated that: a) the beams with nonmetallic anchors exhibited a pseudoductile failure due to the contribution of CFRP anchors, b) beams with mechanically anchored U-wraps and side sheets exhibited a capacity close to that of the control beam; and c) the beams fitted with nonmetallic anchors displayed better stress redistributions compared to the beam with steel anchors (Kim et al. 2008b).

It has been shown that when an anchorage system is used, the anchored prestressed sheets fail at a greater load than the nonanchored prestressed sheets since anchorage greatly reduces the chance of premature 'end peel debonding' failure of the repair (Wight et al. 2001, El-Hacha et al. 2003, Kim et al. 2008a, Kim et al. 2008b and Yu et al. 2008b).

One unique approach did not use anchors, but rather gradually reduced the prestressing force of the strip until the force was zero at the ends of the strip (Aram et al. 2008). The concept behind this was that peeling failure of the strip could be avoided if the force at the strip terminations is zero. Results show that the gradient anchorage method was not effective and premature debonding failure occurred.

2.4.2 Commercially-Available PCFRP System

The only known commercially available 'standardized' PCFRP system (i.e.: not customized for each application) is made by SIKA Corporation and marketed primarily in Europe. The SIKA CarboStress system is shown in Figure 2-12. The anchorage has a capacity of 67 kips (300 kN)

and is intended for a maximum applied prestress force of 45 kips (200 kN). Material properties of the CFPR strips are given later in Table 5-2. This system is comprised of CFRP strips with 'potted' CFRP anchorages referred to as 'stressheads' manufactured on each end. These stressheads are captured by steel anchorages mounted on the concrete (Figure 2-12a) or by the jacking hardware (Figures 2-12b and d). One anchor is the fixed or 'dead' end (Figure 2-12a) while the other is the jacking end (Figure 2-12b). The jacking end stresshead connects into a movable steel frame which connects to a hydraulic jack, thus allowing the strip to be stressed. Once the desired stress level is reached, the jack can be mechanically locked to retain the stress in the CFRP or the CFRP strip can be anchored by 'clamps' (Figure 2-12c) near the jacking end. Anchor points can also be located at the beam diaphragms. The introduced stress in the strips can vary according to the structural needs and is limited to the tensile strength of the strip (in many cases, the strength of the beam at the anchor location controls the amount of prestress force that can be applied). Herman (2005) reports an application of this system on two prestressed concrete box girder bridges. The intended repair of the prestressed concrete box girders was to restore flexural capacity as well as replace some of the lost prestressing forces; employment of the Carbostress system as the repair technique proved successful at restoring flexural capacity and prestressing force. Additionally, this method saved monetary and material resources and minimized construction time and traffic closures.

2.5 NSM CFRP REPAIRS

Near-surface mounted (NSM) CFRP repairs provide an alternative to externally bonded CFRP strip repairs. The NSM technique places the CFRP in the cover concrete of the member (see

Figure 2-13). This protects the laminate from impact forces and environmental exposure (Nordin et al. 2002). Similar to external CFRP repairs, an NSM repair can be prestressed if serviceability is a concern or non prestressed if ultimate capacity is the only design consideration. It is noted, however, that prestressing NSM applications is very difficult and has only been demonstrated in laboratory applications using a stressing procedure that is not practical for use in the field (Nordin et al. 2002 and Casadei et al. 2006). An NSM CFRP repair is completely enclosed in epoxy, making it possible to achieve higher bond strength as compared to external strip bonding due to the larger surface area which is bonded. Additionally, an NSM application engages more cover concrete and is able to transfer greater stresses into the concrete substrate (Quattlebaum et al. 2005). Therefore, NSM repairs will typically use less CFRP material than an externally bonded strip repair. However, NSM repairs are sensitive to the amount of concrete cover and are not a viable option when cover is not sufficient. Laboratory studies have shown that both prestressed and non prestressed NSM repairs have been successful in restoring ultimate girder capacity (Nordin et al. 2002 and Casadei et al. 2006).

2.6 EXPECTED DAMAGE

In designing repair measures, it is of the utmost importance for the designer to thoroughly understand the condition of the member prior to repair. Incorrect assumptions regarding the structure's condition result in a poor or improper repair design. It is important to also consider the nature or cause of the damage in order to understand the damage and address the source of the damage in addition to facilitating the repair. For example, based on findings of the investigation of the Lake View Drive Bridge collapse (Harries 2006 and Naito et al. 2006) a

recommendation was proposed that when considering observable corrosion damage to strands, that the contribution of between 50% and 100% of adjacent (unobservable) strands be neglected in rating the damaged structure. Based on these recommendations, PennDOT adopted the '150% rule' for assessing the area of lost prestressing strand: [paraphrasing] *when assessing corrosion damage to a prestressed concrete girder, the area of prestressing strand assumed to be ineffective due to corrosion shall be taken as 150% of that determined by visual inspection*.

Similarly, the strength capacity of a girder suffering impact damaged may change significantly. For example, a prestressed concrete structure is impacted by a truck and only one strand is visible and severed. Small strand spacing results in little concrete between strands. In this case, there may be insufficient concrete surrounding the adjacent strand(s) to allow the prestressing force of these strands to be transferred into the structure. As a result, a portion or all of the prestressing force near the impact may be ineffective. It may be prudent to disregard a portion or all of the contribution from surrounding strands in repair design.

Damaged strands in larger spans or long girders may be 'redeveloped' if there is sufficient undamaged length remaining. There has been no study on the 'redevelopment' of severed or corroded strands; therefore, for repair design, it is conservative to neglect the strand in the analysis of the structure (Harries 2006).

Table 2-1 Repair Selection Criteria (Shanafelt and Horn 1980).

Damage Assessment Factor	Repair Method			
	External PT	**Strand Splicing**	**Steel Jacket**	**Girder Replacement**
Behavior at Ultimate Load	Excellent	Excellent	Excellent	Excellent
Overload	Excellent	Excellent	Excellent	Excellent
Fatigue	Excellent	Limited	Excellent	Excellent
Adding Strength to Non-Damaged Girders	Excellent	N/A	Excellent	N/A
Combining Splice Methods	Excellent	Excellent	Excellent	N/A
Splicing Tendons or Bundled Strands	Limited	N/A	Excellent	Excellent
Number of Strands Spliced	Limited	Limited	Large	Unlimited
Preload Required	Perhaps	Yes	Probably	No
Restore Loss of Concrete	Excellent	Excellent	Excellent	Excellent
Speed of Repair	Good	Excellent	Good	Poor
Durability	Excellent	Excellent	Excellent	Excellent
Cost	Low	Very Low	Low	High
Aesthetics	Fair*	Excellent	Excellent	Excellent

N/A: not applicable

*can be improved to excellent by extending corbels on fascia girder

Table 2-2 Comparison of Various Beam-End Numerical Ratings and Overall Ratings (Tabatabi et al. 2004).

Beam End	Description	Chlorides*	Cracking*	Corrosion*	Overall Rating*
1A	Epoxy Coated From Day 1	1	2	3	**6**
1B	Epoxy Coated After 6 Months of Exposure	2.5	4	7	**13.5**
2A	No Treatment Applied	2	6	5.5	**13.5**
2B	Patch Repair After 6 Months of Exposure	8	7	8	**23**
3A	Silane Sealer Applied from Day 1	1	5	3.5	**9.5**
3B	Silane Sealer Applied After 6 Months of Exposure	2	8	5.5	**15.5**
4A	Polymer Resin Coating Applied After 6 Months of Exposure	4.5	3	6	**13.5**
4B	FRP Wrap Applied After 6 Months of Exposure	2.5	1	7	**10.5**
5A	Polymer Resin Coating Applied from Day 1	1	1	2	**4**
5B	FRP Wrap Applied From Day 1	1.5	1	2	**4.5**

*Individual criterion ratings were based on 1 –8 scale, 1 indicating best effect, 8 indicating worst effect. The overall ranking was based on a scale of 3 to 24 with 3 indicating the best condition and 24 indicating the worst condition. Shaded rows indicate beam-ends that were treated after 6 months of exposure.

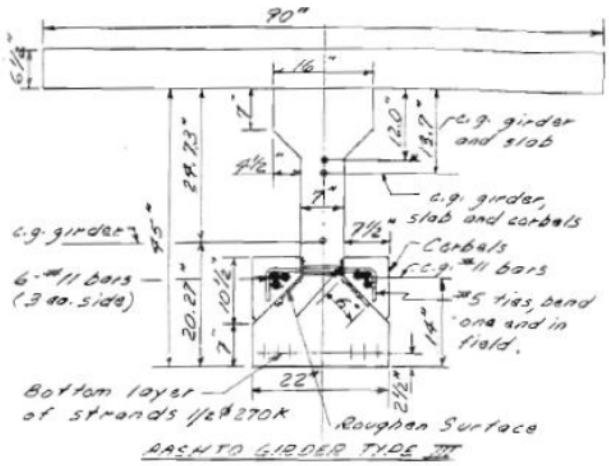

(a) Splice 1: mild reinforcing anchored by bolster.
PT provided by preload.

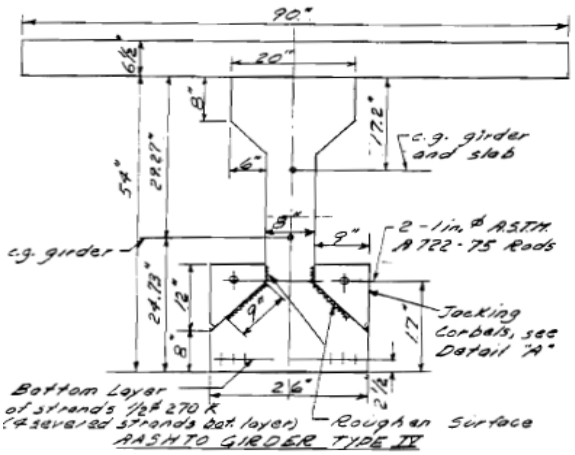

(b) Splice 2: PT anchored by bolster.
Bar is usually mounted in duct or greased sleeve to affect environmental protection.

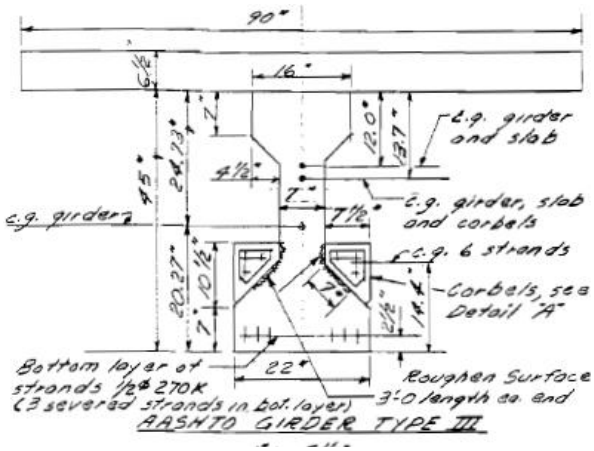

(c) Splice 4: Prestressing strand in continuous bolsters.
Strand may be harped. PT provided by jacking.
Unbonded strand in a greased sleeve is conventionally used.

Figure 2-1 External post-tensioned repair methods (Shanafelt and Horn 1980).

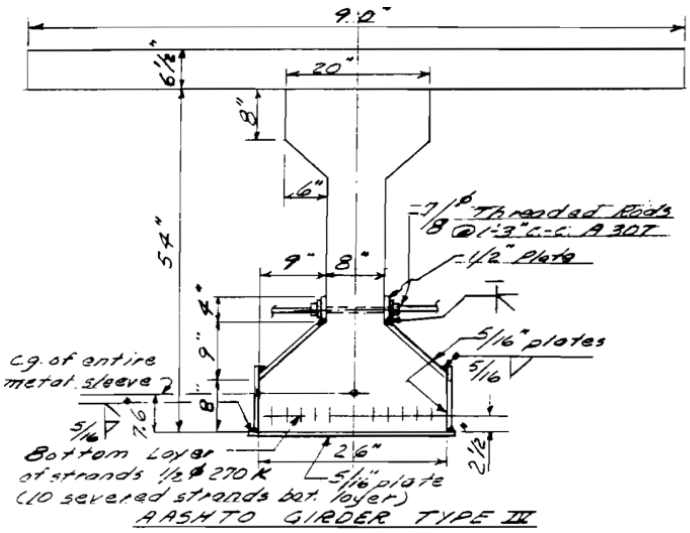

Figure 2-2 Splice 3: Steel jacket repair method (Shanafelt and Horn 1980).

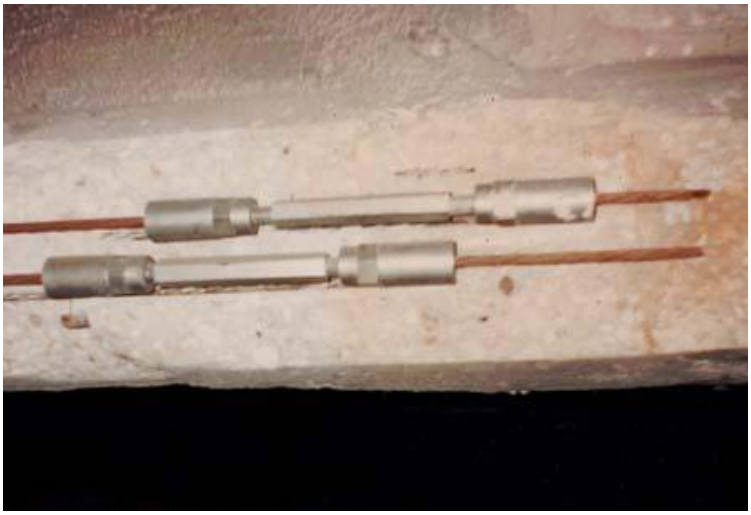

Figure 2-3 Commercially available 'turnbuckle' style strand splice repair method (PCI).

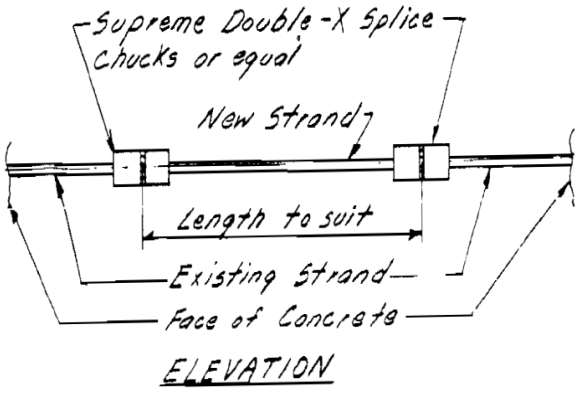

(a) Splice 6: Strand chucks used to splice strand. Prestressing reintroduced by heating strand during installation

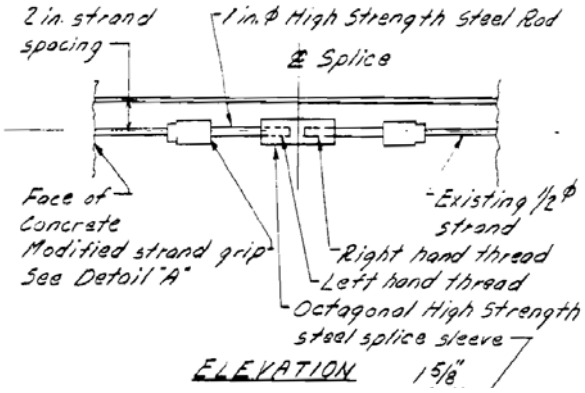

(b) Splice 7: 'Turnbuckle' style strand splice. Coupler draws strand ends together.

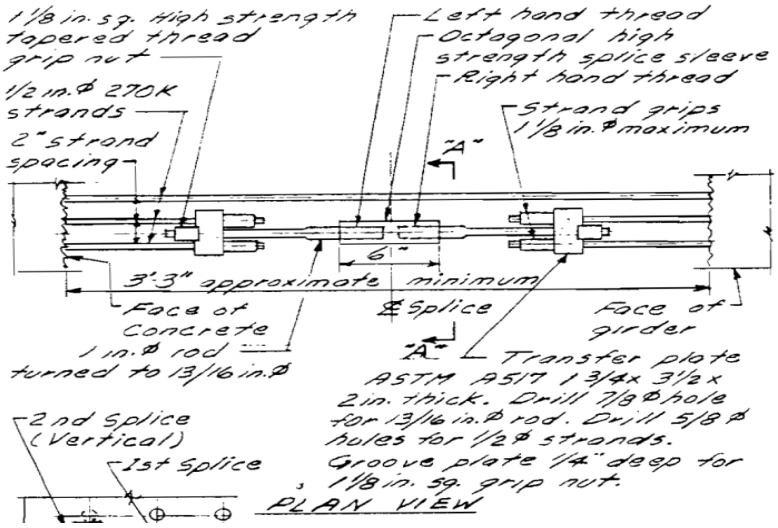

(c) Splice 8: Multiple strand 'turnbuckle' style strand splice.

Figure 2-4 Strand splicing methods (Shanafelt and Horn 1980).

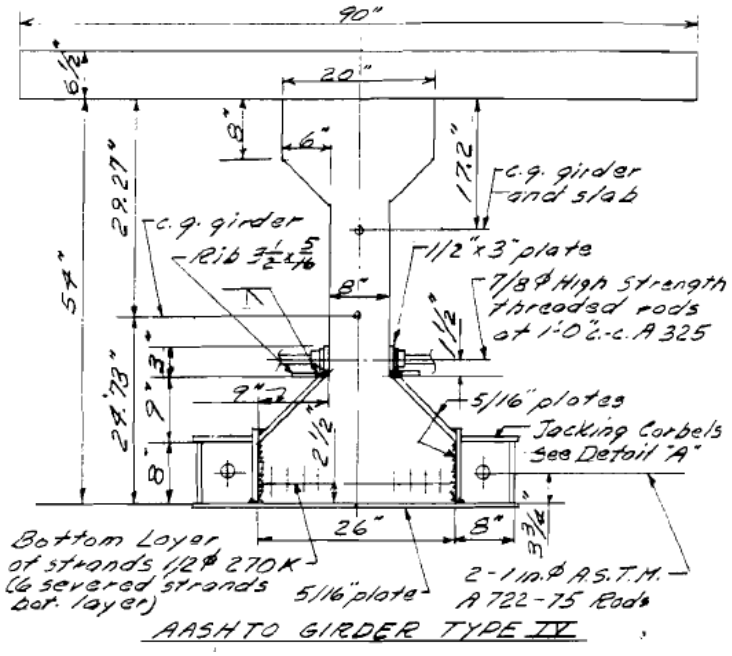

Figure 2-5 Combination of repair methods (Splice 5) (Shanafelt and Horn 1980).

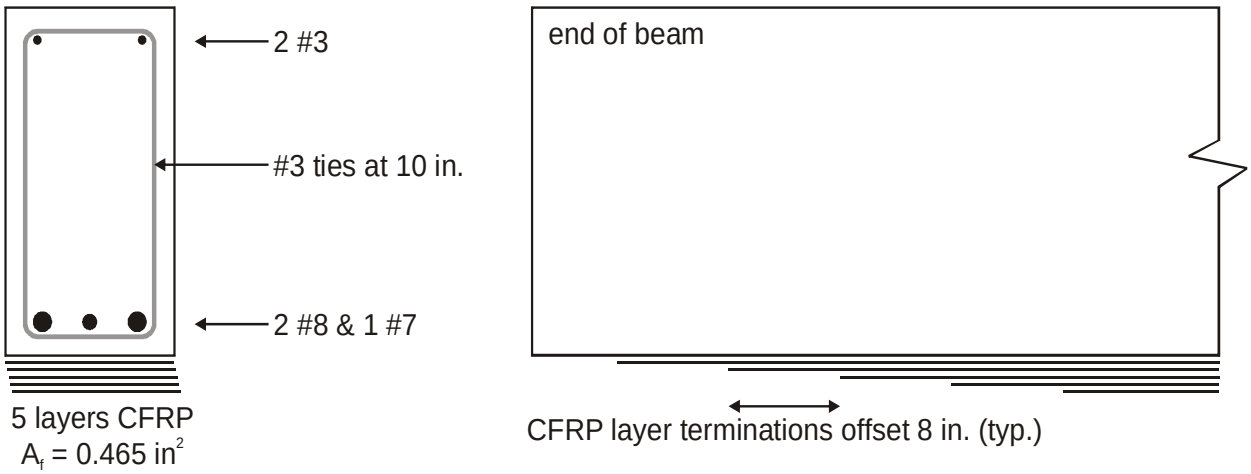

Figure 2-6 Specimen cross sections tested by Wight et al. (2001).

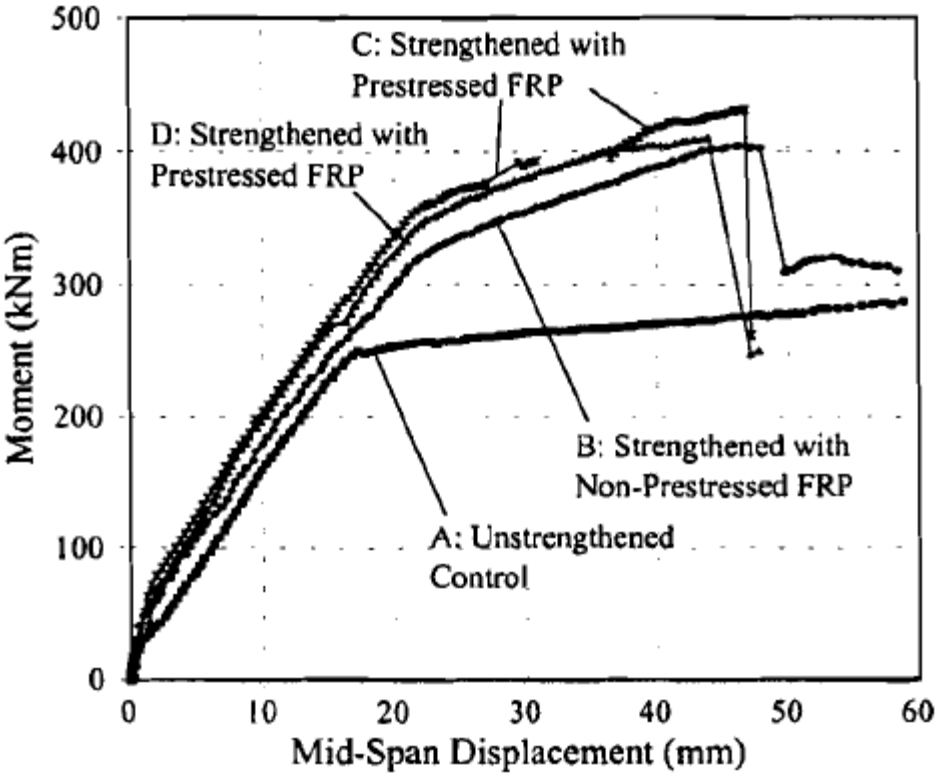

Figure 2-7 Moment –displacement plots for beams tested by Wight et al. (2001).

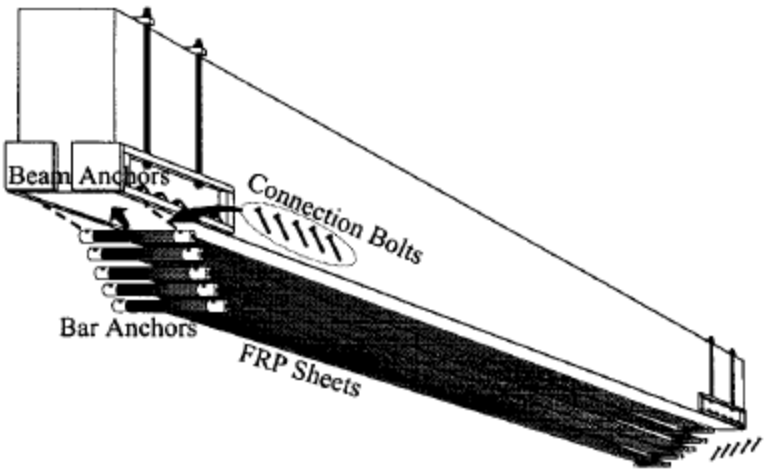

Figure 2-8 Proposed direct prestressing system (Wight et al. 2001).

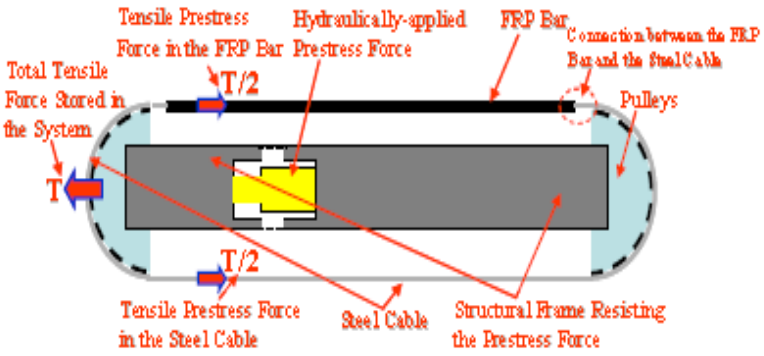

(a) Schematic of closed loop prestressing system.

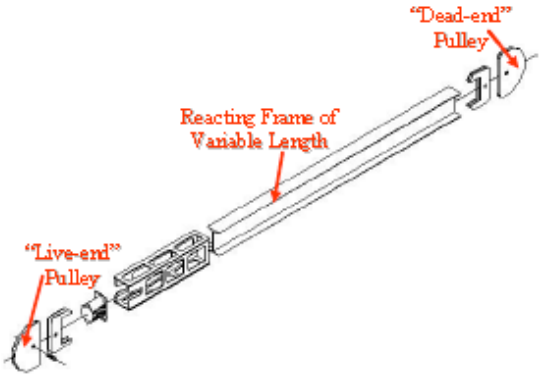

(b) Prototype system under development.

Figure 2-9 Proposed indirect prestressing system (Casadei et al. 2006).

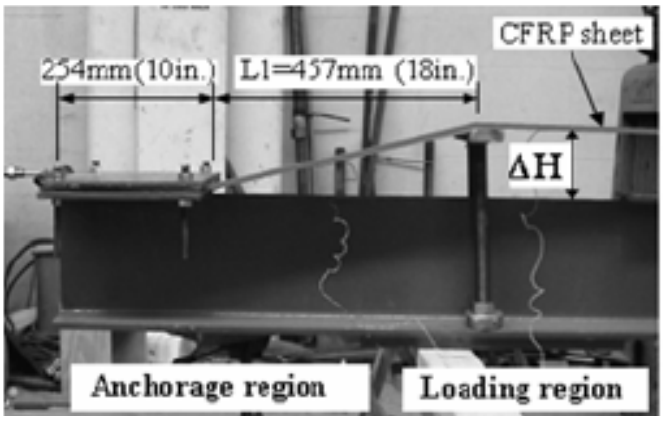

Figure 2-10 Proposed deflection controlled indirect prestressing system (Yu et al. 2008a).

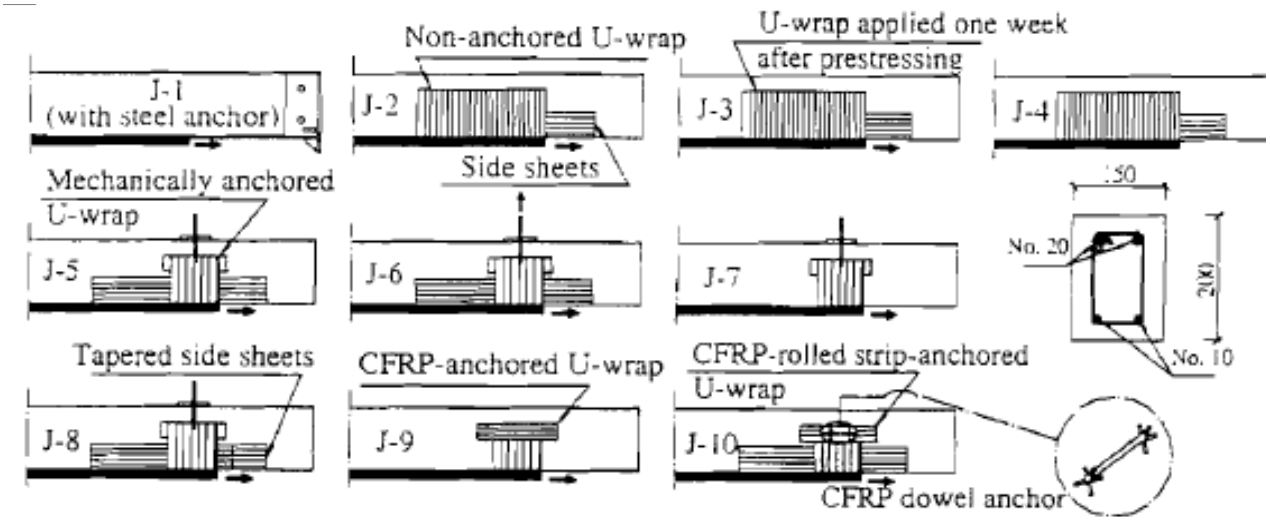

Figure 2-11 Nonmetallic anchoring systems (Kim et al. 2008a).

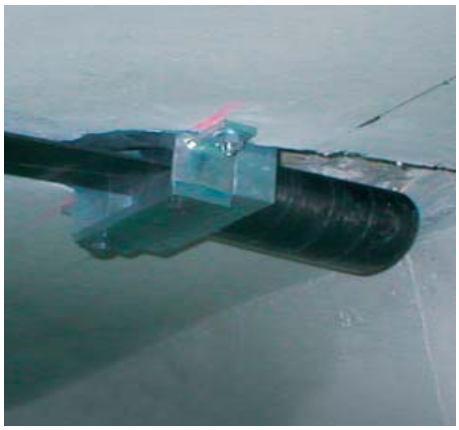

(a) dead end anchor.

(b) jacking end anchor in movable frame.

(c) multiple live end anchors at one location.

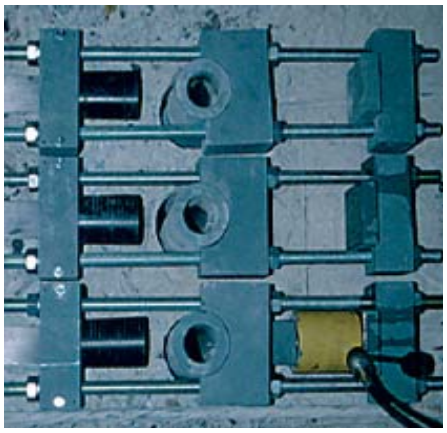

(d) stress head system.

Figure 2-12 Sika CarboStress system (SIKA).

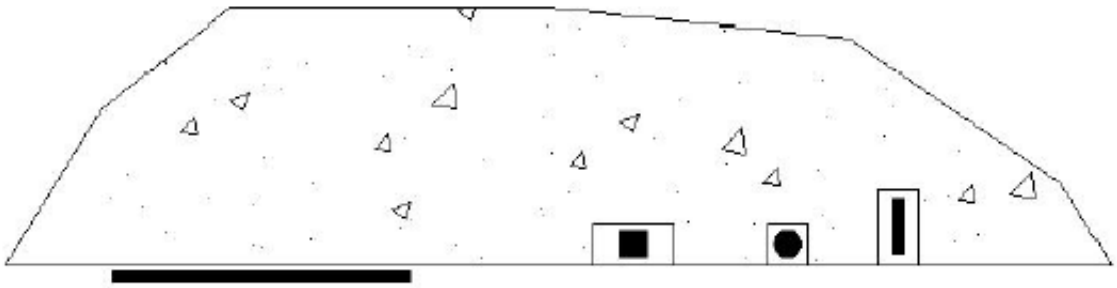

Figure 2-13 Schematic of externally bonded and NSM CFRP techniques.

3.0 INVENTORY CONDITION ASSESSMENT

A review of all prestressed concrete bridge structures in Pennsylvania was conducted. All bridges having a 'structure type' coded 4xxxx (i.e.: prestressed concrete) in the PONTIS database were included. Data was considered on a statewide basis (including District 11) and for District 11 (Allegheny, Beaver and Lawrence counties) only. The intent of this exercise was to establish a snapshot of the condition of the prestressed concrete bridge inventory in Pennsylvania and to ensure that the bridges considered for further study (from District 11) were representative of the statewide distribution.

3.1 BRIDGE INVENTORY REVIEWED

Table 3-1 provides a summary of the data obtained based on bridge type considering statewide and District 11 data. For this exercise, only structures rated as 'structural deficient' (SD) are considered. Additionally, the data is divided into those bridges rated deficient for 'any' (deck, superstructure, substructure) reason and for only superstructure ('super') deficiency; the latter is the focus of the present study. In reading Table 3-1, the percentages reported in the 'No.' columns are determined based on the total number of prestressed bridges reported; thus statewide, 33% of prestressed bridges are 'simple composite multi-box beams' (1921/5874 = 0.33). The percentages reported in the 'SD' columns are based on the total number of bridges of

a particular type; thus statewide, 11% of the 'simple composite multi-box beams' are structurally deficient (214/1921 = 0.11). The following observations are made based on this data:

- Statewide, the inventory of prestressed bridges has proportionally fewer deficient structures (15.1%) than the total inventory (21.4%). This should be expected since prestressed concrete is a relatively durable material and the average age of the prestressed inventory is younger than the inventory as a whole.
- District 11 has a greater proportion of prestressed bridges (37.7%) than the statewide inventory (23.3%).
- District 11 reports a greater proportion of deficient structures (28.4%) than the statewide inventory. Additionally, the proportion of prestressed bridges reported as being deficient in District 11 (28.0%) is comparable to the total inventory deficient in this district (28.4%). However, the majority of deficient structures in District 11 are not rated as deficient based on their superstructure condition and District 11 has essentially the same proportion of deficient prestressed superstructures as the statewide inventory (7.8% in each case).
- Four bridge types dominate the prestressed inventory: simple, noncomposite adjacent box beams (14% of prestressed inventory statewide and 10% in District 11); simple composite I-beams (22%/25%); simple composite multi-box beams (33%/26%); and simple composite adjacent box beams (19%/14%).
- Considering only prestressed bridges rated deficient based on their superstructure rating, noncomposite adjacent box beams represent the majority of such bridges (40% of such bridges are deficient statewide representing 71% of the deficient prestressed structures in the state). Composite I-beam, adjacent box beam and multi-box beams also represent

large numbers of such deficient bridges. The trends and the dominance of these four bridge types are similar when considering District 11 only.

Based this review, 28 bridges from District 11 were selected for an in-depth review of their inspection reports in order to assess the nature of damage resulting in a 'structural deficient' superstructure rating. As indicated in Table 3-1, five bridge types[1], reflective of the District 11 inventory, were selected. Initially, 22 bridges (Bridges A – H in Table 3-2) were selected based on: a) having a superstructure rating less than 4; and b) having low reported clearance over a roadway. The latter criterion was selected to ensure some vehicle impact damage would be present in the sample. Five additional bridges having known vehicle impacts were added (Bridges J – P). Finally, the collapsed Lake View Drive bridge (Harries 2006) from District 12 was also added (Bridge LV). Table 3-2 summarizes the 29 bridges selected for further study. The bridges have been assigned an alphanumeric identification as shown in Table 3-2 which will be adopted for clarity in further reporting and to obscure the identity of the in-service bridges.

3.2 SOURCES OF DAMAGE TO PRESTRESSED CONCRETE GIRDERS

Observed ***sources*** damage to prestressed concrete girders are classified as indicated in Table 3-3. Vehicle impact damage (Source I) was the basis for bridge selection and is thus disproportionately represented in the sample. As of July 16, 2008, only 18 bridges in District 11 were listed as having undergone significant damage from vehicle impact; 7 of these were

[1] There is some confusion in the inventory. 'Simple noncomposite multi-box beams' are reported although there is not believed to be such a structure type. It is believed that this classification represents a mis-classification either 'simple composite multi-box beams' or 'simple noncomposite adjacent box beams'.

prestressed concrete structures. Impact damage (Figures 3-1 to 3-5) ranges from significant loss of section and reinforcing (Figure 3-1), which was not observed in the bridges investigated, to minor 'scrape' marks on the bridge soffit (Figure 3-2). Impact may result in spalling, typically resulting in exposed (although rarely damaged) strands (Figures 3-3 and 3-4). Feldman et al. (1996) identified a commonly occurring damage pattern associated with side impact. The impact causes a torsion-induced shear cracking pattern in the exterior (or fascia) girder as shown in Figure 3-5. This was observed in Bridge P, reviewed for this study (Figure 3-5).

The most common source of damage observed results from 'environmental distress' and simple aging of the structure coupled with limited or inadequate maintenance (Source II). Chloride intrusion resulting from the use of road salt is the most significant environmental stressor. Chloride-laden water from the bridge surface may affect the bridge deck, sides of the bridge and soffit region where no 'drip strips' are present (Figure 3-6). Additionally, chlorides may be introduced into regions assumed to be 'protected' as a result of leaking expansion joints and drain systems (Figure 3-7). Deterioration of shear keys in adjacent box girders (observed in the Lake View Drive bridge (Harries 2006)) and anecdotally throughout southwestern Pennsylvania[2]) results in chloride laden water accessing all webs and most of the soffit (Figure 3-6). Spray from trucks travelling beneath the bridge may introduce additional chloride-laden water to the underside of the bridge superstructure. Although not an issue in the present study, bridges located near an ocean environment are also subject to enhanced chloride attack. Related to the presence of water (whether chloride-laden or not) is the potential for damage associated with freezing and thawing cycles. Such freeze/thaw damage in prestressed structures typically requires other damage to be present (allowing water ingress) before initiating.

[2] Many noncomposite adjacent box girders display icicles between their beams during winter. These icicles are often 'stained' indicating some degree of active corrosion.

Improper retrofit or repair practices can initiate damage (Source III). For example, a concrete patch having a lower chloride content than the adjacent concrete can result in the formation of a localized corrosion cell at the patch interface resulting in accelerated corrosion in this region even without further chloride load (as the chloride ions migrate from the older concrete into the patch). This source of damage is most commonly observed on patched decks. Another damage source (IV) associated with bridge retrofit was observed where a barrier rail system was replaced and the original bolted attachment locations not patched. This led to local spalling as shown in Figure 3-8. Additionally, the possibility that the new rail mounting (Figure 3-8a) is drilled through a strand or may cause future spalling cannot be discounted.

Inadequate maintenance practices may not be a primary source of damage; however they will exacerbate existing damage (Source V). Clogged drain systems, exposed strands, concrete that remains un-patched and clogged weep holes are all maintenance issues that must be corrected before further damage results. For example, weep holes in the adjacent box girders of the Lake View Drive Bridge (Harries 2006) were clearly clogged as evidenced by significant water residing in the beam voids (collapsed void forms can be seen in Figure 3-9). This internal water may affect chloride attack of the girder soffit from the top-down (not observed in the Lake View Drive bridge) and adds an unaccounted-for dead load to the girder.

Construction error (Source VI) may result in bridge damage if uncorrected. Minor errors may exacerbate degradation from other sources. For example, Figure 3-9 shows that some strands in the Lake View Drive Bridge had only one half of their prescribed 1.5 inch concrete cover. Such misplacement results in less protection to the steel from chloride intrusion and is likely to exacerbate spalling.

Bridges may be damaged by overload (Source VII) or extreme events (Source VIII). Such loads may be from overloaded or oversized vehicles or from natural causes including seismic effects (Figure 3-10a) or floods. In general, damage flood-borne debris will be similar to that caused by vehicle impact but may be located anywhere in the bridge depth. No such damage was observed in the present study. Bridges may also be damaged by fire (Figure 3-10b). Due to the nature of such damage, bridges affected by fire should be assessed on a case-by-case basis. Fire damage is beyond the scope of the present work.

3.3 TYPES OF DAMAGE TO PRESTRESSED CONCRETE BRIDGE GIRDERS

Observed ***types*** of damage to prestressed concrete girders are classified as indicated in Table 3-4. This classification may be interpreted as a damage continuum. Left uncorrected, less significant damage types (Types i and ii) will progress to becoming more significant (Types iii to v) as corrosion becomes manifest. Eventually corrosion will lead to section loss of the strand (Types vi and vii) and resulting loss of prestress and member capacity. Figure 3-11 schematically illustrates this continuum of corrosion damage. In general, the progression of corrosion-related damage tends to be exponential in time. Repairing such ***types*** of damage must be accompanied my mitigating the ***source*** of the damage where possible.

Mechanical damage resulting in strand rupture may also result from significant impact events (Type viii) or other overloads (Types ix to xi), although the latter are rare and not generally observed in the present study. It should be noted that the load tests carried out on girders recovered from the Lake View Drive Bridge (Harries 2006) resulted in examples of both shear (Type ix) and flexural (Type x) damage as shown in Figures 3-12 and 3-13, respectively.

Longitudinal cracking (Type xi) may result from impact (Fig. 3-5) or from corrosion of reinforcement prior to spalling. The latter will generally be accompanied by staining.

Table 3-1 Summary of statewide and District 11 prestressed bridge inventory.

	Structure Type Code	Statewide			District 11[1]			bridges considered for further study[5]	
		No.	SD (rating < 4)		No.	SD (rating < 4)			
			Any[2]	Super		Any[2]	Super	review	design
all bridges[3]	xxxxx	25203	5385 (21.4%)	3465 (13.7%)	1781	505 (28.4%)	318 (17.9%)		
all prestressed[4]	4xxxx	5874 (23.3%)	887 (15.1%)	456 (7.8%)	671 (37.7%)	188 (28.0%)	52 (7.8%)		
simple, noncomposite slab	4x101	42	3 (7%)	2 (5%)	0	0	0		
simple, noncomposite hollow slab	4x102	4	2 (50%)	0	4	2 (50%)	0		
simple, noncomposite I beam	4x104	56	16 (29%)	1 (2%)	29	15 (52%)	0	2	x
simple, noncomposite multi-box beam[8]	4x106	84	20 (24%)	11 (13%)	41	16 (39%)	9 (22%)	9[6]	x
simple, noncomposite adjacent box beam	4x107	821 (14%)	350 (43%)	326 (40%)	69 (10%)	19 (28%)	14 (20%)	6	x
simple, composite slab	4x201	55	1 (2%)	0	6	0	0		
simple, composite I beam	4x204	1275 (22%)	173 (14%)	29 (2%)	167 (25%)	59 (35%)	9 (5%)	4	
simple, composite multi-box beam	4x206	1921 (33%)	214 (11%)	55 (3%)	177 (26%)	53 (30%)	12 (7%)	5	
simple, composite adjacent box beam	4x207	1110 (19%)	95 (9%)	29 (3%)	95 (14%)	17 (18%)	8 (8%)	3	
simple, composite other	4x299	3	1 (33%)	0	1	0	0		
continuous, noncomposite I beam	4x304	5	0	0	3	0	0		
continuous, noncomposite multi-box beam[8]	4x306	1	0	0	0	0	0		
continuous, noncomposite adjacent box beam	4x307	1	0	0	0	0	0		
continuous, composite I beam	4x404	210	7 (3%)	0	50	7 (14%)	0		
continuous, composite multi-box beam	4x406	197	0	0	20	0	0		
continuous, composite adjacent box beam	4x407	65	1 (2%)	0	9	0	0		
other I beam	4x504/804	6	1 (17%)	0	0	0	0		
other multi-box beam	4x806	5	0	0	0	0	0		
other adjacent box beam	4x807/907	10	3 (30%)	3 (30%)	0	0	0		
other	4xxxx	2	0	0	0	0	0		

[1]Allegheny, Beaver and Lawrence Counties
[2]Deck, Superstructure and Substructure only (culverts not considered)
[3]data from September 10, 2007
[4]prestressed data from: statewide: February 12, 2008; District 11: December 26, 2007
[5]only bridges from District 11 were considered for further study
[6]more 4x106 bridges were selected for review as many had vertical clearance issues
[7]includes Lake View Drive Bridge.
[8]there is not believed to be such a structure as a *noncomposite multi box beam*. It is believed that this classification represents a mis-classification either *simple composite multi-box beams* (4x406) or *simple noncomposite adjacent box beams* (4x107).

Table 3-2 Bridges Selected for further investigation of inspection records.

ID	Structure Type		Min Vert. Clear (ft)	Year		Rating			Suff. Rate
				Built	Recon.	Deck	Super	Sub	
A	S-NC-multi box beam	42106[1]	17.25	1962	1976	5	3	4	27.1
A	S-NC-multi box beam	42106[1]	[2]	1962	1976	5	3	4	27.1
A	S-NC-multi box beam	42106[1]	[2]	1962	1976	5	3	4	27.1
A	S-NC-multi box beam	42106[1]	53.00	1962	1976	5	3	4	27.1
B	S-NC-multi box beam	42106[1]	[2]	1967	-	4	4	4	47.3
B	S-NC-multi box beam	42106[1]	14.58	1967	-	4	4	4	47.3
C	S-NC-multi box beam	42106[1]	[2]	1963	-	5	4	4	49.0
C	S-NC-multi box beam	42106[1]	14.42	1963	-	5	4	4	49.0
C	S-NC-multi box beam	42106[1]	14.42	1963	-	5	4	4	49.0
D	S-NC-adjacent box beam	42107	[2]	1957	-	4	3	5	41.3
D	S-NC-adjacent box beam	42107	10.00	1957	-	4	3	5	41.3
E	S-NC-adjacent box beam	42107	[2]	1901	1957	5	4	5	22.7
E	S-NC-adjacent box beam	42107	8.00	1901	1957	5	4	5	22.7
F	S-C-I beam	42204	32.00	1969	-	3	4	4	63.1
F	S-C-I beam	42204	32.00	1969	-	3	4	4	63.1
F	S-C-I beam	42204	[2]	1969	-	3	4	4	63.1
G	S-C-multi box beam	42206	14.75	1973	-	3	4	4	56.5
G	S-C-multi box beam	42206	14.75	1973	-	3	4	4	56.5
G	S-C-multi box beam	42206	[2]	1973	-	3	4	4	56.5
G	S-C-multi box beam	42206	[2]	1973	-	3	4	4	56.5
H	S-C-adjacent box beam	42207	15.58	1966	-	3	4	3	33.0
H	S-C-adjacent box beam	42207	[2]	1966	-	3	4	3	33.0
H	S-C-adjacent box beam	42207	15.58	1966	-	3	4	3	33.0
J	S-C-multi box beam	42206	15.00	1988	-	-	5	-	80.0
K	S-NC I beam	42104	14.42	1970	-	-	5	-	63.6
M	S-NC I beam	42104	15.92	1971	-	-	5	-	43.6
N	S-C-I beam	42204	14.42	1970	-	-	5	-	48.8
P	S-NC-adjacent box beam	42107	-	-	-	-	-	-	-
LV	S-NC-adjacent box beam	42107	14.50	1961	-	-	-	-	-

[1]there is not believed to be such a structure as a *noncomposite multi box beam*. It is believed that this classification represents a mis-classification either *simple composite multi-box beams* (42406) or *simple noncomposite adjacent box beams* (42107).

[2]bridge does not pass over active roadway.

S = simple; NC = noncomposite; C = composite

Table 3-3 Sources of Observed Damage.

Damage Source	Description	Representative Photograph(s)	Bridges where observed
I	Impact by over height vehicle	Figs. 3-1 to 3-5	A, C, J-P & LV
II	Environmental Distress/Aging including freeze-thaw and water-induced	Figs. 3-6 and 3-7	A, E, F, G, H, N & LV
III	Construction error or poor practice associated with previous repair	-	H & LV
IV	Construction error associated with appurtenance mounting	Fig. 3-8	C & E
V	Poor maintenance practice	Figs 3-7 and 3-8	A, C, E, F, H & LV
VI	Construction error	Fig. 3-9	LV
VII	Load-related damage (other than impact), including effects of natural disasters	Figs. 3-12 and 3-13	E
VIII	Extreme events such as natural disaster and fire	Fig. 3-10	none

Table 3-4 Types of Observed Damage.

Damage Type	Observed Damage	Representative Photograph(s)	Bridges where observed	Damage Source
i	Concrete spalling	Fig 3-11	A, C, D, E, F, G & LV	all
ii	Exposed prestressing strands		A, C, D, E, F, G, K, N & LV	all but VI
iii	Corroded prestressing strand without pitting		A, E, J, N & LV	all but VI
iv	Corroded prestressing strand with light pitting		A, LV	all but VI
v	Corroded prestressing strand with heavy pitting		A, LV	all but VI
vi	Partial loss of strand area due to corrosion (rupture of individual wires)		A, LV	all but VI
vii	Complete loss of strand area due to corrosion		A, LV	all but VI
viii	Strand rupture associated with load or impact	Figs 3-3 – 3-4	K, N &LV	I, IV, VII & VIII
ix	Shear cracking of girder	Fig. 3-12	C, G & LV	I, VI, VII &VIII
x	Flexural cracking of girder	Fig. 3-13	none	VI, VII & VIII
xi	Longitudinal cracking of girder	Figs 3-3(c) and 3-5	J, N & P	I, II, VII,& VIII

Figure 3-1 Loss of section of AASHTO girder due to vehicle impact (Harries; not taken in PA).

Figure 3-2 Scraping due to minor vehicle impact
(Lake View Drive Bridge prior to collapse; PennDOT and Harries 2006).

(a) damage to girder soffit.

(b) close up view of (a) showing severed strands.

(c) longitudinal cracking resulting from impact.

Figure 3-3 Impact damage to I beam (PennDOT).

Figure 3-4 Exposed and ruptured strand due to vehicle impact (Lake View Drive Bridge; Harries 2006).

(a) following vehicle impact (PennDOT).

(b) typical impact damage pattern (PennDOT).

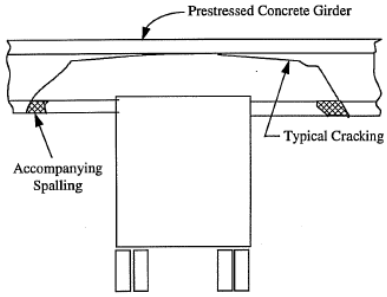

(c) typical impact damage due to side impact (Feldman et al. 1996).

Figure 3-5 Vehicle impact due to collision.

(a) water coming down exterior face of adjacent box girder (Harries 2006).

(b) water leaking between adjacent box girders (PennDOT).

Figure 3-6 Evidence of water on soffits of adjacent box girders.

(a) water pooling due to clogged deck drain (PennDOT).

(b) damaged drain system resulting in water affecting superstructure (PennDOT).

Figure 3-7 Water from unanticipated sources.

(a) spalling at original attachment and possible future damage at sight of new attachment.

(b) unpatched holes at sight of original attachment result in exposed strands.

Figure 3-8 Damage to strands caused by relocating barrier supports (PennDOT).

¾" center of strand to soffit

inconsistent spacing

Figure 3-9 Girder with insufficient cover and inconsistent strand spacing (Lake View Drive Bridge; Harries 2006).

(a) earthquake (FEMA). (b) fire (SIKA Corporation).

Figure 3-10 Damage due to extreme events-beyond the scope of the present study.

(a) concrete spalling.

(b) exposed strands without corrosion (Fig. 3-8b).

(c) corrosion without pitting (strand intentionally cut).

(d) corroded strand with light pitting

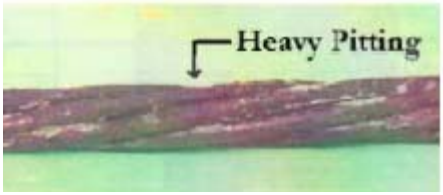

(e) corroded strand with heavy pitting.

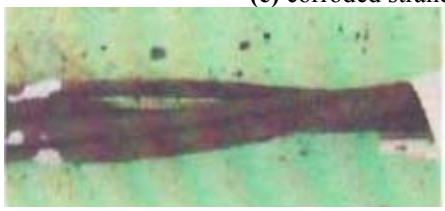

(f) partial loss of strand area.

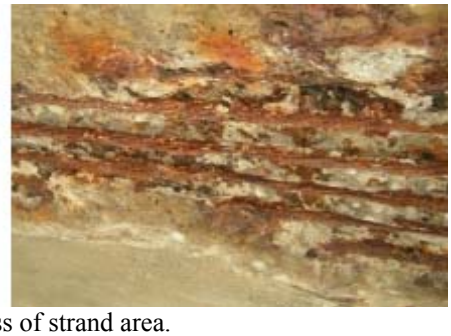

(g) complete loss of strand area.

Figure 3-11 Continuum of corrosion damage (Naito et al. 2006; Harries 2006).

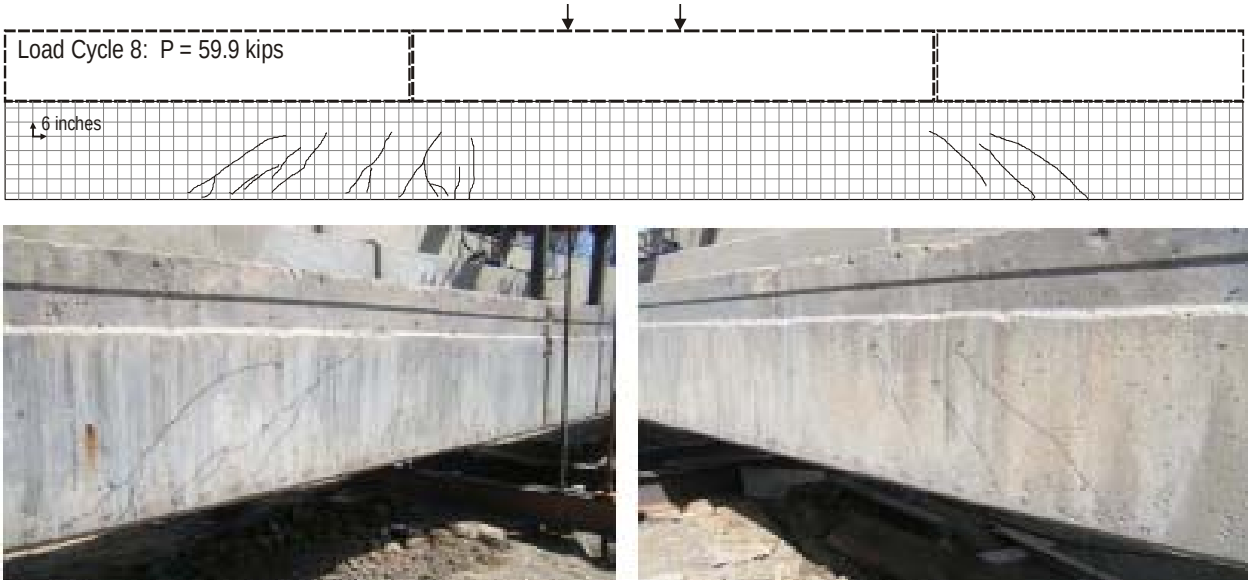

Figure 3-12 Representative shear distress (Lake View Drive EXTERIOR test girder; Harries 2006).

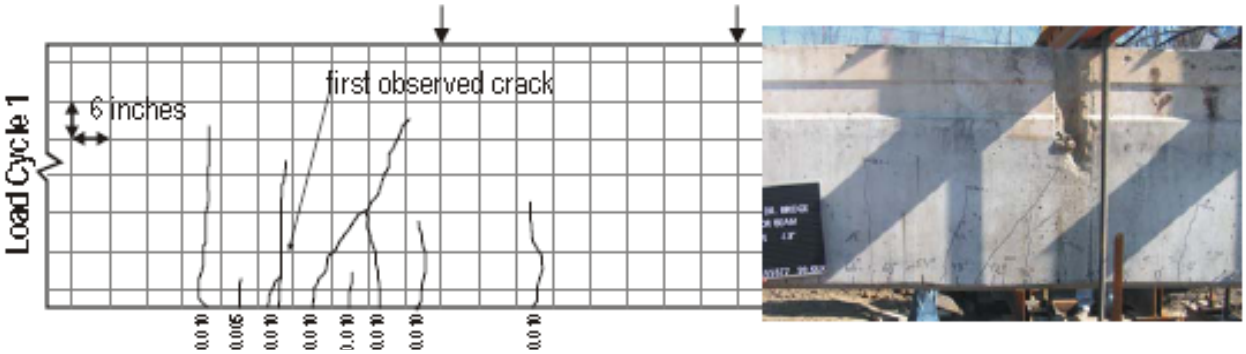

Figure 3-13 Representative flexural distress (Lake View Drive INTERIOR test girder; Harries 2006).

4.0 PROTOTYPE PRESTRESSED GIRDER SELECTION

It was initially anticipated that specific bridges would be used as prototype structures for repair, however, based on the inventory review (Chapter 3) it was decided that prototypes will be prepared having greater damage than has been reported on any of the bridges investigated (Table 3-2). For simplicity, only simply supported, non-composite prototypes are considered. There are few continuous prestressed bridge elements and the nature of repair techniques will not generally be affected by whether the structure is composite or non-composite. Based on the Chapter 3, only three bridge types will be considered: a) Adjacent box beams (AB); b) Multi-box (spread box) beams (SB); and c) I-beams (AASHTO-type beams) (IB). Cross sections of the prototype girders used for the repair designs are shown in Figures 4-1, 4-2 and 4-3, respectively. These prototypes are based on the as-built details of bridges LV, A and K, respectively as reported in Table 3-2 and will be described in greater detail in Chapter 5.

4.1 DAMAGE CLASSIFICATION

The NCHRP 12-21 study (Shanafelt and Horn 1980 and 1985) established three damage classifications: minor, moderate and severe. These are defined in Section 2.1. Based on the potential for more effective retrofit of more heavily damaged members, a further division of the 'severe' category is proposed as follows:

MINOR Concrete with shallow spalls, nicks and cracks, scrapes and some efflorescence, rust or water stains. Damage at this level does not affect member capacity. Repairs are for aesthetic or preventative purposes.

MODERATE Larger cracks and sufficient spalling or loss of concrete to expose strands. Damage does not affect member capacity. Repairs are intended to prevent further deterioration.

SEVERE I Damage requires structural repair that can be affected using a non-prestressed/post-tensioned method. This may be considered as repair to affect the strength (or ultimate) limit state (ULS).

SEVERE II Damage requires structural repair involving replacement of prestressing force through new prestress or post-tensioning. This may be considered as repair to affect the service limit state (SLS) in addition to the ultimate limit state (ULS).

SEVERE III Damage is too extensive. Repair is not practical and the element must be replaced.

Damage may be quantified in a variety of ways. Table 4-1 may be viewed as a guide for both selecting a method by which to quantify damage to prestressed members and for quantifying the damage. The entries are tentative at this time; based on the findings of the repair scenarios presented and additional parallel studies values will be proposed. Nonetheless, it is informative to describe the approach to damage quantification.

Defining damage based on the number of strands lost is not felt to be rational in so far as this value does not take into account the contribution of an individual strand to the member capacity. That is; 4 strands missing from a girder having only 16 strands is significant, whereas 4 strands missing from a girder having 72 strands may not require immediate repair. Classification by girder deflection, while likely an excellent indicator of performance, is felt to be impractical to establish in the field. Attention will be focused on live load and ultimate capacity replacement.

Washington State DOT (2008) has provided limited guidance as to when girder replacement is required. This guidance would correspond to the threshold between SEVERE II and SEVERE III. Replacement is required in cases where:

1. Over 25% of the strands have been severed.
2. The bottom flange is displaced from the horizontal position more than ½" per 10' of girder length.
3. If the alignment of the girder has been permanently altered by the impact.
4. Cracks at the web/flange interface remain open.
5. Abrupt lateral offsets may indicate that stirrups have yielded.
6. Concrete damage at harping point resulting in permanent loss of prestress.
7. Severe concrete damage at girder ends resulting in permanent loss of prestress.

Items 3-7 are additional qualitative considerations for determining SEVERE III level damage.

4.2 REPAIR EXAMPLE SELECTION

Based on the review of repair methodologies available and the proposed damage classification, a 'flow chart' of appropriate repair methods was established for each type of beam

considered, adjacent box (AB), multi-box (SB) and AASHTO girder (IB). These flow charts are shown in Figure 4-4. The resulting matrix of repair examples is shown in Table 4-2. Three variants of non-prestressed CFRP, one variant of prestressed CFRP, one variant of post-tensioned CFRP, one variant of strand splicing and one variant of external steel post-tensioning will be demonstrated in examples presented in the following chapter.

The viable selections outlined in Figure 4-4 were developed based on some practical considerations of girder and retrofit geometry. For example, due to the large dimension of the splices and the need to stagger splices is felt that strand splicing is only marginally applicable in sections having relatively thin wall or flange dimensions (box girders). Such splices would be more appropriate for prestressed slabs having only a single layer of strands and reasonable cover dimensions.

No example of steel jacketing is provided. This method is felt to be very cumbersome to apply in the field and offers no advantages over the non-corrosive, lighter and easier to apply CFRP systems. An example of a steel jacket design is provided in Shanafelt and Horn (1980).

All repair approaches should also include mitigation of the damage source, the adoption of passive or active corrosion mitigation measures and finally concrete patching. These steps are shown in Figure 4-4 but are beyond the scope of the present work.

Table 4-1 Proposed damage classifications.

Damage Classification	**SEVERE I**	**SEVERE II**	**SEVERE III**
Repair philosophy	ULS only	ULS and SLS	-
Action	non PT repair	PT repair	replace
Live load capacity replacement	up to 5%	up to 30%	100%
Ultimate load capacity replacement	up to 8%	up to 15%	100%
Replace lost strands	2-3 strands	up to 8 strands	>8 strands
Deflection	loss of camber	up to 0.5%	>0.5%

Table 4-2 Repair Examples.

Beam	**Damage**	**Retrofit**
Adjacent Box Beam	4-0-0 & 8-2-1	Non-prestressed preformed CFRP strip
	8-2-1	Prestressed CFRP strips
	8-2-1	Post-tensioned CFRP strips
Spread Box Beam	4-0-0 & 8-2-1	Non-prestressed preformed CFRP strip
	8-2-1	Prestressed CFRP strips
	8-2-1	Post-tensioned CFRP strips
AASHTO I-girder	4-0-0	Strand Splice
	4-0-0, 6-2-1 & 10-2-1	Non-prestressed CFRP fabric
	4-0-0, 6-2-1 & 10-2-1	Non-prestressed NSM CFRP
	4-0-0, 6-2-1 & 10-2-1	Prestressed CFRP strips
	4-0-0, 6-2-1 & 10-2-1	Post-tensioned CFRP strips
	6-2-1 & 10-2-1	External steel post-tensioning

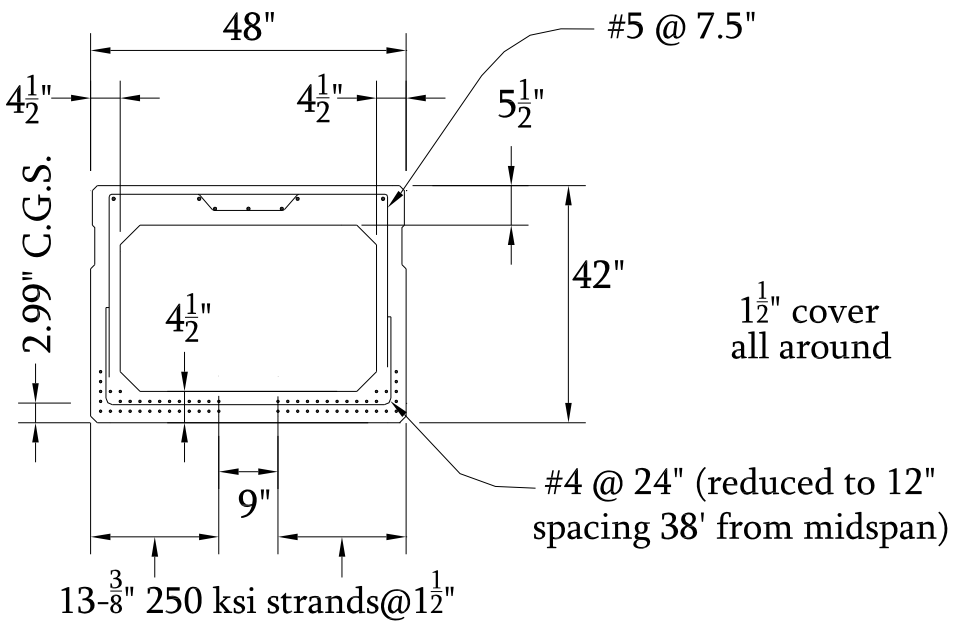

Figure 4-1 Prototype AB girder cross section.

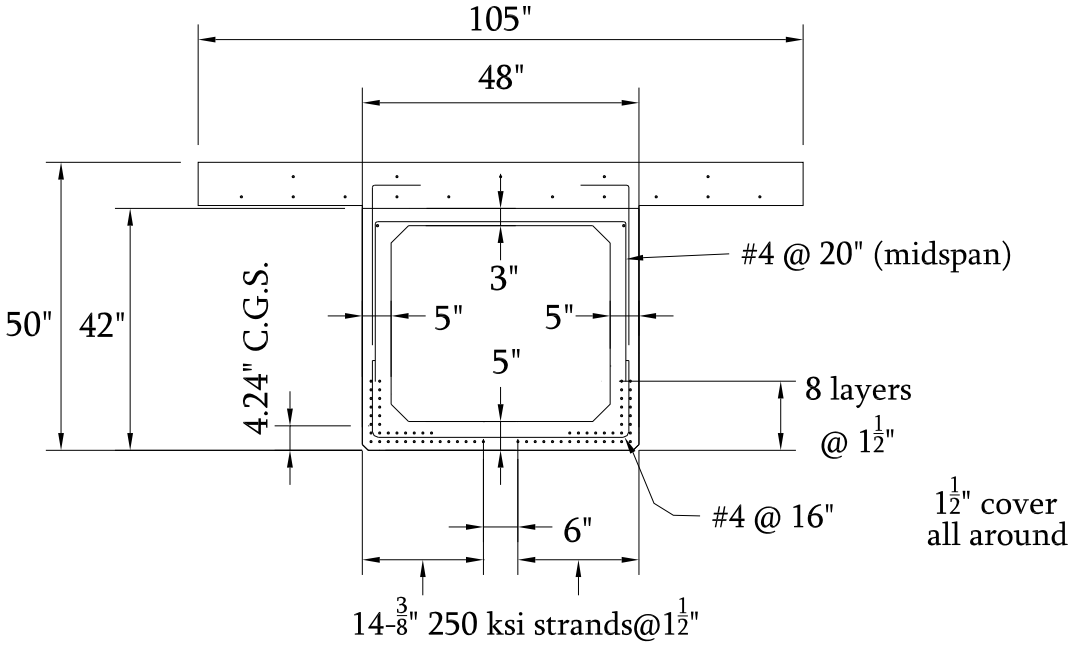

Figure 4-2 Prototype SB girder cross section.

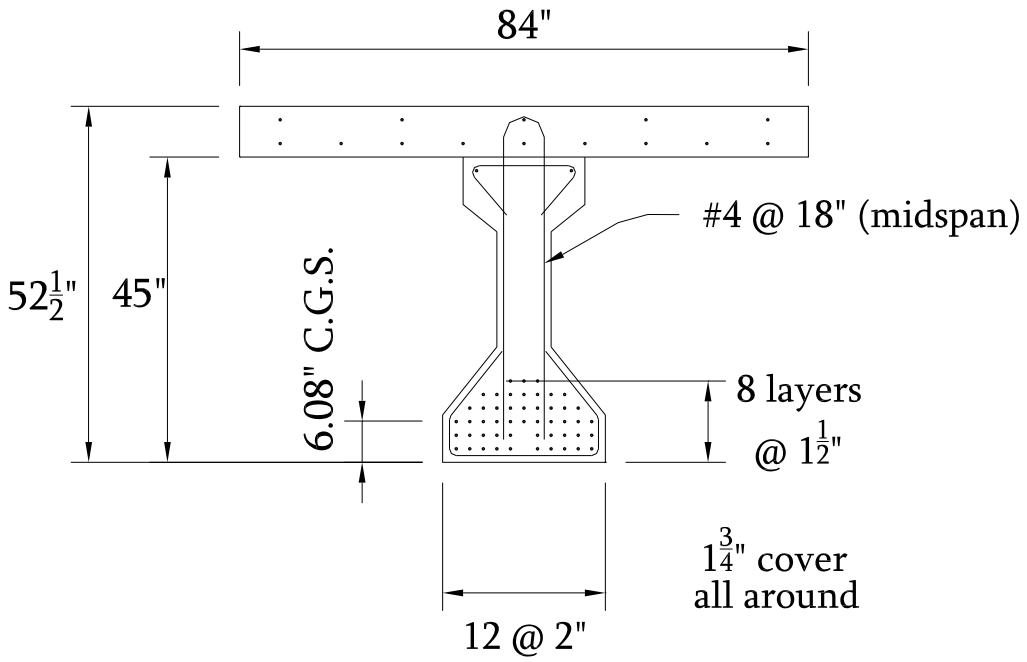

Figure 4-3 Prototype IB girder cross section.

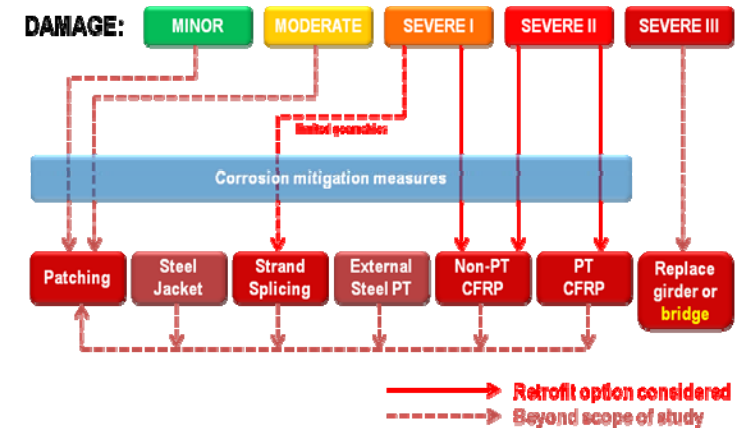

(a) Adjacent box girders

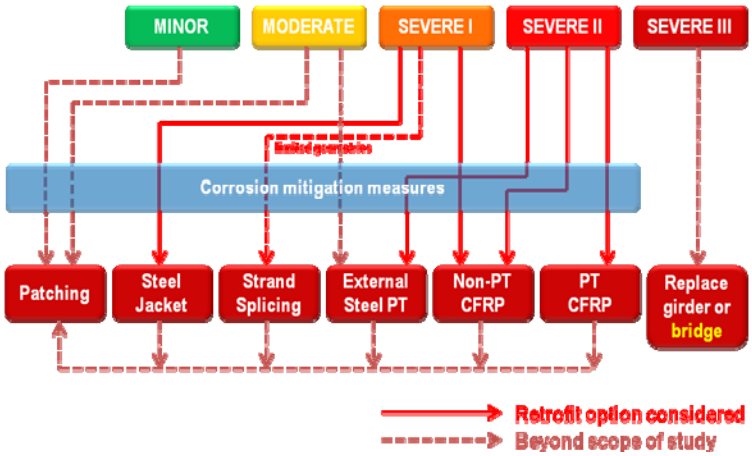

(b) Multi-box beam

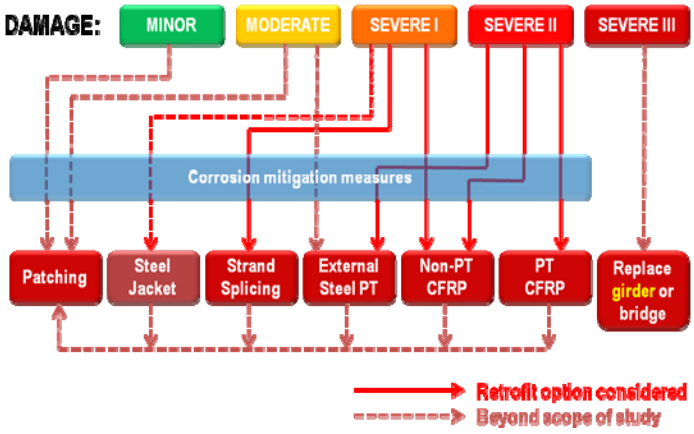

(c) I-beam

Figure 4-4 Flow charts illustrating viable retrofit techniques based on level of damage.

5.0 PROTOTYPE REPAIR DESIGNS

This chapter describes prototype repair designs which include CFRP repairs, strand splicing and steel post tensioning repairs. CFRP repairs are designed primarily using ACI 440.2R-08 *Guide for the Design and Construction of Externally Bonded FRP Systems for Strengthening Concrete Structures* (ACI 2008) as a guide and are based on strain compatibility of the section. Comparable strand splicing and steel post-tensioning repairs are designed using the previously established guidance provided by the NCHRP 12-21 project (Shanafelt and Horn 1985). The objective of this section is to provide design examples where the repair is intended to restore the section flexural capacity of a damaged prestressed girder. The repair method chosen for each girder type and damage is outlined in Table 4-2.

5.1.1 Materials

Section geometry and material properties of the prototype girders are compiled in Table 5-1. CFRP repair materials and post-tensioning steel material properties are compiled in Tables 5-2 and 5-3, respectively. The material strengths and girder geometries used are based on representative/prototype structures LV, A and K as described in Chapter 4. CFRP material and geometric properties are based on manufacturer's data for Sika CarboDur strips (preformed CFRP strips) (Sika 2008a) and SikaWrap Hex 103C (unidirectional CFRP 'fabric') materials.

Data for SikaWrap assumes the use of with Sikadur Hex 300 epoxy (Sika 2008c). Post-tensioning steel material and geometric properties are based on the use of 150ksi Williams all thread bar (Williams 2008). These properties were used for convenience; the use of Sika or Williams products is not specifically endorsed in this document.

5.1.2 Assumptions and Simplifications

For the analysis and repair of the girders some assumptions and simplifications have been made to allow generalized representative designs to be prepared. It is noted that every structure is different and all designs must consider local conditions and circumstances.

All prototype girders are interior girders. It is understood that impact damage is more likely to occur on the exterior girders, but the inclusion of barrier walls complicates the analysis (Harries 2006), clouding the issues relevant in the present work. The main goal is to provide repair designs and model the repaired girder in order to verify the strength of the repair. Therefore, all girders modeled have been considered to be interior and have not included barrier walls. A parallel study (Russell 2009) has as its objective simplifying the analysis of exterior girders so that a simple plane sections approach (as is applied here) may be used for exterior girders subject to biaxial bending.

The design method of FRP repairs accounts for the initial state of the girder by including the strain distribution present at the time of FRP installation in design calculations. The state of strain at the soffit at this time is assumed to be only the strain due to the dead load of the structure. In field applications, additional loads may be presented which need to be included in the calculation of initial strain conditions. Due to limitations of the plane-sections analysis program *XTRACT* (see following section), it is not possible to correctly account for the initial

soffit strain for the CFRP repairs. Therefore, the moment curvature plots created for the CFRP repairs are not representative at load levels below the dead load of the structure (of course, the structure will never be subject to loads below this level).

The damage, modeled by removing strands from the section, was chosen to mimic truck impact damage. Strands are removed from the exterior bottom corner and progress inward (this is discussed later in Section 5.1.4). As a result, the section is no longer symmetric and a rotation of the neutral axis occurs resulting a torsional moment being introduced to the girder. Harries (2006) has shown that the effect of this torsional moment is negligible for interior girders (although it can be significant for exterior girders having composite barrier walls). Additionally, the presence of adjacent girders and the coupling effect of the slab further negate the effects of torsion on interior girders. The analyses presented in this document do not account for girder twist.

5.1.3 XTRACT Program

XTRACT is the commercial version of the University of California at Berkeley program *UCFyber* (Chadwell and Imbsen 2002). *XTRACT* is a biaxial nonlinear fiber element sectional analysis program. As it is biaxial (2D in the parlance of this report), it permits the input of any section shape. While *XTRACT* can perform moment-curvature (M-φ) and axial load-moment interaction (P-M) analyses about the traditional horizontal (x) and vertical (y) axes. Its "orbit analysis" tool additionally permits a M_{xx}-M_{yy} failure surface to be generated based on specified failure criteria. Only moment-curvature analyses are presented in this work.

XTRACT provides both customizable analysis reports and an interactive mode to view results. A strong graphical component allows the user to see the outcome of their analyses.

Finally, all data is easily exported in text format for further processing. *XTRACT* is not able to run 'batch jobs' and thus multiple scenarios (as done for this study) require individual runs and data processing. The ease of use (particularly in editing models) of *XTRACT* however makes up for the necessity of this 'brute force' approach for multiple analyses.

The sections analysis design methodology for FRP repair systems is based on strain compatibility and does not consider beam curvature. In modeling the repair designs for the FRP systems, for convenience the target repair capacity has been determined based on the moment capacity at a selected curvature, $\varphi = 0.00015$. Because the objective is to consider ultimate capacity, the maximum capacity of the repaired girder, determined from a fiber section analysis (*XTRACT*), is presented in Table 5-4. The ultimate curvature at which this value is achieved is also reported in Table 5-4. The ultimate curvature in all CFRP analyses presented is determined by CFRP debonding failure. While the ultimate curvature varies considerably, all reported values continue to represent a reasonable degree of ductility (see moment-curvature plots in this chapter, i.e. Figure 5-3).

5.1.4 Girder Damage

It is assumed that the most significant damage is related to truck impact. Thus it is appropriate to remove strands beginning at the exterior web-soffit corner and move inward across the soffit of the girder. Even if truck impact is not the source of damage, removing strands in this manner is rational since it represents a worst-case scenario (Harries 2006).

In the analyses to follow, strands were removed from the lower three layers only. The three-digit identification of each analysis indicates the number of strands ***removed*** from the lower, second and third layers, respectively. Thus, IB 6-2-1 indicates 6 strands removed from the

lower layer, 2 from the second and 1 from the third, for a total of 9 strands removed from the I-beam section (Figure 4-3). In all cases the strands were removed from the exterior face and moved inward. An example is shown in Figure 5-1. Table 5-4 lists all cases considered. In Table 5-4, the nominal capacity of the damaged girders is given along with the nominal capacity of the undamaged girder. The objective of all repairs is to restore the undamaged girder capacity. Figures 4-1 through 4-3 show the girder prototypes and their strand arrangement.

5.1.5 Bridge Loading

Bridge load calculations were completed according to AASHTO LRFD (2007) specifications and are compiled in Tables 5-5 to 5-8 for the various girder types. Loads are calculated based on the HS-25 vehicle. It is suggested that in adjacent box (AB) beam bridges with inadequate or damaged shear keys that a moment distribution factor of g = 0.50 be used (Harries 2006). Table 5-6 shows this case and illustrates the potential difference between the assumed load distribution, where the distribution factor is approximately g = 0.30 (Table 5-5) and *possible in situ* conditions (Table 5-6). Most bridges reviewed in this study were originally built around 1960, therefore the bridges were originally designed for a lower HS-20 loading according to the 1960 AASHO Specifications. The HS-20 and HS-25 loads are shown in Tables 5-5 through 5-8 to contrast the difference between current rating loads and original design loads. Select load levels from these tables are superimposed onto the repaired girder moment-curvature plots presented later.

5.2 NON PRESTRESSED PREFORM CFRP STRIP REPAIRS

Non-prestressed CFRP strip repairs assume the use of Sika CarboDur strips (Table 5-2). The explanation of the repair design is best seen via example. This example illustrates the necessary steps in designing a CFRP repair as well as provides a brief explanation of each step. All equations, equation numbers and clause references shown in the example are from ACI 440.2R-08 unless noted otherwise. The girder and damage considered for this example repair is the AB 4-0-0 case. Subsequent cases refer to the steps described in this example and identify appropriate modifications. A summary of the parameters, intermediate values obtained during the calculations and results of this repair are shown in Table 5-9. Schematic drawings of the resulting repair are presented in Figure 5-2. Non-prestressed perform CFRP strip repairs have been modeled using *XTRACT* and the moment-curvature plots are shown in Figures 5-3 and 5-4.

5.2.1 Design Example AB 4-0-0

The design example is presented below. A brief description of each step and the associated equations are provided in the left column. The calculations associated with AB 4-0-0 are provided in the right column. All subsequent CFRP designs use the approach presented with some modification as indicated in the sections to follow.

In the following example, the capacity of the damaged AB 4-0-0 is 3160 k-ft (Table 5-4). The objective of the repair is to restore the undamaged nominal moment capacity of the girder: 3395 k-ft (Table 5-4).

Procedure	Calculation
Define objective of repair. For all examples discussed, the objective is to restore the undamaged moment capacity, M_u. Values of M_u and the capacity of the damaged girders are given in Table 5-4.	Restore undamaged moment capacity: $M_n = 3395\ k\text{-}ft$ Capacity of damaged girder without repair: $M_{n\ 4\text{-}0\text{-}0} = 3160\ k\text{-}ft$
Step 1: Calculate the FRP system design material properties. The repair is of a bridge girder exposed to the elements. Per ACI Table 9.1, a reduction factor, C_E, of 0.85 is suggested. $f_{fu} = C_E f^*_{fu}$ $\varepsilon_{fu} = C_E \varepsilon^*_{fu}$	$f_{fu} = 0.85 \times 406ksi = 345ksi$ $\varepsilon_{fu} = 0.85 \times 0.017in/in = 0.0145in/in$
Step 2: Assemble beam properties. Assemble geometric and material properties for the beam and FRP system. An estimate of the area of FRP (A_f) is chosen here. If the section capacity does not meet the demand after the completion of all steps in this procedure, the FRP area is iterated upon.	$E_c = 6800\ psi$ $A_{cg} = 786\ in^2$ $h = 42\ in$ $d_p = 38.91\ in$ $y_t = 20.59\ in$ $y_b = 21.41\ in$ $e = 18.28\ in$ $I = 204000\ in^4$ $r = 16.11\ in$ $A_p = 4.48\ in^2$ $E_{ps} = 28500000\ psi$ $\varepsilon_{pe} = 0.0048$ $P_e = 616000\ lb$ $E_f = 23200000\ psi$ $A_f = 0.556\ in^2$ $d_f = 42.0\ in$ $cgstrands = 3.09\ in$

Step 3: Determine the state of strain on the beam soffit, at the time of FRP installation. The existing strain on the beam soffit is calculated. It is assumed that the beam is uncracked and the only load applied at the time of FRP installation is dead load. M_{DL} is changed to reflect a different moment applied during CFRP installation. If the beam is cracked, appropriate cracked section properties may be used. However, a cracked prestressed beam may not be a good candidate for repair due to the excessive loss of prestress required to result in cracking. $\varepsilon_{bi} = \frac{-P_e}{E_c A_{cg}}\left(1+\frac{ey_b}{r^2}\right)+\frac{M_{DL}y_b}{E_c I_g}$	$\varepsilon_{bi} = \frac{-616000lb}{6800psi \times 768in^2}\left(1+\frac{18.28in \times 21.41in}{(16.11in)^2}\right)$ $+\frac{(1199k-ft \times 12000)\times 21.41in}{6800psi \times 204000in^4} = -0.001in/in$
Step 4: Estimate the depth to the neutral axis. Any value can be assumed, but a reasonable initial estimate of c is 0.1h. The value of c is adjusted to affect equilibrium.	$c = 0.1 \times 42in = 4.2in$

Step 5: Determine the design strain of the FRP system.

The limiting strain in the FRP system is calculated based on three possible failure modes: FRP debonding (Eq. 10-2), FRP rupture (Eq. 10-16) and FRP strain corresponding to prestressing steel rupture (Eq. 10-17). The strain in the FRP system is limited to the minimum value obtained from (Eq. 10-2), (Eq. 10-16) and (Eq. 10-17).

$$\varepsilon_{fd} = 0.083\sqrt{\frac{f_c'}{nE_f t_f}} \qquad (10\text{-}2)$$

$$\varepsilon_{fe} = \frac{\varepsilon_{cu}(d_f - c)}{c} - \varepsilon_{bi} \le \varepsilon_{fd} \qquad (10\text{-}16)$$

$$\varepsilon_{fe} = \frac{(\varepsilon_{pu} - \varepsilon_{pi})(d_f - c)}{(d_p - c)} - \varepsilon_{bi} \le \varepsilon_{fd} \qquad (10\text{-}17)$$

where

$$\varepsilon_{pi} = \frac{P_e}{E_p A_p} + \frac{P_e}{E_c A_c}\left(1 + \frac{e^2}{r^2}\right) \qquad (10\text{-}18)$$

$$\varepsilon_{fd} = 0.083\sqrt{\frac{6800\,psi}{1 \times 23200000\,psi \times 0.047in}}$$

$$\varepsilon_{fd} = 0.0066in/in$$

$$\varepsilon_{fe} = \frac{0.003in/in \times (42.0in - 4.2in)}{4.2in} - (-0.001)$$

$$\varepsilon_{fe} = 0.0271in/in$$

$$\varepsilon_{pi} = \frac{616000lb}{28500000\,psi \times 4.48in^2} + \frac{616000lb}{4700000\,psi \times 786in^2}\left(1 + \frac{(18.28in)^2}{(16.11in)^2}\right)$$

$$\varepsilon_{pi} = 0.0052in/in$$

$$\varepsilon_{fe} = \frac{(0.035 - 0.0052)(42.0 - 4.2)}{(38.91 - 4.2)} - (-0.001)$$

$$\varepsilon_{fe} = 0.0326in/in$$

Therefore, the limiting strain in the FRP system is $\varepsilon_{fd} = 0.0066in/in$ and the anticipated mode of failure is FRP debonding

Step 6: Calculate the strain in the existing prestressing steel.

The strain in the prestressing steel can be calculated using Eq. (10-22):

$$\varepsilon_{ps} = \varepsilon_{pe} + \frac{P_e}{E_c A_c}\left(1 + \frac{e^2}{r^2}\right) + \varepsilon_{pnet} \le 0.035$$

ε_{pnet} is calculated for concrete crushing (Eq. 10-23a) or FRP rupture or debonding (Eq. 10-23b). The value used in Eq. (10-22) is based on the failure mode of the system.

$$\varepsilon_{pnet} = 0.003\frac{(d_p - c)}{c} \qquad \text{(10-23a)}$$

$$\varepsilon_{pnet} = (\varepsilon_{fe} + \varepsilon_{bi})\frac{(d_p - c)}{(d_f - c)} \qquad \text{(10-23b)}$$

For concrete crushing:

$$\varepsilon_{ps} = 0.0048in/in + \frac{616000lb}{4700000psi \times 786in^2} \times \left(1 + \frac{(18.28in)^2}{(16.11in)^2}\right) + 0.0248in/in \le 0.035$$

$$\varepsilon_{ps} = 0.0300in/in$$

For FRP rupture or debonding:

$$\varepsilon_{ps} = 0.0048in/in + \frac{616000lb}{4700000psi \times 786in^2} \times \left(1 + \frac{(18.28in)^2}{(16.11in)^2}\right) + 0.0059in/in \le 0.035$$

$$\varepsilon_{ps} = 0.0111in/in$$

Therefore, FRP debonding represents the expected failure mode of the system and $\varepsilon_{ps} = 0.0111$ in/in.

Step 7: Calculate the stress level in the prestressing steel and FRP.

The stresses are calculated in the prestressing steel and FRP using Eq. (10-24) and Eq. (10-9), respectively.

$$f_{ps} = 28500psi \times \varepsilon_{ps} \quad (when \quad \varepsilon_{ps} \le 0.0076)$$

or

$$f_{ps} = 250ksi - \frac{0.04}{\varepsilon_{ps} - 0.0064} \quad (when \quad \varepsilon_{ps} > 0.0076) \qquad \text{(10-24)}$$

$$f_{ps} = 250ksi - \frac{0.04}{(0.0111) - 0.0064} = 241.5ksi$$

$$f_{fe} = E_f \times \varepsilon_{fe} \qquad \text{(10-9)}$$

$$f_{fe} = 23200000psi \times 0.0066in/in = 152ksi$$

Step 8: Calculate the equivalent stress block parameters. From strain compatibility, the strain in the concrete at failure can be calculated as: $\varepsilon_c = (\varepsilon_{fe} + \varepsilon_{bi})\frac{c}{(d_f - c)}$ The strain $\varepsilon_c^{'}$ corresponding to $f_c^{'}$ is calculated as: $\varepsilon_c^{'} = \frac{1.7 f_c^{'}}{E_c}$ Using ACI 318-08, the equivalent stress block factors can be calculated as: $\beta_1 = \frac{4\varepsilon_c^{'} - \varepsilon_c}{6\varepsilon_c^{'} - 2\varepsilon_c}$ $\alpha_1 = \frac{3\varepsilon_c^{'}\varepsilon_c - \varepsilon_c^2}{3\beta_1 \varepsilon_c^{'2}}$	$\varepsilon_c = (0.0066in/in - 0.0001in/in)\times \frac{4.2in}{42.0in - 4.2in} = 0.0007in/in$ $\varepsilon_c^{'} = \frac{1.7 \times 6800psi}{40700000psi} = 0.0025in/in$ $\beta_1 = \frac{4 \times 0.0025 - 0.0007}{6 \times 0.0025 - 2 \times 0.0007} = 0.685$ $\alpha_1 = \frac{3 \times 0.0025 \times 0.0007 - (0.0007)^2}{3 \times 0.685 \times (0.0025)^2} = 0.384$
Step 9: Calculate the internal force resultants. Use Eq. (10-25) $c = \frac{A_p f_{ps} + A_f f_{fe}}{\alpha_1 f_c^{'} \beta_1 b}$ (10-25)	$c = \frac{4.48in^2 \times 241ksi + 0.556in^2 \times 152ksi}{0.384 \times (6800psi \div 1000) \times 0.685 \times 48}$ $c = 13.6in$
Step 10: Adjust c until estimate creates equilibrium. The value of c calculated in Step 9 must be equal to the estimate in Step 4. If not, choose another value of c and repeat Steps 5 through 9 with the new c value until equilibrium is achieved.	By iteration, *c = 10 in.*

Step 11: Calculate the flexural strength corresponding to the prestressing steel and FRP components. The flexural strength is calculated using Eq. (10-26). The component of flexural strength contributed by the FRP system includes an additional (empirical) reduction factor, ψ. $M_{np} = A_p f_{ps}\left(d_p - \frac{\beta_1 c}{2}\right)$ $M_{nf} = A_f f_{fe}\left(d_f - \frac{\beta_1 c}{2}\right)$ The nominal capacity of the section is found as: $M_n = M_{np} + \psi M_{nf}$	$M_{np} = 4.48in^2 \times 241ksi \times \left(38.91in - \frac{0.728 \times 10.0in}{2}\right)$ $M_{np} = 38132k - in$ $\psi = 0.85$ $M_{nf} = 0.556in^2 \times 152ksi \times \left(42.0in - \frac{0.728 \times 10.0in}{2}\right)$ $M_{nf} = 3242k - in$ $\psi \times M_{nf} = 2755k - in$ The nominal section capacity is: $M_n = 38132k - in + 2755k - in$ $M_n = 40887k - in$ $M_n = 3407k - ft$
Step 12: Verify that the repair provides sufficient strength as compared to the demand on the structure. The area of CFRP provided, A_f, is adjusted and the procedure repeated until the desired flexural capacity is achieved.	$M_n = 3407k - ft$ $M_u = 3395k - ft$ $M_n > M_u$ Therefore, the repair is sufficient.
Design Summary	$A_f = 0.556\ in^2$ Use 6-2 in. wide CFRP strips as shown in Figures 5-2a and 5-6.

The outlined approach is easily programmed as a spreadsheet (as was done for this study) allowing the designer to investigate the effects of varying any of the parameters with relative ease. The iteration procedures (c and A_f) are also easily automated.

Following the flexural design, the shear capacity should be verified. If the flexural capacity is increased beyond the undamaged girder capacity, the shear demand at ultimate capacity will increase. Typically, for long prestressed highway bridge girders, shear will not be a

problem provided the objective of the repair is to simply restore the undamaged capacity of the girder.

The use of 2 in. CFRP strip width in the examples is arbitrary. However, Ramanathan and Harries (2008) have shown that, analogous to reinforcing steel, a larger number of less wide strips (i.e.: using 2-2 in. strips instead of 1-4 in. strip) results in marginally improved debonding performance. Based on interaction of adjacent strips it is recommended that the clear spacing between strips be greater than 0.25 in. (Oehlers and Seracino 2004). Finally, where possible, the strips should be located in the vicinity of the damaged strands. For example, the repair of AB 4-0-0 would likely be arranged as shown in Figure 5-5.

A summary of all non prestressed CFRP strip repairs (AB 4-0-0, AB 8-2-1, SB 4-0-0 and SB 8-2-1) is provided in Table 5-9. Resulting CFRP repairs are shown in Figure 5-2. Finally, detailed moment-curvature responses of: a) the undamaged beams (target values); b) damaged beams; and c) repaired beams are shown in Figures 5-3 and 5-4 for the AB and SB examples, respectively. Also shown in these figures are the 1960 AASHO and 2007 AASHTO design moment and dead load moments for the girders (Tables 5-5 through 5-8).

A fiber section analysis (*XTRACT)* is used to determine the moment-curvature responses of the beams. Modeling the repairs using a fiber sections analysis is more refined since the material stress strain behaviors are better captured than in a simplified plane section analysis utilizing stress block factors. Therefore, the results of the sections analysis of Step 11 and the *XTRACT* program are slightly different. The moment-curvature plots produced to model the repairs (such as Figures 5-3 and 5-4) display a pronounced ‘kink’ in the curves representing section cracking. This kink is an artifact of the transition from uncracked to cracked behavior and

is typical of the moment curvature response of prestressed concrete elements as shown in Figure 5-6 (Collins and Mitchell 1997).

5.2.2 Further Examples

The following sections report other repair methods utilizing the preceding detailed example. The sections highlight the differences in parameters and equations used in this method. Like the presented AB 4-0-0 example, each section includes summary tables of the procedure followed, summary drawings of the resulting designs and moment-curvature plots of the target and repaired beam behaviors.

5.3 NON PRESTRESSED CFRP FABRIC REPAIR

The difference between this and the previous repair is the CFRP material. The CFRP fabric is flexible and can be wrapped around complex shapes and thus is particularly useful for 'wrapping' the complex tension flange shape of an I-beam. However, the fabric should not be wrapped around the entire bulb since 'pull off' failures at inside corners can occur easily. Additionally, a significant amount of effort is required to wrap over a sharp corner because the corner must be rounded to accommodate the CFRP fabric. Typically, fabric manufactures recommend a minimum outside corner radius of 1 in. and do not recommend wrapping around an inside corner (such as the flange-to-web interface in an I-beam). Therefore, repairs conducted with the fabric are practically restrained to the bulb only (consisting of the bottom soffit and the vertical sides). The repairs conducted for the IB 6-2-1 and IB 10-2-1 cases use multiple layers of

fabric on the soffit (as seen in Figure 5-7). With the exception of CFRP material properties (Table 5-2), the repair design is identical to that presented in Section 5.2.1. Input parameters and results are shown in Table 5-10 and drawings of the repairs are shown in Figure 5-7. The repairs are modeled in *XTRACT* and moment-curvature plots are shown in Figure 5-8. It is noted that the repairs prescribed for IB 6-2-1 and 10-2-1 did not completely restore the undamaged girder moment capacity. This will be discussed in Chapter 6.

5.4 NSM CFRP REPAIRS

The design of near-surface mounted (NSM) CFRP repairs is similar to that for CFRP strips presented in Section 5.2. The geometric difference is that the CFRP of an NSM repair is located in the concrete cover of the member (as seen in Figure 2-13) thereby affecting the FRP lever arm, d_f, in Step 11. The same material is used for NSM repair as the CFRP strip repair, although the geometry of the material is customized by cutting the strips longitudinally. For the repairs done here, a strip size of 0.875 in. x 0.047 in. was used (see following section for rationale). Additionally, two strips were glued together and inserted into each slot in the beam. This method of increasing the available area of CFRP per slot has been successfully demonstrated by Aidoo et al. (2006), among others. The advantage of an NSM repair is that a greater debonding strain can be achieved. The design of an NSM repair is the same as the example in Section 5.2.1 with the exception of the calculation of equation (10-2) in Step 5. For NSM, rather than making the calculation of equation (10-2), the debonding strain is calculated by $\varepsilon_{fd} = k_m \times \varepsilon_{fu}^*$, (where $k_m = 0.7$) (ACI 440.2R-08). Input parameters and results are shown in Table 5-11 and drawings

of the repairs are shown in Figure 5-9. NSM repaired girder moment-curvature plots are seen in Figure 5-10. It is noted that the repair prescribed for IB 10-2-1 did not completely restore the undamaged girder moment capacity. This will be discussed in Chapter 6.

5.4.1 NSM Strip Size Optimization

NSM slot geometry (required slot size and spacing) is prescribed by ACI 440.2R-08. Therefore, for a given soffit width, an optimal strip size can be determined so as to maximize the area of NSM reinforcement that may be provided. A typical slot, cut with a concrete saw is 0.25 in. wide (Aidoo 2004 and Quattlebaum et al. 2005). This is the maximum width for the cut (if made in one pass) and therefore restricts the width of NSM reinforcement that may be used[3]. ACI 440.2R-08 recommends that the slot be at least 3 times the width of the inserted strip. Based on this, it is assumed that two strips (glued together) may be inserted into a 0.25 in. slot; this was demonstrated by both Aidoo (2004) and Quattlebaum et al. (2005). The clear concrete cover depth also restricts the NSM strip size. The depth of the slot clearly must not exceed the clear cover as this will result in cutting into the transverse reinforcement. Some margin is required when cutting slots. For prestressed construction where dimensions are well controlled and primary reinforcement does not sag, a margin of 0.125 in. is suggested. Therefore, for the I-beam, for instance, the maximum depth of cut was determined using the depth to the strand (2 in.) and subtracting half of the diameter of the strand (0.219 in.), the diameter of #3 stirrups (0.375 in.) and the safety margin (0.125 in.). Therefore, the maximum slot depth was determined

[3] Alternate methods of cutting the slot include using a concrete grinding wheel (very inefficient), tuck pointing blade (rather inefficient for concrete) or making multiple, overlapping passes with a concrete saw (efficient, but each pass doubles the cost of the slot). Each of these approaches would allow a wider slot to be formed.

to be approximately 1.25 in. Finally, slot spacing and edge distance is a function of slot depth; ACI 440.2R-08 recommends that spacing exceed twice the slot depth and edge distance be four times the slot depth. Considering these restrictions, an optimal slot size may be determined such that the amount of CFRP is maximized for a given soffit dimension. The optimized NSM reinforcement size for the 24 in. soffit of the IB chosen for NSM repairs is 0.875 x 0.094 in. Allowing for the slot to be 0.125 in. deeper than the CFRP dimension, this arrangement requires 1 in. deep slots located 2 in. on center having a 4 in. edge distance. The optimization process is summarized in Table 5-12.

5.5 PRESTRESSED CFRP STRIP REPAIR

CFRP strip dimension and material properties are based on Sika CarboDur strips. This system does not use mechanical anchorage; therefore the prestressing force is transferred to the beam over the entire bond length of the strip. Since no anchorage is used, it is suggested that CFRP U-wraps be used to help mitigate the possibility of peeling failure at strip ends (Klaiber et al. 2003, Green et al. 2004, Reed and Peterman 2004, Reed and Peterman 2005, Scheibel et al. 2001, Tumialan et al. 2001, and Wipf et al. 2004). Experiments have shown that a sustained prestress force of 30% of the ultimate strain capacity of the strip is achievable (El-Hacha et al. 2003) with a prestressed CFRP system; this value is used in the present example. The differences in design of the prestressed CFRP strip repair as compared to the example presented in Section 5.2.1 are as follows:

1. The strain introduced by the prestressed strip is considered in the calculation of the initial soffit condition, ε_{bi} : (Step 3)

$$\varepsilon_{bi} = \frac{-\left(P_e + 0.30 f_{fu} A_f\right)}{E_c A_{cg}}\left(1 + \frac{e y_b}{r^2}\right) + \frac{M_{DL} y_b}{E_c I_g}$$

2. Adding the anchored strain of the prestressed strip to the debonding strain, ε_{fd} : (Step 5, Equation 10-2)

$$\varepsilon_{fd} = 0.083\sqrt{\frac{f_c^{'}}{nE_f t_f}} + 0.30\varepsilon_{fu}$$

The prestressed CFRP repair design follows the same procedure as the example with the exception of the changes noted in steps 3 and 5, respectively. Input parameters and results are shown in Table 5-13 and drawings of the repairs are shown in Figures 5-11 to 5-13. Prestressed CFRP repaired girder moment-curvature plots are seen in Figures 5-14 to 5-16. It is noted that the repair prescribed for IB 10-2-1 did not completely restore the undamaged girder moment capacity. This will be discussed in Chapter 6.

5.6 BONDED POST-TENSIONED CFRP REPAIR

Bonded post-tensioned CFRP repairs include the use of mechanical anchorage at each end of the beam. As a result, a greater strain can be sustained when compared to the prestressed CFRP system described in the previous section. Sika CarboStress system technical data suggests that 50% of the CFRP strip's ultimate strain can be sustained. This value is used in present example. CFRP anchorage is discussed below. Design of bonded post-tensioned CFRP repairs is the same as that of the prestressed CFRP repair design except that the debonding strain, ε_{fd}, calculated in Step 5, is increased to 50% of the strip's ultimate strain (rather than 30% described in the previous section). Additionally, the original state of strain in the soffit, ε_{bi} (Step 3) is also

calculated accounting for the amount of post tensioning provided the CFRP. Since this system includes anchorage at the ends, peeling failures are not a concern. Input parameters and results are shown in Table 5-14 and drawings of the repairs are shown in Figures 5-17 to 5-19. Post-tensioned CFRP repaired girder moment-curvature plots are seen in Figures 5-20 to 5-22.

5.6.1 Anchorage of CFRP

CFRP anchorage is usually secured to proprietary anchorage hardware which in turn is anchored to the concrete substrate. The CFRP-to-anchor connections may rely on adhesive bond, friction or bearing of a preformed CFRP 'stresshead' (the SIKA system uses the latter as shown in Figure 2-12a; Sika 2008b). Manufacturer recommendations must be followed in considering the CFRP to-anchor connection.

The proprietary anchor, in turn, is secured to the concrete substrate. Anchor bolts (Figure 2-12c) and shear keys are conventional methods of transferring the force. Anchorage requirements such as available space and bolt spacing may affect the amount of post-tensioned CFRP that may be installed. Due to their size, anchorages will have to be staggered longitudinally (analogous to staggering reinforcing steel lap splice locations) if a large amount of CFRP is required. Temporary jacking anchorages may be bolted or utilize temporary shear keys. An example of a temporary shear key comprised of a pipe inserted into a hole cored through the beam web is shown in Figure 2-12d.

For anchorages bolted to the concrete substrate, the recommendations ACI 318-08 Appendix D for bolting to concrete should be followed. For anchorages relying on a shear key arrangement, the key should be designed to carry 100% of the prestress force and bolts should be provided to carry any moment and to keep the shear key fully engaged. In cases where the end of

the beam is available for anchorage (Figure 2-8), this is preferred although bearing stresses should be considered in designing the prestressing anchorage.

5.7 STRAND SPLICE REPAIR

Conceptually, the goal of a strand splice is to recreate the original strand, including the prestressing force. Due to geometric constraints of concrete cover, strand spacing and strand splice dimensions, this repair can only be used to repair a small number of strands at a particular section. The 'turn of the nut method' is suggested (rather than the torque wrench method) to ensure that the proper stress is reintroduced in the strand (Labia et al. 1996 and Olson et al. 1992). Determining the amount of stress introduced into the strand by the strand splice is done using the stiffness of the strand splice and the stiffness of the undeveloped strand (i.e.: at least the exposed strand being connected) and balancing these with the 'shortening' of the splice as the nut is turned. The stiffness of the strand splice is a function of its geometry, length and strand diameter being developed. This stiffness must be calculated on an individual basis. Based on the desired prestress force, P, stiffness of the strand splice, K_{splice}, exposed length of strand, $L_{exposed}$ and strand transfer length, L_{tr} into the concrete, the required shortening of the strand splice may be calculated as:

$$\Delta_{splice} = \frac{P}{K_{splice}} + \frac{P\left(\sum L_{exposed} + L_{tr}\right)}{A_p E_p} \qquad \text{(Eq. 5-1)}$$

For the I-beam, for instance, the stress in the 7/16 in. strand after long term losses was found to be 133.6 ksi. Suggested practice is to add 5 ksi for dead load stress and 5 ksi for error to the target stress value and use this value as the target value for the strand splice induced stress

(Labia et al. 1996). This resulted in a target stress of 143.6 ksi (corresponding to a force of 15.5 kips) per strand. Assuming a splice stiffness of 187.7 k/in. (reported by Labia et al. 1996), that there is 24 inches of exposed strand to either side of the splice and that the strand transfer length is equal to $d_b(f_{pe}/3000) = 21$ *in.* (ACI 318-08), a shortening of 0.42 in. is required. There are 16 threads per inch on the splice; therefore, to reach the required deformation, 6.7 nut revolutions are required. The use of the strand transfer length assumes a linear development of strand force in the sound concrete. Thus the strand strain associated with development of the strand force is $PL_{tr}/2A_pE_p$. Considering both sides of the splice, the ½ coefficient cancels and Equation 5-1 results.

The use of the preload technique is often used with the strand splice method. The preload technique is discussed in Section 5.9.

5.8 EXTERNAL STEEL POST-TENSIONING

The goal of external steel post-tensioning is to restore the compressive stress in the bottom of the girder as intended by the original prestressed strands as well as increase the flexural capacity. Although not covered in this document, external steel post tensioning can be used to restore original stress levels in the bottom of the girder even if there is no damage. In this document, this method is used to repair the IB 6-2-1 and 10-2-1 cases.

Analysis of the section after strand loss is done by sections analysis. A general procedure is provided here as an example.

1. Determine the amount of stress lost at the girder soffit due to the loss of strands:

$$f_{loss} = \left(-\frac{P}{A} - \frac{Pe}{S} + \frac{M_{DL}}{S} \right)_{undamaged} - \left(-\frac{P}{A} - \frac{Pe}{S} + \frac{M_{DL}}{S} \right)_{damaged} \quad \text{(Eq. 5-2)}$$

It should be noted that the section modulus, S, and effective area, A, may be different for the undamaged and damaged terms particularly if the damaged girder is cracked under the influence of dead load. The P and Pe terms are the axial prestressing force and its resulting moment (e is the strand eccentricity), respectively. The M_{DL} term is the moment due to girder dead load.

2. Determine the required force in the post tensioning steel needed to replace the lost strands:

$$f_{loss} = \left(-\frac{P}{A} - \frac{Pe}{S} \right)_{PT} \quad \text{(Eq. 5-3)}$$

3. Design the bolster for the post-tensioning system. The bolster should anchor the additional forces and should be designed such that in the event of overstress, the post-tensioning bar, rather than the bolster, fails.

Drawings of the example repairs are shown in Figures 5-23 and 5-24 and the repaired girder moment-curvature plots are seen in Figure 5-25.

Post-tensioning steel will typically take the form of solid high strength post-tensioning rods (such as Williams all thread bars) or prestressing strand. Due to the dimension of the post-tensioning system and the possibility of impact damage, external post-tensioning systems are conventionally mounted along the girder web rather than the soffit below. As a result, this repair method is inappropriate for adjacent box girders. Appropriate environmental protection (such as using encapsulated strand, epoxy-coated or galvanized rod, etc.) is provided for external applications.

Bolsters can be made of either concrete or steel. Bolster material is the preference of the designer, but cost and constructability must be considered. Regardless of bolster material, bolster

design is to be carried out as a shear friction connection following AASHTO (2007) Section 5.8.4. Figure 5-26a shows an example of a concrete bolster and Figure 5-26b shows a schematic of a steel angle bolster.

5.9 PRELOAD TECHNIQUE

Preload is the application of a load to a girder during the repair process. Used primarily to improve the performance on concrete patches, the preload results in a tension stress applied to the beam soffit. The patch is executed in this condition and when the preload is released, the patch is drawn into compression (even if there is still a net tension at the soffit). The goal of a preload is to sufficiently compress the concrete patch in order to counteract live load effects reducing the possibility of patch 'pop-out' failure. Although covered in this document for completeness, it should be realized that this method is not applicable for all structures or repair types.

A generalized preload application procedure is provided here as an example (adopted and corrected from Labia et al. 1996). In this procedure, tension is represented by positive stress.

1. Using AASHTO (2007) Table 5.9.4.2.2-1, the maximum permissible tensile stress, f_t, at the bottom of the patch can be selected. Typically a value of $0.19\sqrt{f_c'}$ (ksi units) is selected.
2. The maximum external moment, M_{EXTmax}, that can be applied can be determined as follows: $f_t \le -\frac{P}{A}\left(1+\frac{ey_b}{r^2}\right)+\frac{M_D}{S_d}+\frac{M_{EXT\max}}{S_d}$. (Eq. 5-4)

3. For completeness, compressive stress due to the prestressing force and dead load at the bottom of the damaged girder should be checked using Table 5.9.4.2.1-1 (AASHTO 2007). These stresses should not exceed $0.45 f_c^{'}$:

$$-\frac{P}{A}\left(1+\frac{ey_b}{r^2}\right)+\frac{M_D}{S_d} \le 0.45 f_c^{'}. \qquad \text{(Eq. 5-5)}$$

Upon release of the preload, the concrete patch is placed in compression with a stress equal to M_{EXT}/S_d. Due to the magnitude of the load required to achieve a useful value of M_{EXT}, the use of preloading is only practical on shorter spans.

Table 5-1 Prototype girder material and geometric properties.

Property	AB	SB	IB
Section	prestressed concrete adjacent box beam	prestressed concrete multi-box beam	prestressed concrete I-girder
prestressing steel	60 - 250 ksi 3/8 in. seven-wire strand	68 - 250 ksi 3/8 in. seven-wire strand	50 - 250 ksi 7/16 in. seven-wire strand
Young's modulus of prestressed steel, E_p	28500 ksi	28500 ksi	28500 ksi
Concrete girder compressive strength, f_c'	6800 psi	5500 psi	5500 psi
Young's modulus of girder, E_c	4700 ksi	4227 ksi	4227 ksi
Concrete deck compressive strength	n.a.	4000 psi	4000 psi
Young's modulus of deck	n.a.	3605 ksi	3605 ksi
girder geometry	Figure 4-1	Figure 4-2	Figure 4-3
girder length	90.0 ft	69.0 ft	75.5 ft

Table 5-2 CFRP material and geometric properties (Sika 2008a and 2008c).

Property	Sika CarboDur strips	SikaWrap Hex 103C (w/Sikadur Hex 300 epoxy)
Material type	preformed unidirectional CFRP strip	unidirectional CFRP fabric
Tensile strength, f_{fu}	406 ksi	104 ksi
Compressive strength	-	-
Young's Modulus, E_f	23,200 ksi	9,446 ksi
Rupture strain, ε_{fu}	0.017	0.0098
Material thickness	0.047 in.	approx. 0.04 in.
Size/packaging	1.97 in. strips[1] 3.15 in. strips 3.94 in. strips	25 in. x 50 ft. rolls 25 in. x 300 ft. rolls
[1] product is fabricated in 50, 75 and 100 mm widths; hard conversions are presented here to facilitate later stress calculations.		

Table 5-3 Post-tensioning steel material and geometric properties (Williams 2008).

Nominal Bar Diameter	Minimum Net Area Through Threads	Minimum Tensile Strength	Minimum Yield Strength
1.25 in.	1.25 in^2	188 kips	150 kips
1.375 in.	1.58in^2	237 kips	190 kips

Table 5-4 Target and repaired flexural capacities for repair designs.

Example	Repair Type	Damaged Capacity at φ = 0.00015 (k-ft)	Target Capacity at φ = 0.00015 (k-ft)	Repaired Capacity (k-ft)	Repaired φ =
AB 4-0-0	CFRP strip	3160	3387	3425	0.00019
AB 8-2-1	CFRP strip	2770	3387	3396	0.00019
SB 4-0-0	CFRP strip	4317	4596	4591	0.00015
SB 8-2-1	CFRP strip	3838	4596	4822	0.00015
IB 4-0-0	CFRP fabric	4200	4590	4596	0.00022
IB 6-2-1	CFRP fabric	3731	4590	4436	0.00013
IB 10-2-1	CFRP fabric	3340	4590	4052	0.00013
IB 4-0-0	NSM CFRP	4200	4590	4703	0.00026
IB 6-2-1	NSM CFRP	3731	4590	4972	0.00026
IB 10-2-1	NSM CFRP	3340	4590	4389	0.00026
AB 8-2-1	Prestressed CFRP	2770	3387	3590	0.00025
SB 8-2-1	Prestressed CFRP	3838	4596	4553	0.00013
IB 4-0-0	Prestressed CFRP	4200	4590	4345	0.00013
IB 6-2-1	Prestressed CFRP	3731	4590	4492	0.00013
IB 10-2-1	Prestressed CFRP	3340	4590	4280	0.00013
AB 8-2-1	Post-tensioned CFRP	2770	3387	3369	0.00018
SB 8-2-1	Post-tensioned CFRP	3838	4596	4461	0.00013
IB 4-0-0	Post-tensioned CFRP	4200	4590	4502	0.00013
IB 6-2-1	Post-tensioned CFRP	3731	4590	4600	0.00013
IB 10-2-1	Post-tensioned CFRP	3340	4590	4554	0.00013
IB 6-2-1	Post-tensioned steel	3731	4590	4291	0.0001
IB 10-2-1	Post-tensioned steel	3340	4590	4040	0.0001

Table 5-5 AB loading with AASHTO-prescribed distribution factor g = 0.285.

	based on load…	Moment	MPF	g	IM	Strength I	Service I	Service III	units
M_{DW}	0.12 klf	118	-	-	-	177	118	118	k-ft
M_{SW}	0.90 klf	909	-	-	-	1137	909	909	k-ft
M_{JB}	0.17 klf	171	-	-	-	214	171	171	k-ft
M_{LANE}	0.64 klf	648	1	0.285	-	323	185	148	k-ft
M_{HS20}	HS20	1344	1	0.285	1.33	891	509	407	k-ft
M_{HS25}	HS25	1680	1	0.285	1.33	1114	637	509	k-ft
M_{TAN}	TANDEM	1076	1	0.285	1.33	713	407	326	k-ft
Dead Load Moment (M_{DL})=						1528	1199	1199	k-ft
Live Load Moment (HS20) =						1214	694	555	k-ft
Live Load Moment (HS25) =						1437	821	657	k-ft
Live Load Moment (TANDEM) =						1036	592	474	k-ft

MPF = multiple lane presence factor
g = distribution factor for moment
IM = impact factor

Table 5-6 AB loading with distribution factor g = 0.5.

	based on…	Moment	MPF	g	IM	Strength I	Service I	Service III	units
M_{DW}	0.12 klf	118	-	-	-	177	118	118	k-ft
M_{SW}	0.90 klf	909	-	-	-	1137	909	909	k-ft
M_{JB}	0.17 klf	171	-	-	-	214	171	171	k-ft
M_{LANE}	0.64 klf	648	1	0.5	-	567	324	259	k-ft
M_{HS20}	HS20	1344	1	0.5	1.33	1564	894	715	k-ft
M_{HS25}	HS25	1680	1	0.5	1.33	1955	1117	894	k-ft
M_{TAN}	TANDEM	1076	1	0.5	1.33	1252	715	572	k-ft
Dead Load Moment =						1528	1199	1199	k-ft
Live Load Moment (HS20) =						2131	1218	974	k-ft
Live Load Moment (HS25) =						2522	1441	1153	k-ft
Live Load Moment (TANDEM) =						1819	1039	831	k-ft

MPF = multiple lane presence factor
g = distribution factor for moment
IM = impact factor

Table 5-7 SB loading.

	based on…	Moment	MPF	g	IM	Strength I	Service I	Service III	units
M_{DECK}	0.77 klf	456	-	-	-	570	456	456	k-ft
M_{DW}	0.20 klf	122	-	-	-	182	122	122	k-ft
M_{SW}	0.80 klf	475	-	-	-	594	475	475	k-ft
M_{JB}	0.09 klf	53	-	-	-	66	53	53	k-ft
M_{LANE}	0.64 klf	381	1	0.648	-	432	247	197	k-ft
M_{HS20}	HS20	968	1	0.648	1.33	1460	834	667	k-ft
M_{HS25}	HS25	1210	1	0.648	1.33	1825	1043	834	k-ft
M_{TAN}	TANDEM	813	1	0.648	1.33	1227	701	561	k-ft
Dead Load Moment =						1411	1105	1105	k-ft
Live Load Moment (HS20) =						1892	1081	865	k-ft
Live Load Moment (HS25) =						2257	1289	1032	k-ft
Live Load Moment (TANDEM) =						1659	948	758	k-ft

MPF = multiple lane presence factor
g = distribution factor for moment
IM = impact factor

Table 5-8 IB loading.

	based on…	Moment	MPF	g	IM	Strength I	Service I	Service III	units
M_{DECK}	0.70 klf	499	-	-	-	623	499	499	k-ft
M_{SW}	0.69 klf	491	-	-	-	614	491	491	k-ft
M_{JB}	0.15 klf	108	-	-	-	135	108	108	k-ft
M_{LANE}	0.64 klf	456	1	0.592	-	472	270	216	k-ft
M_{HS20}	HS20	867	1	0.592	1.33	1194	682	546	k-ft
M_{HS25}	HS25	1084	1	0.592	1.33	1493	853	682	k-ft
M_{TAN}	TANDEM	894	1	0.592	1.33	1232	704	563	k-ft
Dead Load Moment =						1372	1098	1098	k-ft
Live Load Moment (HS20) =						1667	952	762	k-ft
Live Load Moment (HS25) =						1965	1123	898	k-ft
Live Load Moment (TANDEM) =						1705	974	779	k-ft

MPF = multiple lane presence factor
g = distribution factor for moment
IM = impact factor

Table 5-9 Non-prestressed perform CFRP strip repair results.

Step #		AB 4-0-0	AB 8-2-1	SB 4-0-0	SB 8-2-1	units
1	f_{fu}	345	345	345	345	ksi
1	ε_{fu}	0.0145	0.0145	0.0145	0.0145	in/in
2	**cg strands**	3.09	3.16	4.41	4.77	in.
2	d_f	42	42	50	50	in.
2	d_p	38.91	38.84	45.59	45.23	in.
2	ε_{cu}	0.003	0.003	0.003	0.003	in/in
2	P_e	616	539	692	616	kips
2	A_p	4.48	3.92	5.12	4.56	in^2
2	E_{ps}	28500	28500	28500	28500	ksi
2	A_{cg}	786	786	1553	1553	in^2
2	E_c	4700	4700	4230	4230	ksi
2	**e**	18.32	18.31	27.44	27.14	in
2	**I**	204000	204000	543000	543000	in^4
2	**r**	16.1	16.1	18.7	18.7	in
2	ε_{pe}	0.0048	0.0048	0.0047	0.0047	in/in
2	A_f	0.56	1.57	0.56	1.67	in^2
2	$f_c'_{DECK}$	-	-	4000	4000	psi
3	ε_{bi}	-0.0001	0	-0.0002	-0.0001	in/in
4	**c**	9.9	10	7.5	7.5	in.
5	ε_{fd}	0.0066	0.0066	0.0059	0.0059	in/in
5	ε_{fe} **(cc)**	0.0098	0.0097	0.0172	0.0172	in/in
5	ε_{pi}	0.0052	0.0052	0.0051	0.0050	in/in
5	ε_{fe} **(psr)**	0.0331	0.0332	0.0336	0.0339	in/in
6	ε_{pnet} **(cc)**	0.0088	0.0087	0.0152	0.0151	in/in
6	ε_{pnet} **(frp)**	0.0058	0.0059	0.0051	0.0051	in/in
6	ε_{ps} **(cc)**	0.0140	0.0138	0.0203	0.0201	in/in
6	ε_{ps} **(frp)**	0.0110	0.0110	0.0102	0.0101	in/in
7	f_{ps}	241	241	239	239	ksi
7	f_{fe}	152	152	137	137	ksi
8	ε_c	0.0020	0.0020	0.0010	0.0010	in/in
8	ε'_c	0.0025	0.0025	0.0016	0.0016	in/in
8	**β1**	0.728	0.730	0.711	0.711	-
8	**α**	0.811	0.820	0.697	0.701	-
9/10	**c** (check)	10.0	10.1	7.6	7.6	in
11	M_{np}	38132	33253	52593	46388	k-in
11	M_{nf}	3242	9175	3596	10782	k-in
11	ψ_f	0.85	0.85	0.85	0.85	-
11	M_n	40888	41052	55650	55553	k-in
11	M_n	3407	3421	4638	4629	k-ft
12	M_u (Table 5-4)	3395	3395	4596	4596	k-ft

Table 5-10 CFRP fabric repair results.

Step #		IB 4-0-0	IB 6-2-1	IB 10-2-1	units
1	f_{fu}	88.4	88.4	88.4	ksi
1	ε_{fu}	0.0102	0.0102	0.0102	in/in
2	**cg strands**	6.43	6.78	7.3	in.
2	d_f	52.5	52.0	52.0	in.
2	d_p	46.07	45.72	45.2	in.
2	ε_{cu}	0.003	0.003	0.003	in/in
2	P_e	664	592	534	kips
2	A_p	4.97	4.43	4.00	in^2
2	E_{ps}	28500	28500	28500	ksi
2	A_{cg}	1272	1272	1272	in^2
2	E_c	4230	4230	4230	ksi
2	**e**	26.45	26.1	25.72	in
2	**I**	402400	402400	402400	in^4
2	**r**	17.8	17.8	17.8	in
2	ε_{pe}	0.0047	0.0047	0.0047	in/in
2	A_f	0.8	3.44	3.44	in^2
2	$f_c'_{DECK}$	4000	4000	4000	psi
3	ε_{bi}	-0.0002	-0.0002	-0.0001	in/in
4	**c**	6.3	7.6	6.7	in.
5	ε_{fd}	0.0100	0.0058	0.0058	in/in
5	ε_{fe} **(cc)**	0.0222	0.0177	0.0204	in/in
5	ε_{pi}	0.0051	0.0050	0.0050	in/in
5	ε_{fe} **(psr)**	0.0350	0.0350	0.0354	in/in
6	ε_{pnet} **(cc)**	0.0189	0.0150	0.0172	in/in
6	ε_{pnet} **(frp)**	0.0084	0.0048	0.0048	in/in
6	ε_{ps} **(cc)**	0.0240	0.0201	0.0222	in/in
6	ε_{ps} **(frp)**	0.0135	0.0099	0.0098	in/in
7	f_{ps}	244	238	238	ksi
7	f_{fe}	95	55	55	ksi
8	ε_c	0.0013	0.0010	0.0010	in/in
8	ε'_c	0.0016	0.0016	0.0016	in/in
8	**β1**	0.731	0.708	0.702	-
8	**α**	0.822	0.677	0.614	-
9/10	**c (check)**	6.4	7.7	6.8	in
11	M_{np}	53100	45394	40413	k-in
11	M_{nf}	3798	9247	9241	k-in
11	ψ_f	0.85	0.85	0.85	-
11	M_n	56328	53254	48268	k-in
11	M_n	4694	4438	4022	k-ft
12	M_u (Table 5-4)	4688	4688	4688	k-ft

Table 5-11 NSM CFRP repair results.

Step #		IB 4-0-0	IB 6-2-1	IB 10-2-1	units
1	**f_{fu}**	345	345	345	ksi
1	**ε_{fu}**	0.0145	0.0145	0.0145	in/in
2	**cg strands**	6.43	6.78	7.3	in.
2	**d_f**	51.9	51.4	51.4	in.
2	**d_p**	46.07	45.72	45.2	in.
2	**ε_{cu}**	0.003	0.003	0.003	in/in
2	**P_e**	664	592	534	kips
2	**A_p**	4.97	4.43	4.0	in^2
2	**E_{ps}**	28500	28500	28500	ksi
2	**A_{cg}**	1272	1272	1272	in^2
2	**E_c**	4230	4230	4230	ksi
2	**e**	26.45	26.1	25.72	in
2	**I**	402400	402400	402400	in^4
2	**r**	17.8	17.8	17.8	in
2	**ε_{pe}**	0.0047	0.0047	0.0047	in/in
2	**A_f**	0.33	0.91	0.99	in^2
2	**$f_c'_{DECK}$**	4000	4000	4000	psi
3	**ε_{bi}**	-0.0002	-0.0002	-0.0001	in/in
4	**c**	6.0	6.0	5.7	in.
5	**ε_{fd}**	0.0119	0.0119	0.0119	in/in
5	**ε_{fe} (cc)**	0.0232	0.0228	0.0242	in/in
5	**ε_{pi}**	0.0051	0.0050	0.0050	in/in
5	**ε_{fe} (psr)**	0.0345	0.0344	0.0348	in/in
6	**ε_{pnet} (cc)**	0.0200	0.0199	0.0208	in/in
6	**ε_{pnet} (frp)**	0.0102	0.0103	0.0102	in/in
6	**ε_{ps} (cc)**	0.0251	0.0249	0.0258	in/in
6	**ε_{ps} (frp)**	0.0153	0.0153	0.0152	in/in
7	**f_{ps}**	246	246	245	ksi
7	**f_{fe}**	276	276	276	ksi
8	**ε_c**	0.0015	0.0016	0.0015	in/in
8	**ε'_c**	0.0016	0.0016	0.0016	in/in
8	**β1**	0.744	0.746	0.740	-
8	**α**	0.873	0.878	0.859	-
9/10	**c (check)**	6.0	6.1	5.8	in
11	**M_{np}**	53464	47240	42242	k-in
11	**M_{nf}**	4511	12270	12304	k-in
11	**ψ_f**	0.85	0.85	0.85	-
11	**M_n**	57298	57670	52701	k-in
11	**M_n**	4775	4806	4392	k-ft
12	**M_u** (Table 5-4)	4742	4742	4742	k-ft

Table 5-12 NSM size optimization.

FRP strip width (in)	**Depth of slot required (in)**	**Edge distance required (in)**	**Required spacing between slots (in)**	**Number of slots in 24 in. wide soffit**	**Available area of FRP[1] (in^2)**
b_b	$b_b + 0.125$	$4(b_b + 0.125)$	$2(b_b + 0.125)$		
0.500	0.625	2.5	1.25	13	0.306 - 0.611
0.625	0.750	3.0	1.5	11	0.323 - 0.646
0.750	0.875	3.5	1.75	9	0.317 - 0.635
0.875	1.000	4.0	2	8	0.329 - 0.658
1.000	1.125	4.5	2.25	6	0.282 - 0.564
1.125	1.250	5.0	2.5	6	0.317 - 0.635

[1]A range is provided to show the area of FRP using one or two strips per slot, respectively. Actual area of FRP can be anywhere between these bounds.

Table 5-13 Prestressed CFRP repair results.

Step #		AB 8-2-1	SB 8-2-1	IB 4-0-0	IB 6-2-1	IB 10-2-1	units
1	f_{fu}	345	345	345	345	345	ksi
1	ε_{fu}	0.0145	0.0145	0.0145	0.0145	0.0145	in/in
2	**cg strands**	3.16	4.77	6.43	6.78	7.3	in.
2	d_f	42	50	52	52	52	in.
2	d_p	38.84	45.23	46.07	45.72	45.2	in.
2	ε_{cu}	0.003	0.003	0.003	0.003	0.003	in/in
2	P_e	539	616	664	592	534	kips
2	A_p	3.92	4.56	4.97	4.43	4.00	in^2
2	E_{ps}	28500	28500	28500	28500	28500	ksi
2	A_{cg}	786	1553	1272	1272	1272	in^2
2	E_c	4700	4230	4230	4230	4230	ksi
2	**e**	18.31	27.14	26.45	26.1	25.72	in
2	**I**	204000	543000	402400	402400	402400	in^4
2	**r**	16.1	18.7	17.8	17.8	17.8	in
2	ε_{pe}	0.0048	0.0047	0.0047	0.0047	0.0047	in/in
2	A_f	0.74	0.83	0.19	0.83	1.02	in^2
2	$f_c'_{DECK}$	-	4000	4000	4000	4000	psi
3	ε_{bi}	-0.0001	-0.0002	-0.0002	-0.0002	-0.001	in/in
4	**c**	7.3	6.1	6.2	6.2	6.0	in.
5	ε_{PT}	0.004	0.004	0.004	0.004	0.004	in/in
5	ε_{fd}	0.0109	0.0102	0.0102	0.0102	0.0102	in/in
5	ε_{fe} **(cc)**	0.0144	0.0218	0.0226	0.0226	0.0234	in/in
5	ε_{pi}	0.0052	0.0050	0.0051	0.0050	0.0050	in/in
5	ε_{fe} **(psr)**	0.0329	0.0338	0.0349	0.0353	0.0358	in/in
6	ε_{pnet} **(cc)**	0.0130	0.0192	0.0193	0.0191	0.0196	in/in
6	ε_{pnet} **(frp)**	0.0098	0.0090	0.0086	0.0086	0.0085	in/in
6	ε_{ps} **(cc)**	0.0181	0.0243	0.0244	0.0242	0.0246	in/in
6	ε_{ps} **(frp)**	0.0150	0.0140	0.0137	0.0136	0.0135	in/in
7	f_{ps}	245	245	245	244	244	ksi
7	f_{fe}	253	237	237	237	237	ksi
8	ε_c	0.0023	0.0014	0.0013	0.0013	0.0013	in/in
8	ε'_c	0.0025	0.0016	0.0016	0.0016	0.0016	in/in
8	**β1**	0.741	0.735	0.731	0.731	0.728	-
8	**α**	0.863	0.840	0.825	0.825	0.811	-
9/10	**c (check)**	7.4	6.1	6.2	6.3	6.1	in
11	M_{np}	34703	47970	53209	46990	41953	k-in
11	M_{nf}	7348	9449	2209	9931	12156	k-in
11	ψ_f	0.85	0.85	0.85	0.85	0.85	-
11	M_n	40949	56002	55087	55431	52285	k-in
11	M_n	3412	4667	4591	4619	4357	k-ft
12	M_u (Table 5-4)	3388	4596	4557	4557	4557	k-ft

Table 5-14 Post-tensioned CFRP repair results.

Step #		AB 8-2-1	SB 8-2-1	IB 4-0-0	IB 6-2-1	IB 10-2-1	units
1	f_{fu}	345	345	345	345	345	ksi
1	ε_{fu}	0.0145	0.0145	0.0145	0.0145	0.0145	in/in
2	**cg strands**	3.16	4.77	6.43	6.78	7.3	in.
2	d_f	42	50	52	52	52	in.
2	d_p	38.84	45.23	46.07	45.72	45.2	in.
2	ε_{cu}	0.003	0.003	0.003	0.003	0.003	in/in
2	P_e	539	616	664	592	534	kips
2	A_p	3.92	4.56	4.97	4.43	4.00	in^2
2	E_{ps}	28500	28500	28500	28500	28500	ksi
2	A_{cg}	786	1553	1272	1272	1272	in^2
2	E_c	4700	4230	4230	4230	4230	ksi
2	**e**	18.31	27.14	26.45	26.1	25.72	in
2	**I**	204000	543000	402400	402400	402400	in^4
2	**r**	16.1	18.7	17.8	17.8	17.8	in
2	ε_{pe}	0.0048	0.0047	0.0047	0.0047	0.0047	in/in
2	A_f	0.56	0.56	0.28	0.74	1.11	in^2
2	$f_c'_{DECK}$	-	4000	4000	4000	4000	psi
3	ε_{bi}	-0.0001	-0.0002	-0.0002	-0.0002	-0.002	in/in
4	**c**	6.3	5.5	5.8	5.8	5.8	in.
5	ε_{PT}	0.007	0.007	0.007	0.007	0.007	in/in
5	ε_{fd}	0.0138	0.0131	0.0131	0.0131	0.0131	in/in
5	ε_{fe} **(cc)**	0.0171	0.0245	0.0244	0.0244	0.0244	in/in
5	ε_{pi}	0.0052	0.0050	0.0051	0.0050	0.0050	in/in
5	ε_{fe} **(psr)**	0.0329	0.0337	0.0349	0.0350	0.0358	in/in
6	ε_{pnet} **(cc)**	0.0155	0.0217	0.0208	0.0208	0.0204	in/in
6	ε_{pnet} **(frp)**	0.0125	0.0116	0.0162	0.0162	0.0159	in/in
6	ε_{ps} **(cc)**	0.0207	0.0267	0.0259	0.0259	0.0254	in/in
6	ε_{ps} **(frp)**	0.0176	0.0166	0.0162	0.0162	0.0159	in/in
7	f_{ps}	246	246	246	246	246	ksi
7	f_{fe}	320	304	304	304	304	ksi
8	ε_c	0.0024	0.0016	0.0016	0.0016	0.0016	in/in
8	ε'_c	0.0025	0.0016	0.0016	0.0016	0.0016	in/in
8	**β1**	0.748	0.749	0.750	0.750	0.750	-
8	**α**	0.883	0.887	0.888	0.888	0.888	-
9/10	**c (check)**	6.5	5.6	5.8	5.9	5.9	in
11	M_{np}	35181	48407	53612	47768	42222	k-in
11	M_{nf}	7033	8105	4256	11345	17015	k-in
11	ψ_f	0.85	0.85	0.85	0.85	0.85	-
11	M_n	41159	55296	57229	57411	56685	k-in
11	M_n	3430	4608	4769	4784	4724	k-ft
12	M_u (Table 5-4)	3388	4596	4742	4742	4742	k-ft

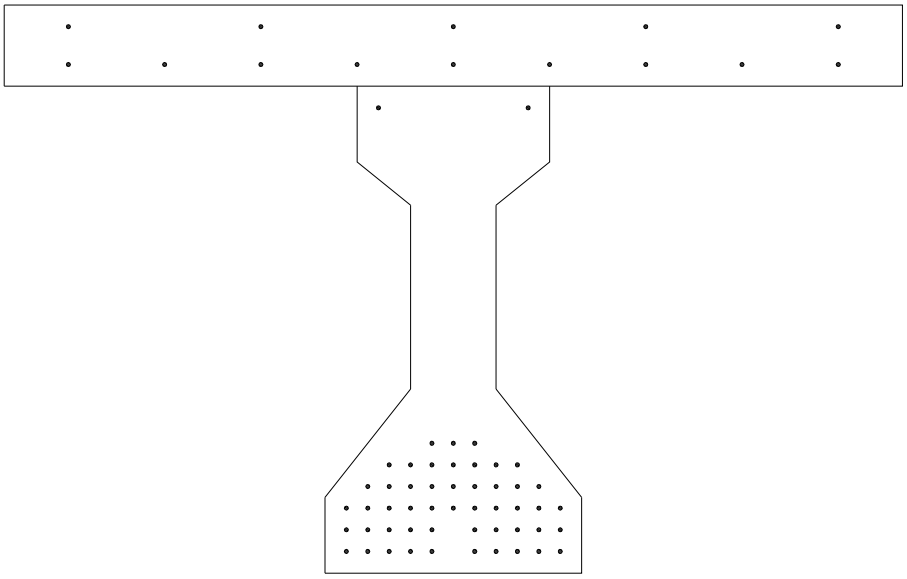

(a) case IB 0-0-0.

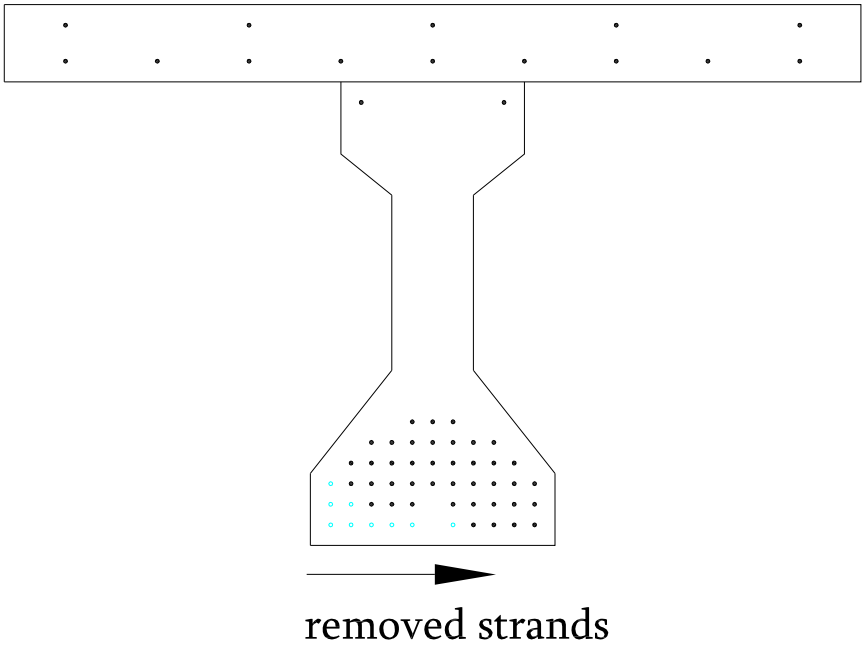

(b) case IB 6-2-1.

Figure 5-1 Example of analysis identification.

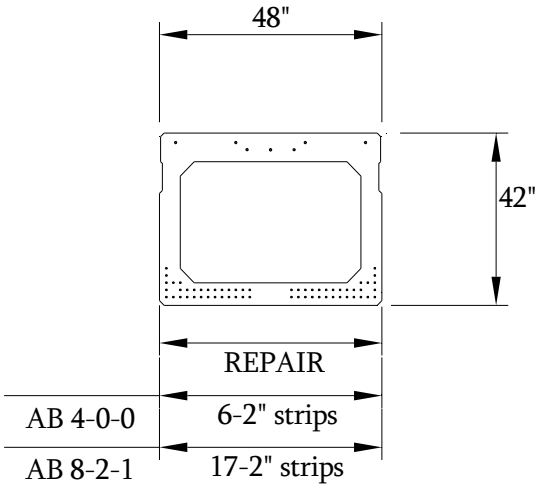

(a) AB CFRP strip repair.

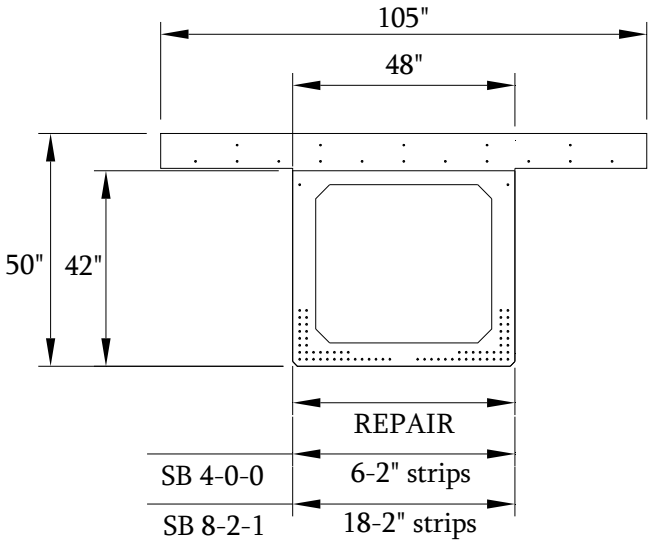

(b) SB CFRP strip repair.

Figure 5-2 Preformed CFRP strip repairs.

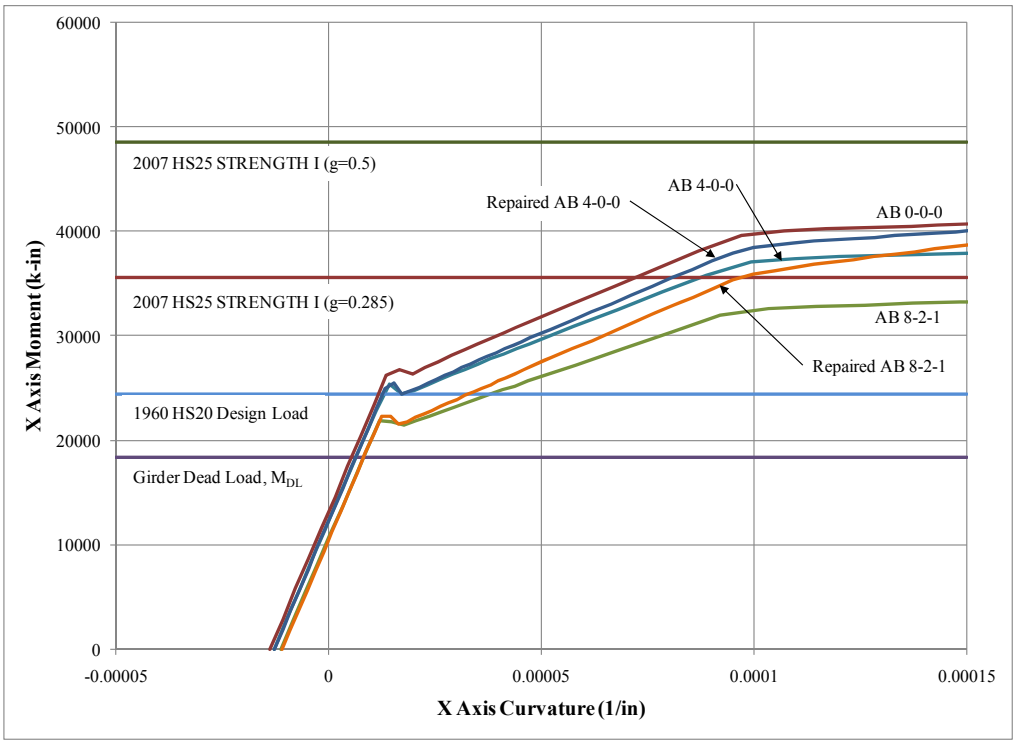

Figure 5-3 Preformed CFRP strip repaired AB moment-curvature plot.

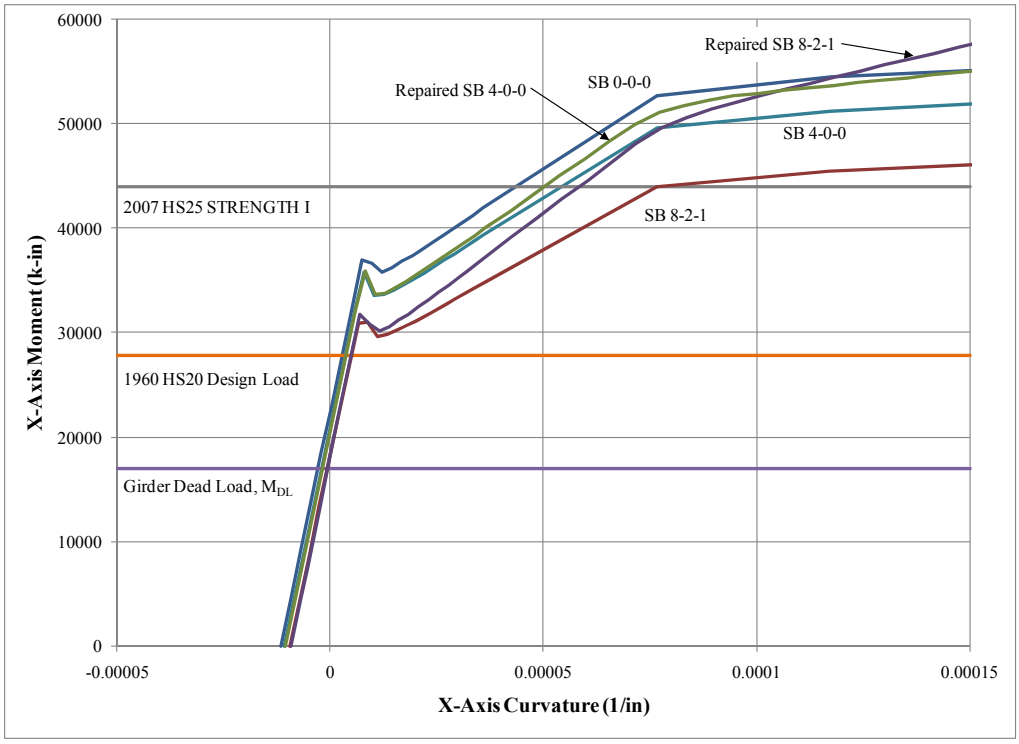

Figure 5-4 Preformed CFRP strip repaired SB moment-curvature plot.

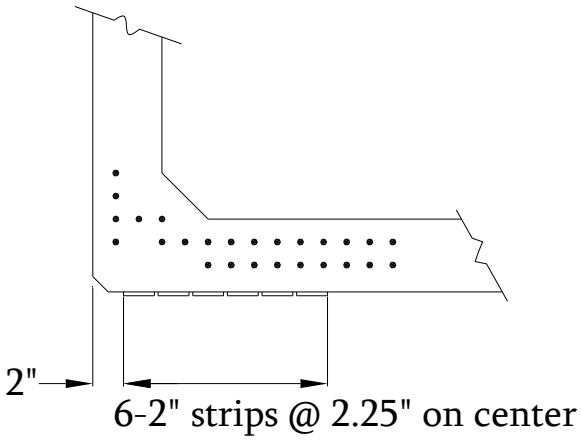

Figure 5-5 Suggested strip location for AB 4-0-0.

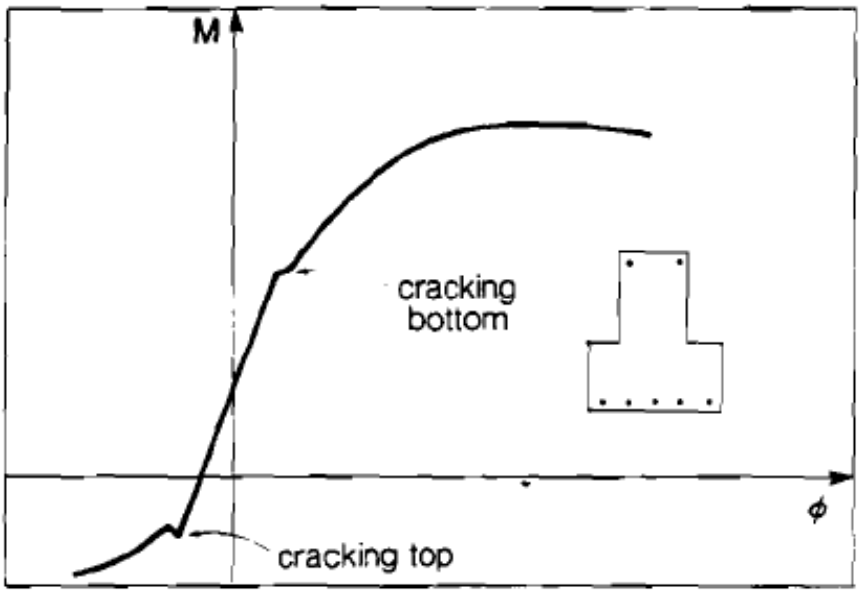

Figure 5-6 Flexural behavior of prestressed girders (Collins and Mitchell 1997).

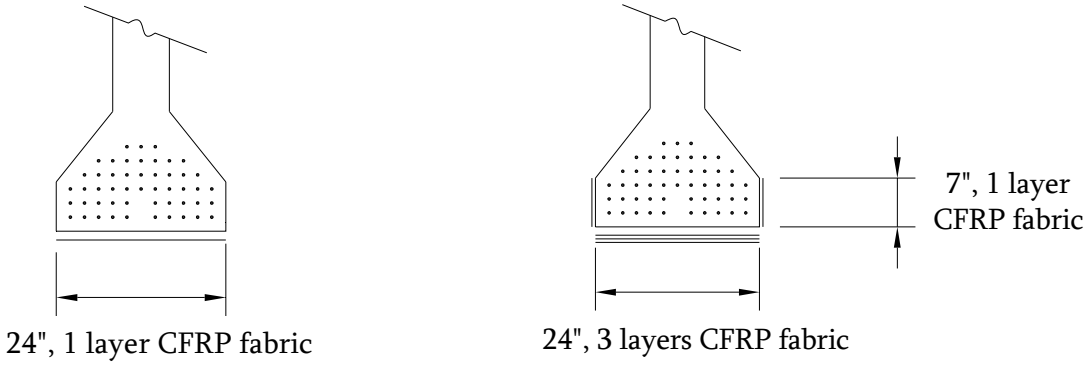

(a) IB 4-0-0 CFRP fabric repair. **(b)** IB 6-2-1 and 10-2-1 CFRP fabric repair.

Figure 5-7 CFRP fabric repairs.

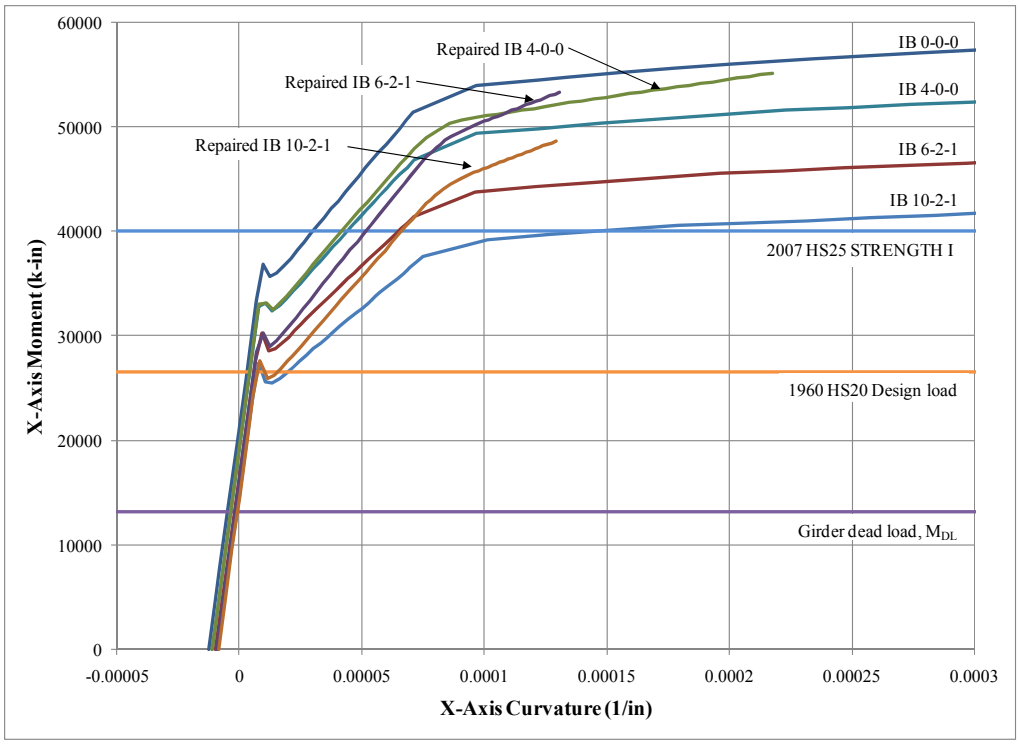

Figure 5-8 CFRP fabric repair moment-curvature plot.

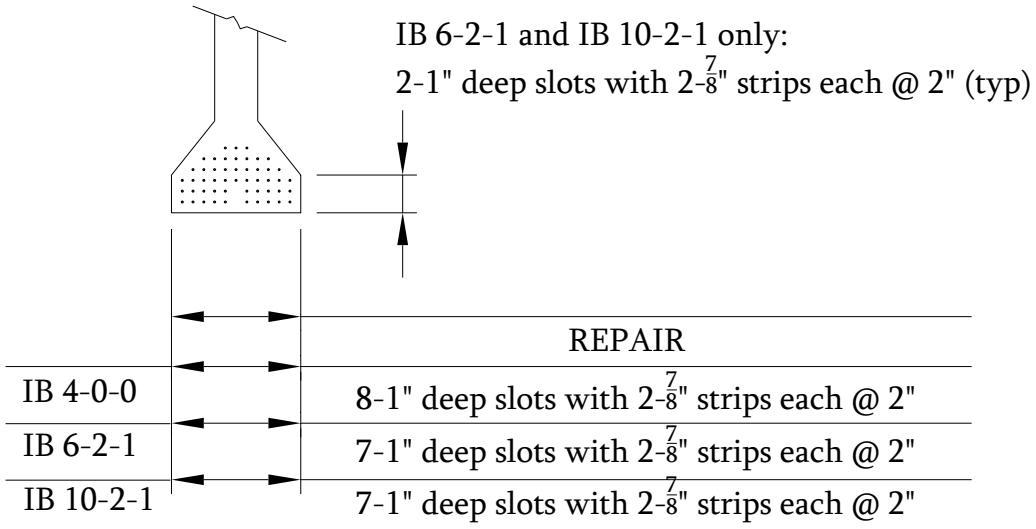

Figure 5-9 NSM repairs.

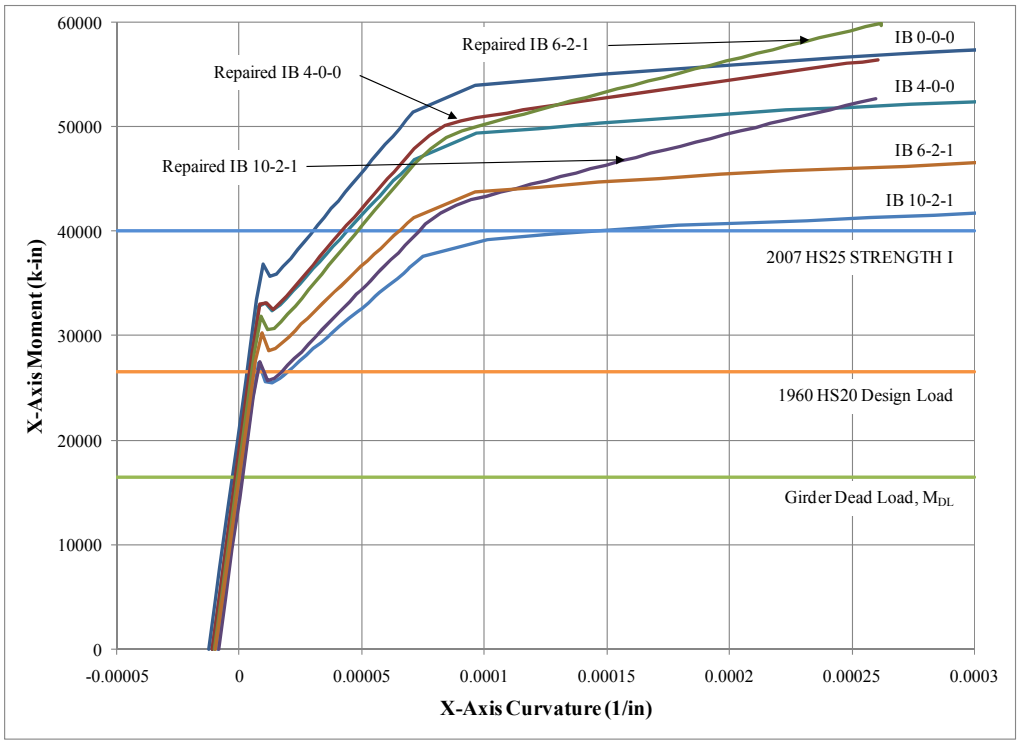

Figure 5-10 NSM repair moment-curvature plot.

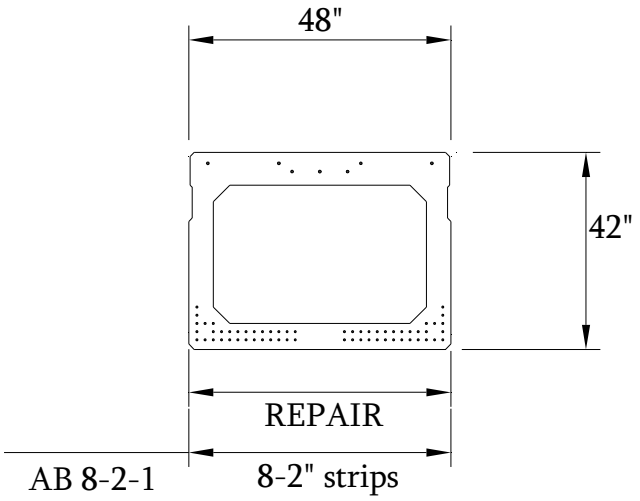

Figure 5-11 Prestressed CFRP repaired AB.

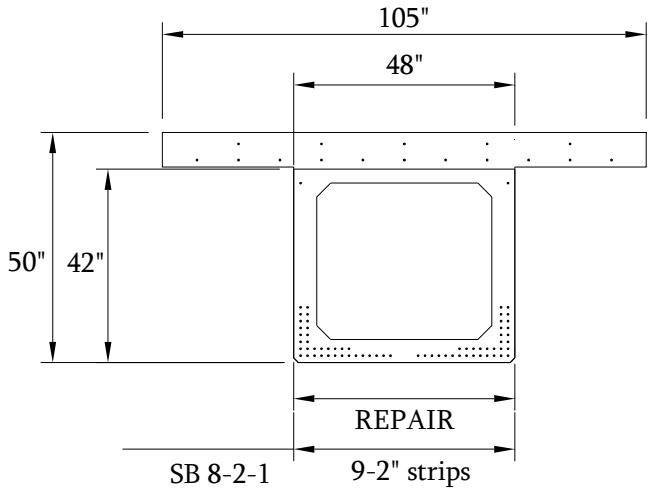

Figure 5-12 Prestressed CFRP repaired SB.

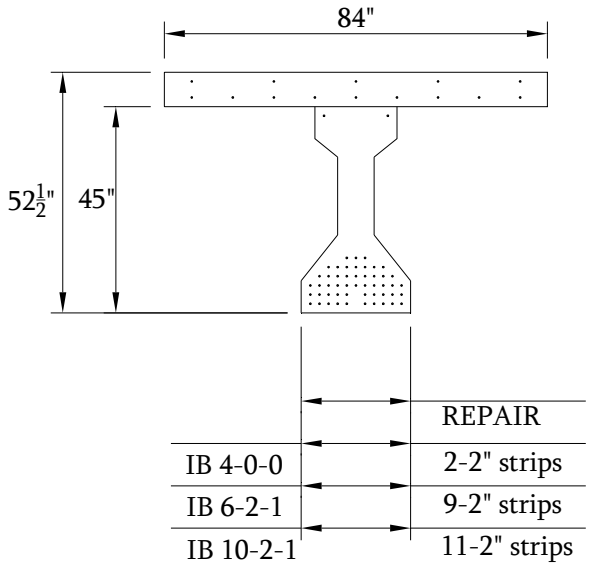

Figure 5-13 Prestressed CFRP repaired IB.

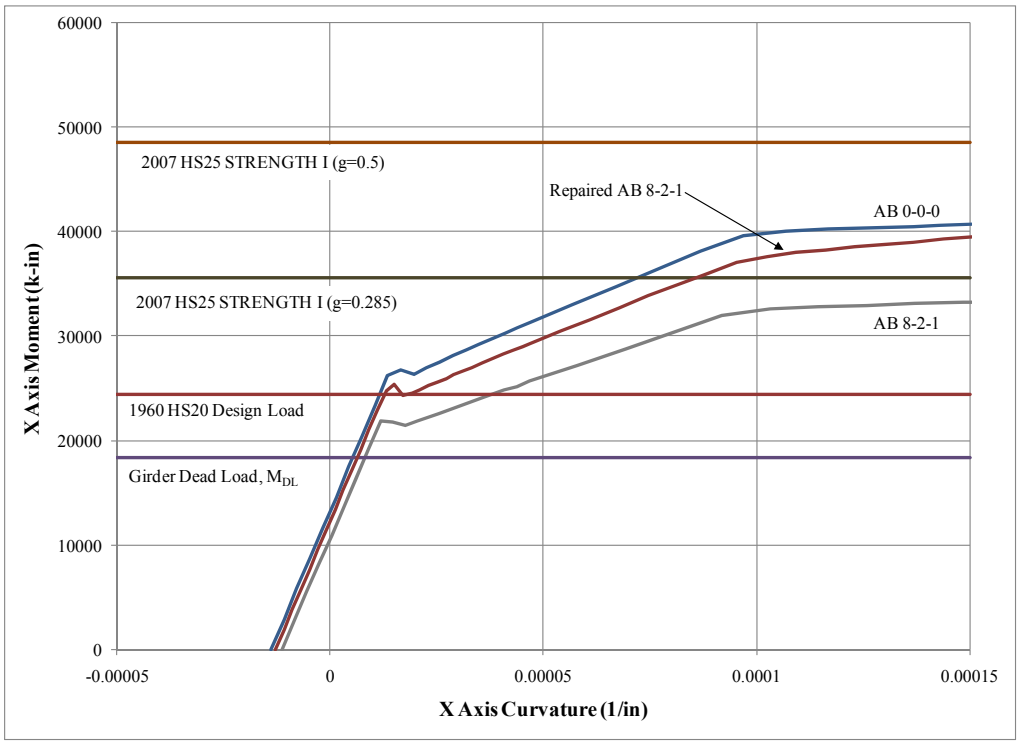

Figure 5-14 Prestressed CFRP repaired AB moment-curvature plot.

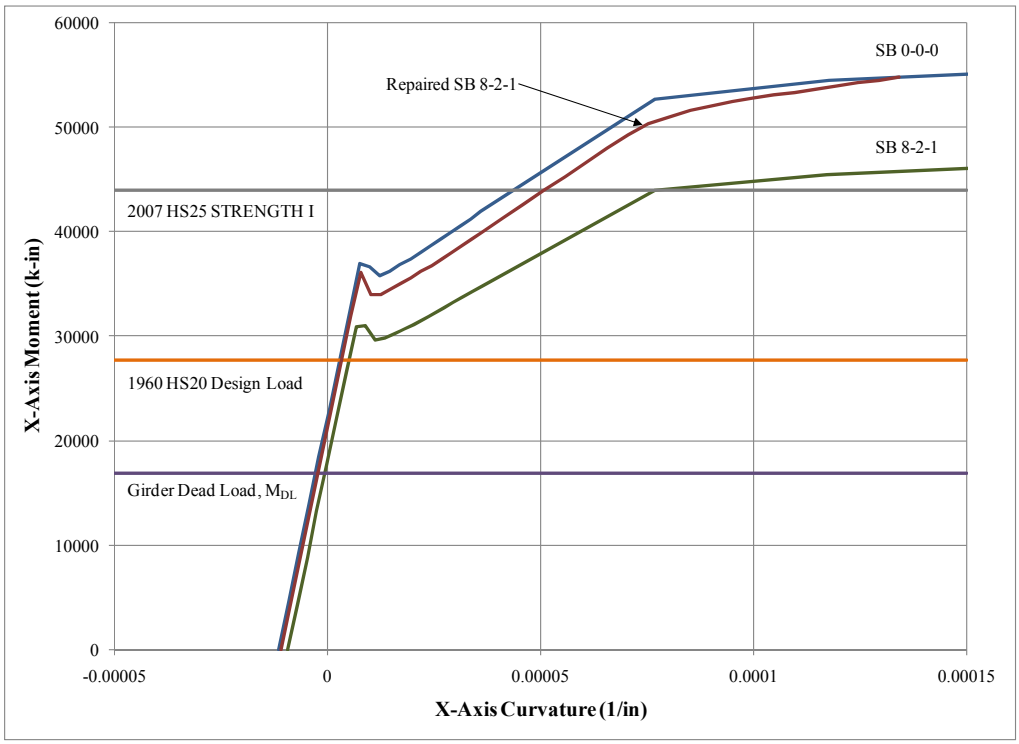

Figure 5-15 Prestressed CFRP repaired SB moment-curvature plot.

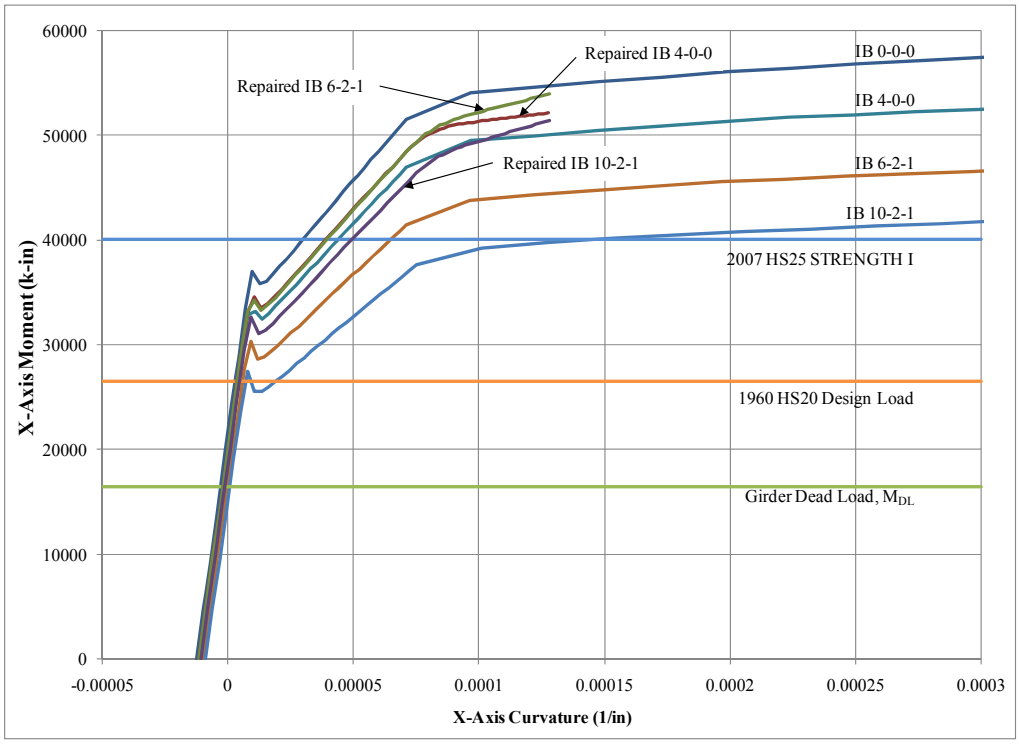

Figure 5-16 Prestressed CFRP repaired IB moment-curvature plot.

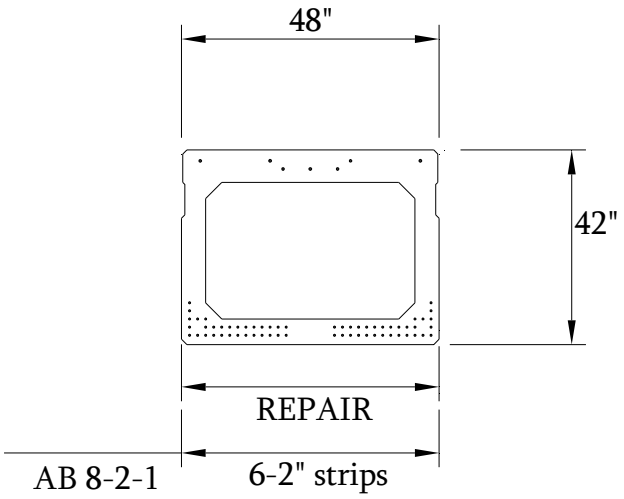

Figure 5-17 Post-tensioned CFRP repaired AB.

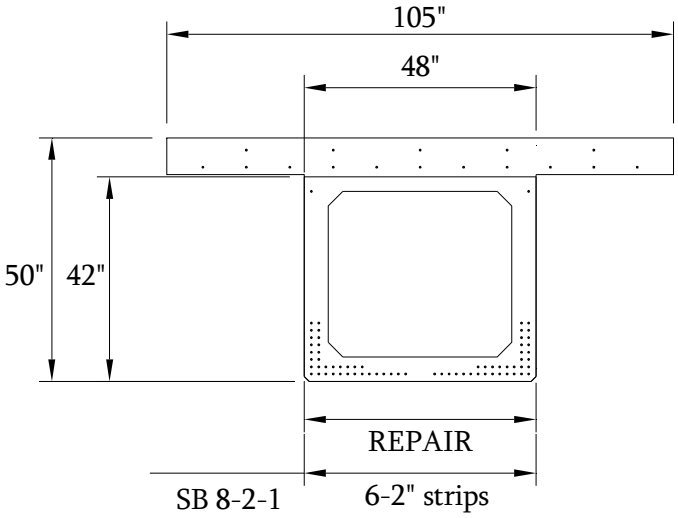

Figure 5-18 Post-tensioned CFRP repaired SB.

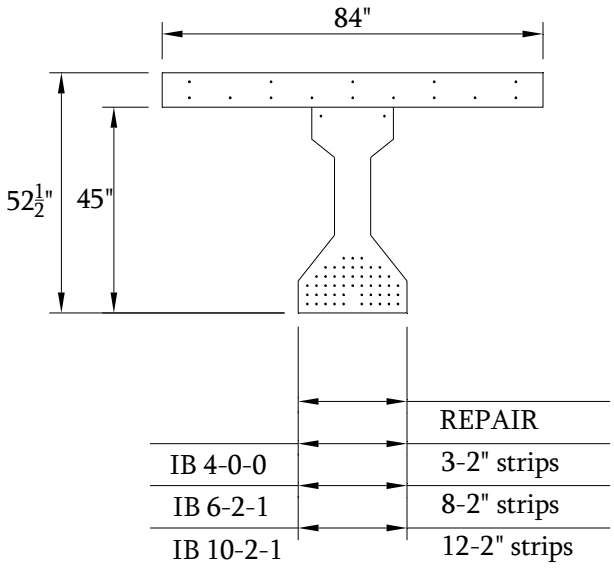

Figure 5-19 Post-tensioned CFRP repaired IB.

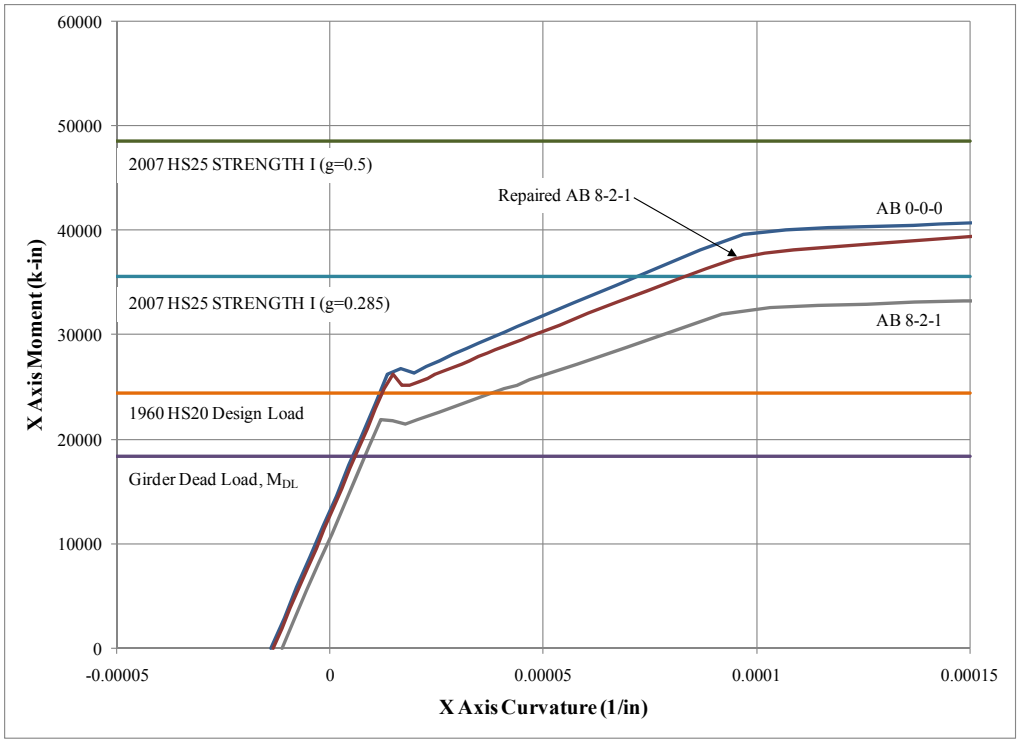

Figure 5-20 Post-tensioned CFRP repaired AB moment-curvature plot.

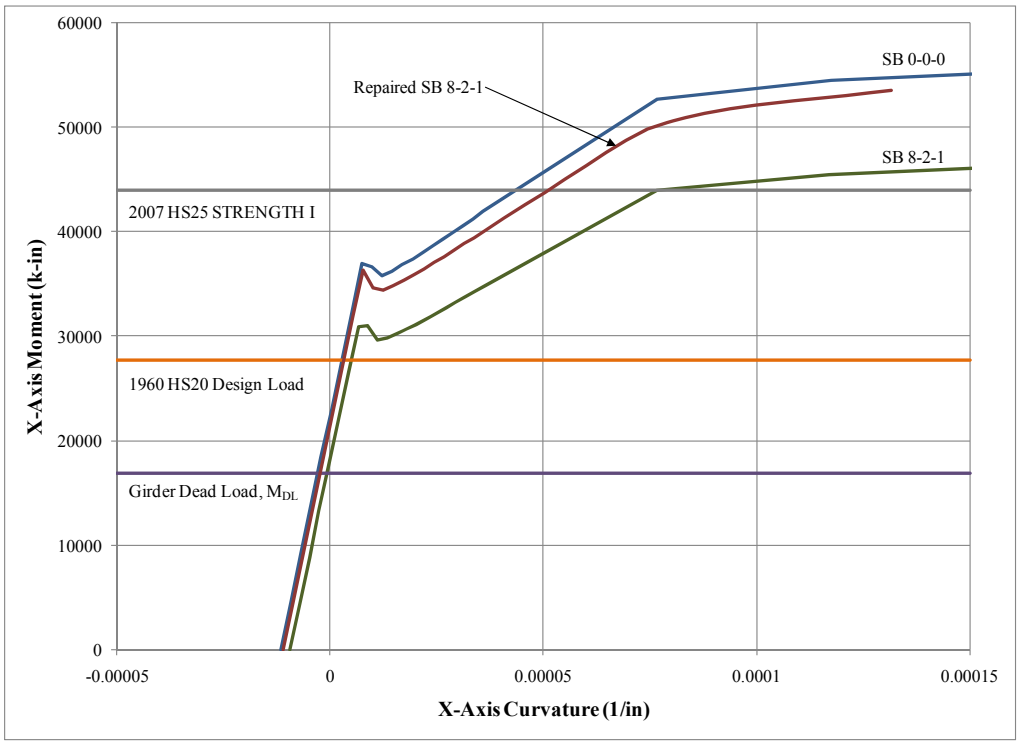

Figure 5-21 Post-tensioned CFRP repaired SB moment-curvature plot.

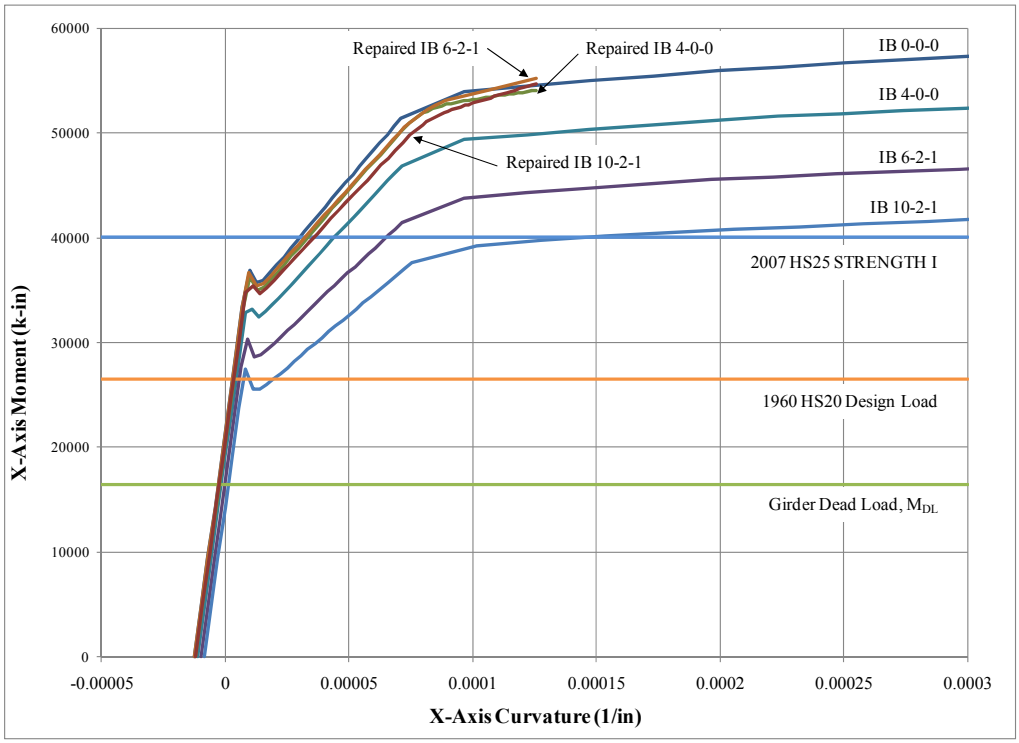

Figure 5-22 Post-tensioned CFRP repaired IB moment-curvature plot.

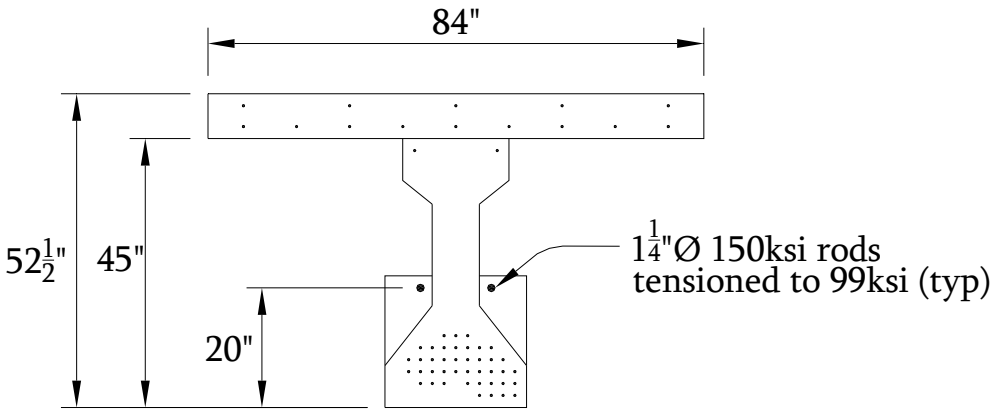

Figure 5-23 External post-tensioned steel repaired IB 6-2-1 drawing.

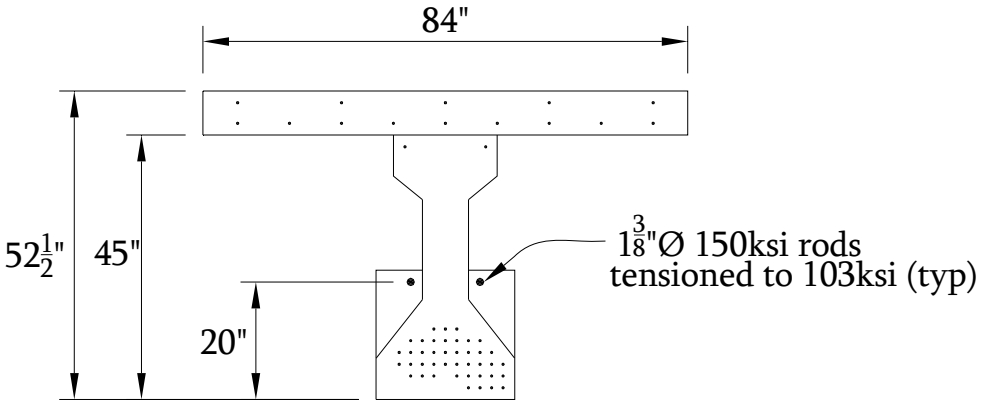

Figure 5-24 External post-tensioned steel repaired IB 10-2-1 drawing.

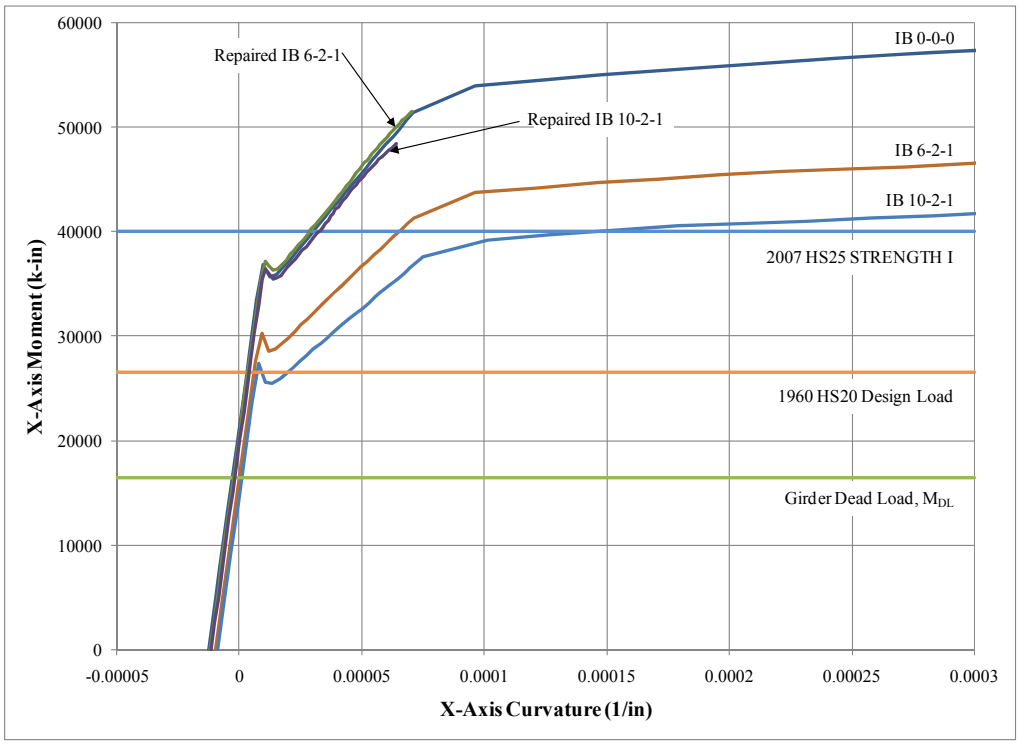

Figure 5-25 External post-tensioned steel repaired IB moment-curvature plot.

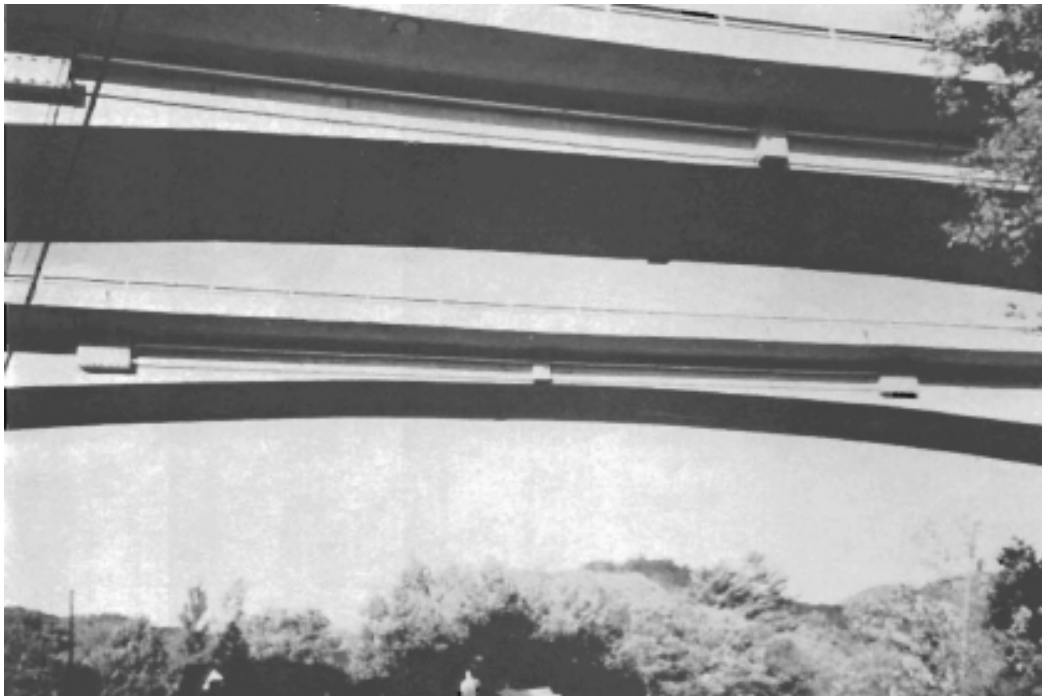

(a) Post-tension tendon retrofit with concrete bolsters (Collins and Mitchell 1997).

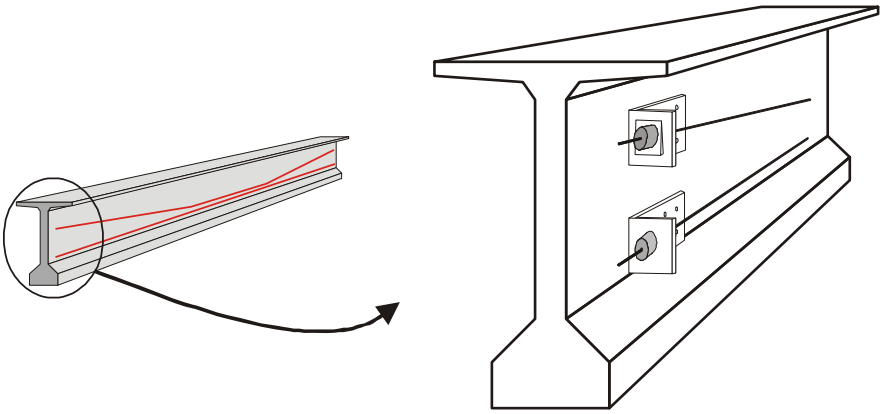

(b) steel angle anchorages for straight or harped strands.

Figure 5-26 Bolster examples.

6.0 CONCLUSIONS, DISCUSSION AND RECOMMENDATIONS

With the continued deterioration of infrastructure and the increase in structurally deficient structures, the need for repair and retrofit strategies and particular measures has become more apparent. In this document, repair methods have been presented for three prototype prestressed concrete highway bridge girder shapes (adjacent boxes (AB), spread boxes (SB), and AASHTO-type I-girders (IB)) having four different damage levels. A total of 22 prototype repair designs are presented. Although not applicable to all structure types or all damage levels, the repair techniques covered include the use of carbon fiber reinforced polymer (CFRP) strips, CFRP fabric, near-surface mounted (NSM) CFRP, prestressed CFRP, post-tensioned CFRP, strand splicing and external steel post-tensioning. It is the author's contention that each potential structural repair scenario should be assessed independently to determine which repair approach is best suited to the unique conditions of a specific project. Therefore, no broad classifications have been presented directly linking damage level (or a range of damage) to specific repair types. Nonetheless, it is concluded that when 25% of the strands in a girder no longer contribute to its capacity, girder replacement is a more appropriate solution. This can be seen most dramatically in the repairs of prototype IB 10-2-1 in which the flexural capacity could not be easily restored. The only instance in which the capacity of IB 10-2-1 was restored was by using external steel post-tensioning (Figure 5-24).

Table 5-4 provides a summary of the target capacities of the beam prototypes; in this study, this value was taken as the capacity of the undamaged girder. Table 5-4 also summarizes the ultimate capacity obtained using each repair approach and the ultimate curvature of the repaired beam at which this capacity was obtained. Despite some repairs failing to achieve their target capacities, the behavior of all examples was improved. This leads to three possible scenarios:

1. The target capacity is achieved and the repair is considered successful.
2. The target capacity is not achieved; however the beam behavior is improved sufficiently to carry required loads. The corollary of this case is that the target capacity is selected only at a level to allow the beam to perform adequately, but not necessarily achieve its original undamaged capacity. That is: the target capacity was selected higher than is necessary to provide adequate performance.
3. The target capacity is not achieved and the beam behavior is not improved sufficiently. In this case an alternate repair method or beam replacement is required. This case permits the limit of each repair method to be assessed.

Additionally, there are some practical limits associated with some of the repair methods presented which may limit their use in certain circumstances; these are discussed further in the following sections.

6.1 DISCUSSION

6.1.1 Damage Assessment and Damaged Girder Rating

Chapter 3 presents a detailed description of observed damage to prestressed concrete bridge members in Southwestern Pennsylvania. NCHRP *Report 226* (Shanafelt and Horn 1980) provides guidance for the assessment and inspection of damaged prestressed concrete bridge girders. Suggestions were given for standardized inspection including proper techniques, tools and forms. Additionally, Harries (2006) provides a guide for inspecting such girders and identifying and assessing damage types. The need to separate the damage assessment tasks (inspection) from the engineering assessment tasks (load rating, etc.) is emphasized by both Shanafelt and Horn (1985) and Harries (2006). A relevant example of damage assessment guidance that should be emphasized is PennDOT's adoption of the '150% rule' for assessing the area of lost prestressing strand: [paraphrasing] *when assessing corrosion damage to a prestressed concrete girder, the area of prestressing strand assumed to be ineffective due to corrosion shall be taken as 150% of that determined by visual inspection*. This guidance, recommended by Harries (2006) and Naito et al. (2006) is believed to conservatively capture the unseen (uninspectable) corrosion of strands adjacent to those damaged by corrosion.

In general, the use of plane sections analysis using standard Whitney stress block factors has been shown to be adequate for assessing the capacity of damaged and repaired girders. Harries (2006) describes some limitations of a plane sections approach for beams having highly eccentric loading or resistance. A parallel study (Russell 2009) has as its objective the simplification of highly eccentric sections such that a plane sections analysis approach may be utilized. In the present work, only sections having nominal eccentricities were considered.

Harries (2006) has shown that these eccentricities have essentially no effect on the capacities derived using conventional plane sections analyses.

A non-linear fiber sections analysis program (*XTRACT)* was used to establish the moment curvature relationships presented in Chapter 5 and girder capacities reported in Table 5-4 for the sections considered. As should be expected, the differences between this analysis and the stress-block approach are small with the code-prescribed stress block approach being somewhat conservative.

6.1.2 Repair Type Selection

The matrices shown in Figure 4-4 present a range of viable repairs for each girder type and do not consider the specific damage level. Nonetheless, the damage level dictates which repair method can be used. For example, in an IB girder, strand splicing is a potential repair approach, but only if a few strands need to be replaced. The geometry of the strand arrangement and strand splice make this method impractical for heavier damage. Although 'percentage of strands lost' appears to be a representative indicator of girder strength, the only correlation found between percentage of lost strands to repair method has been at the level of 25% of strands lost. At this level of damage, repair (restoration of undamaged capacity) becomes impractical (as seen in the case of IB 10-2-1). This is not to say that the girder cannot be repaired, but the resources necessary to repair this girder would be significant and thus replacement may become a more attractive solution.

Often times, the girders have been designed to have a specific stress level at the soffit. To restore this, an active repair (i.e. strand splicing, prestressed or post-tensioned repairs) should be

selected so that as much of the prestressing force is restored as possible. However, when soffit stress is not the main consideration, any of the described techniques, active or passive, may be used.

The repair type chosen must be done so on a project-by-project basis. At this point, it is not feasible to standardize repair type selection based on damage level due to the variability between structures, the unique nature of damage to a particular girder and the original girder's design or stress requirements. Nonetheless, Figure 4-4 provides a summary of viable repair techniques for each scenario and some additional guidelines (rules of thumb) are presented in the following sections.

6.1.3 Repair Technique Applicability

The repair method chosen is a function of the original girder's design considerations such as soffit stress (Preston et al. 1987), girder shape, strand spacing or layout and damage, amongst other factors. Also, the goal of the repair must be considered, i.e. if the repair must restore prestressing force (an active repair) or flexural capacity (achievable with a passive repair). Table 6-1 summarizes the potential applications and a number of selection and design considerations for each repair type. Although specific damage levels are not suggested, this table suggests the limits of applicability of each repair type. Table 6-1 updates and revises the performance comparison matrix presented by Shanafelt and Horn (1980) and presented in Table 2-1. Due to the different bases for comparison (inclusion of CFRP methods), the ranking and practicality of various methods reported by Shanafelt and Horn have changed. For instance, steel jackets are not considered practical. They are cumbersome, untested, and their design, installation and performance are all expected to be exceeded by CFRP methods. While strand splicing is felt to

viable for localized repairs associated with individual impacts, this method is limited by the degree of damage it can reasonably mitigate.

In terms of CFRP methods, non-prestressed methods are well established in both the literature and practice (see Chapter 2). Prestressed or post-tensioned methods are presently limited to proprietary systems and have similarly limited field experience. Nonetheless, post-tensioned CFRP holds great promise for highway bridge applications. NSM CFRP out performs surface-mounted CFRP, however this performance comes at a cost in terms of constructability. Additionally, NSM repairs may be more limited than surface mounted methods due to slot geometry and spacing requirements.

All external methods require protection from the environment. Steel methods may use galvanizing, epoxy coating or encased (unbonded post-tensioning type) strand. CFRP itself requires little environmental protection, although adhesive systems do. Therefore, CFRP systems are often painted with a gel coat to limit moisture intrusion and protect against UV radiation.

External repair methods must also be protected from mechanical damage. Repairs that are attached to the beam soffit encroach upon the roadway clearance below. The only viable method for protecting against mechanical damage is ensuring the repair is not impacted. This therefore, should be an initial design consideration. In general, external CFRP systems are smaller and have a 'lower profile' than steel systems. NSM and strand splicing are internal repairs and have little effect on beam geometry.

Cost and aesthetic rankings given in Table 6-1 are quantitative assessments of the author. Once again, due to the unique nature of each repair project, it is difficult to provide cost efficiency in a general sense.

6.1.4 Girder Shape

As has been discussed in a few instances, girder shape plays a role in repair selection and design. For instance, IB girders have a more vertically distributed arrangement of strands resulting in a higher center of gravity of strands than AB and SB girders. As a result, strands lost on the bottom row in an IB girder have a greater proportional affect on the strand center of gravity (and thus girder capacity) when compared to the same damage for an AB or SB girder. That is, one lost strand has more of an impact on the flexural capacity in an IB girder than for an AB or SB girder. This results in the repairs for IB girders being more substantial as compared to those for AB or SB girders having the same damage level. This can be seen in the repairs presented in this document. Furthermore, the bulb of an IB girder results in certain geometric constraints on the repair. As has been seen, NSM slots are limited and external CFRP requires rounding of the bottom corners in order to be extended up the side of the bulb. Extending the CFRP vertically from the soffit also results in proportionally less efficient use of the CFRP (as its centroid rises).

6.1.5 Ductility

Using ultimate curvatures as an indicator of ductility, it can be seen that passive repair methods are more ductile than active methods. It is believed that the active utilization of the material (i.e. post-tensioning) creates a greater possibility of material yielding and thus a less ductile failure than a passive repair application. This relationship can be seen in Table 5-4. As a result, it is concluded that maximizing an active repair for a girder is not ideal and other solutions

should be investigated. One possibility not considered here is a 'partially prestressed' repair where only a portion of the CFRP provided is post-tensioned.

6.2 FUTURE WORK

6.2.1 Strand 'Redevelopment Length'

In determining the flexural capacity of a damaged structure, the damage strands are discounted over their entire length. Often times, damage is localized and forensic studies have shown that, away from the damage, the strand is still in excellent shape (Harries 2006). Therefore, it is proposed that the damaged strand can redevelop prestressing force (as it extends into sound concrete) and thus contribute to section capacity at some distance away from the damage. As a result, determining this 'redevelopment length' is of importance in order to be certain that the prestressing force has been developed. A small project using the recovered Lake View Drive girders is planned to investigate the redevelopment of severed strand.

6.2.2 Best Practices Document

The work included in this document was funded by PennDOT and will be compiled into a 'best practices' document. For reasons of liability and contractual obligation these specific best practices recommendations cannot be presented here

Table 6-1 Repair Selection Criteria.

Damage Assessment Factor	Repair Method								
	preform CFRP strips	**CFRP fabric**	**NSM CFRP**	**prestressed CFRP**	**PT CFRP**	**PT steel**	**Strand Splicing**	**Steel Jacket[1]**	**Replace Girder**
Damage that may be repaired	Severe I	low Severe I	Severe I	Severe II	Severe II	Severe II	low Severe I	Severe II	Severe III
Active or Passive repair	passive	passive	passive	marginally active	active	active	active or passive	passive or marginally active	n/a
Applicable beam shapes	all	all	IB, limited otherwise	all	all	all	IB, limited otherwise	IB	all
Behavior at ultimate load	excellent	excellent	excellent	excellent	excellent	excellent	excellent	uncertain	excellent
Resistance to overload	limited by bond	limited by bond	good	limited by bond	good	excellent	excellent	uncertain	excellent
Fatigue	limited by bond[2]	limited by bond[2]	good	limited by bond[2]	excellent (unbonded)	excellent	poor	uncertain	excellent
Adding strength to non-damaged girders	excellent	good	excellent	excellent	excellent	excellent	n/a	excellent	n/a
Combining splice methods	possible	possible	unlikely	possible	good (unbonded)	good	excellent	excellent	n/a
Number of strands spliced	up to 25%	limited	limited by slot geometry	up to 25%	up to 25%	up to 25%	few strands	up to 25%	unlimited
Preload for repair[3]	no	no	no	no	no	no	possibly	possibly	n/a
Preload for patch[3]	possibly	no	yes	possibly	possibly	possibly	yes	no	n/a
Restore loss of concrete	patch prior to repair	patch prior to repair	patch prior to repair	patch prior to repair	patch prior to repair	patch prior to repair	excellent	patch prior to repair	n/a
Constructability	easy	easy	difficult	difficult	moderate	moderate	difficult	very difficult	difficult
Speed of repair	fast	fast	moderate	moderate	moderate	moderate	fast	slow	very slow
Environmental impact of repair process	VOCs from adhesive	VOCs from adhesive	VOCs from adhesive & concrete sawing dust	VOCs from adhesive	minimal	minimal	minimal	welding	typical erection issues
Durability	requires environmental protection	requires environmental protection	excellent	requires environmental protection	requires environmental protection	requires corrosion protection	excellent	requires corrosion protection	excellent
Cost	low	low	moderate	moderate	moderate	low	very low	moderate	high
Aesthetics	excellent	excellent	excellent	excellent	fair	fair	excellent	excellent	excellent

n/a: not applicable

[1] Due to their complexity and the fact that they are untested, steel jacket repairs are not recommended; it is believed that CFRP repairs address all advantages of steel jackets while overcoming some of their drawbacks.

[2] see Harries et al. (2006) for a discussion of fatigue of bonded CFRP repair systems.

[3] Preload may be required for the repair or simply to pre-compress associated concrete patches. Jackets render the need to pre-compress the patch unnecessary.

APPENDIX A

BRIDGE DRAWINGS

A.1 BRIDGE LV

Structural drawings for bridge LV (Spancrete 1960).

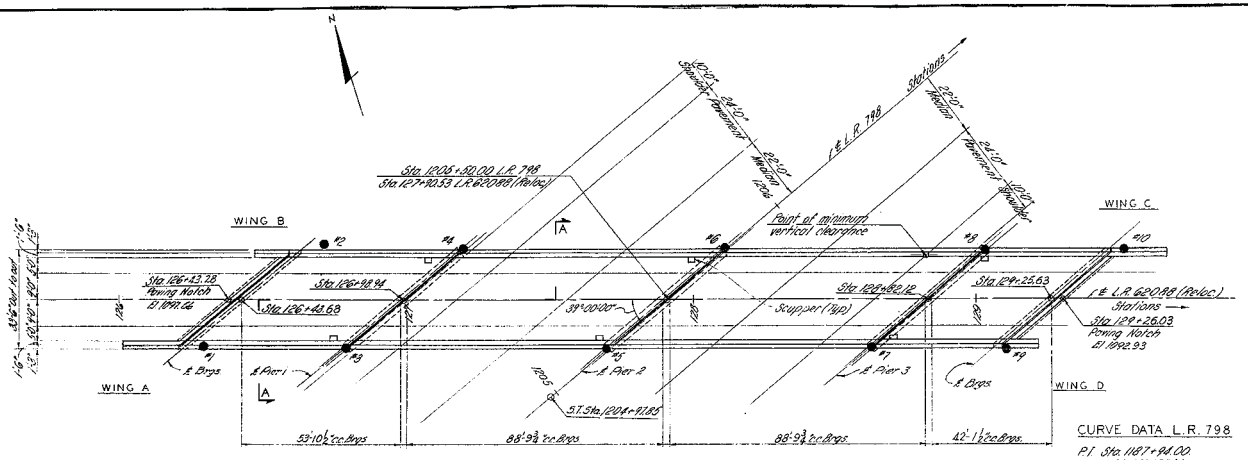

● — Indicates core boring location

PLAN
Scale 1" = 20'

CURVE DATA L.R. 798

P.I. Sta. 1187+94.00
Δ = 18°-14'-16" Lt.
D = 2°-00'
Rn = 2864.93'
Ls = 150.00'
θs = 1°-30'
Ts = 275.04'
Es = 10.60.42'
Lc = 4181.09'
p = 0.63'
k = 75.00'
Superelevation = ⅜"/Ft.

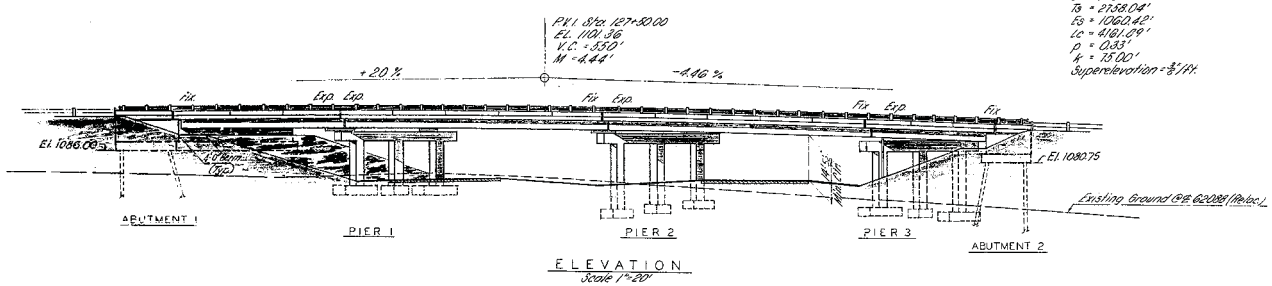

ELEVATION
Scale 1" = 20'

NOTES:

1 — Live load: H 20-S 16-44.
2 — Design: A.A.S.H.O. Standard Specifications for Highway Bridges (1953)
Earth pressure: 120 lbs/cu.ft. vertical; 35 lbs/cu.ft. fluid pressure, horizontal
3 — Specifications: — Penna. Depart ment of Highways Forms 408 (1954) and 409 (1949).
4 — All superstructure concrete shall be Class A. All abutment concrete shall be Class B except wingwall parapets which shall be Class A. All concrete in piers shall be Class A except footings which shall be Class B.
4a. Embankment shall be thoroughly compacted up to bottom elevation of Abutment before driving piles.
5 — All exposed concrete edges shall have a 1"x1" chamfer unless noted.
6 — Reinforcement bars are designed for fs = 18,000 psi & are detailed in accordance with A.C.I. recommendations.
7 — All reinforcement bars carrying design or temperature stresses shall be lapped at least 40 diameters where splicing is required.
8 — The bases of the structure may be ordered by the Engineer to be at any elevation or at any dimensions necessary to provide a proper foundation.
9 — Place two-coat painted waterproofing on top of footing heels and on rear face of abutment walls and wingwalls up to a line 1'0" below top of finished grade.
10 — Fabricated structural steel shall be A.S.T.M. designation A7, current
11 Provide 2" Cover on reinforcement bars unless otherwise Noted.
12 — W.P. - denotes Work Point.
13 — For parapet railing and guard fence connections, see P.D.H. Std. Dwgs. [illegible]
14 — Prestressed, Precast beams shall be designed in accordance with Pennsylvania Department of Highways Specifications Form 408 (1954) Supplement Section 6.24 (1958) [illegible]
15 — All piles shall be steel beam piles 10 BP 42.
16 — Piles shall be driven to refusal, or to practical refusal as directed by the Engineer but, in no case, to a bearing value less than 70 Tons for Test Piles and 50 Tons for Bearing Piles.
17 — All dowels in Pier Cap shall be set in preformed holes. Drilling of holes for dowels in Pier Cap will not be permitted.
18 — All Parapet, Parapet Railing will be considered a part of the Bridge Superstructure.

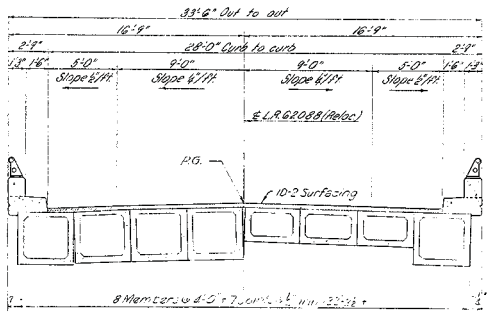

SECTION A-A
Scale 4'-1-0"

QUANTITIES

Item	Cu. Yds. Class 3 Excavation	Cu. Yds. Class A Concrete	Sq. Ft. Prestressed Precast Conc. Box Beam	Cu. Yds. Class B Concrete	Lbs. Reinforcement Bars	Lbs. Fabricated Structural Steel	Lin. Ft. Parapet Railing	Steel Beam Piles 10 BP 42		Each Guard Fence Connections	Sq. Yds. Bituminous Surface 10-2
								Test Piles	Lin. Ft.		
Abutment 1	—	4	—	104	5,530	—	27	1 @ 20'	300	2	—
Pier 1	98	46	—	25	13,840	—	—	—	—	—	—
Pier 2	89	49	—	18	17,440	—	—	—	—	—	—
Pier 3	74	53	—	25	15,310	—	—	—	—	—	—
Abutment 2	—	4	—	108	5,590	—	27	1 @ 32'	470	2	—
Superstructure	—	114	9,143	—	8,770	6450	570	—	—	—	878
Totals	261	270	9,143	280	66,480	*6450	624	Lump Sum	770	4	878

* Includes: 3720 Lbs. Malleable Iron or Cast Steel
2340 Lbs. Wrought Iron

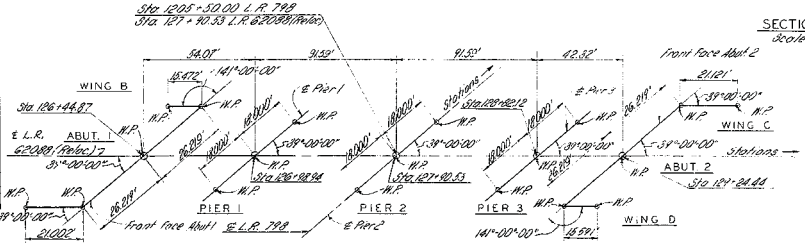

STAKE-OUT PLAN
Not to Scale

These drawings supersede S-3661 Approved June 16, 1959

PRESTRESS ALTERNATE REVISIONS BY
MACOMBER & FABER
CONSULTING ENGINEERS
HARRISBURG, PENNA.

PREPARED BY
GROF & MYERS
CONSULTING ENGINEERS
HARRISBURG, PENNA.

APPROVED JUN 13 1960
BRIDGE ENGINEER

Commonwealth of Pennsylvania
Department of Highways
BRIDGE UNIT
WASHINGTON COUNTY
L.R. 798 SECTION 1
L.R. 798 UNDER L.R. 62088 (RELOC)
GENERAL PLAN
STA. 1205+5000
SCALE: AS NOTED
SHEET 1 OF 6 + S-1614 B, S-3361

S-3661 A

DESIGNED F.S.F.
DRAWN H.N.W.
TRACED H.N.W.
CHECKED E.R.L.

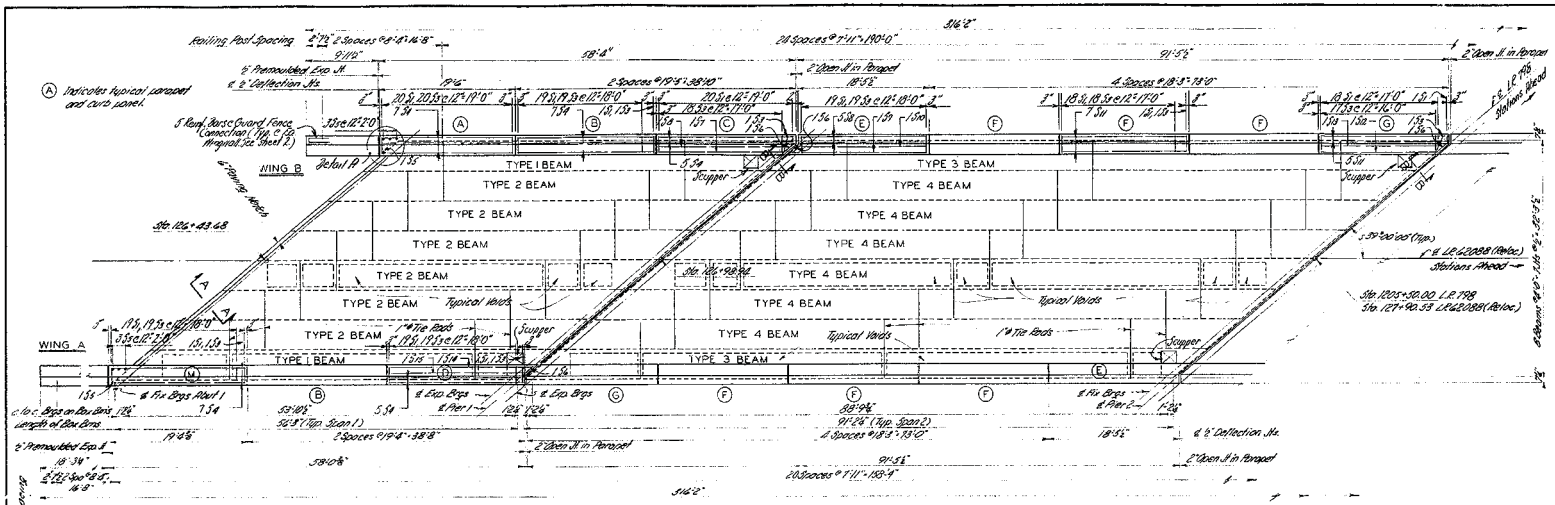

PLAN - SPANS 1 & 2

Scale: 1/8"=1'-0"

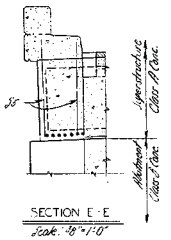

SECTION E-E

Scale: 1/8"=1'-0"

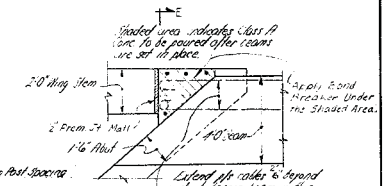

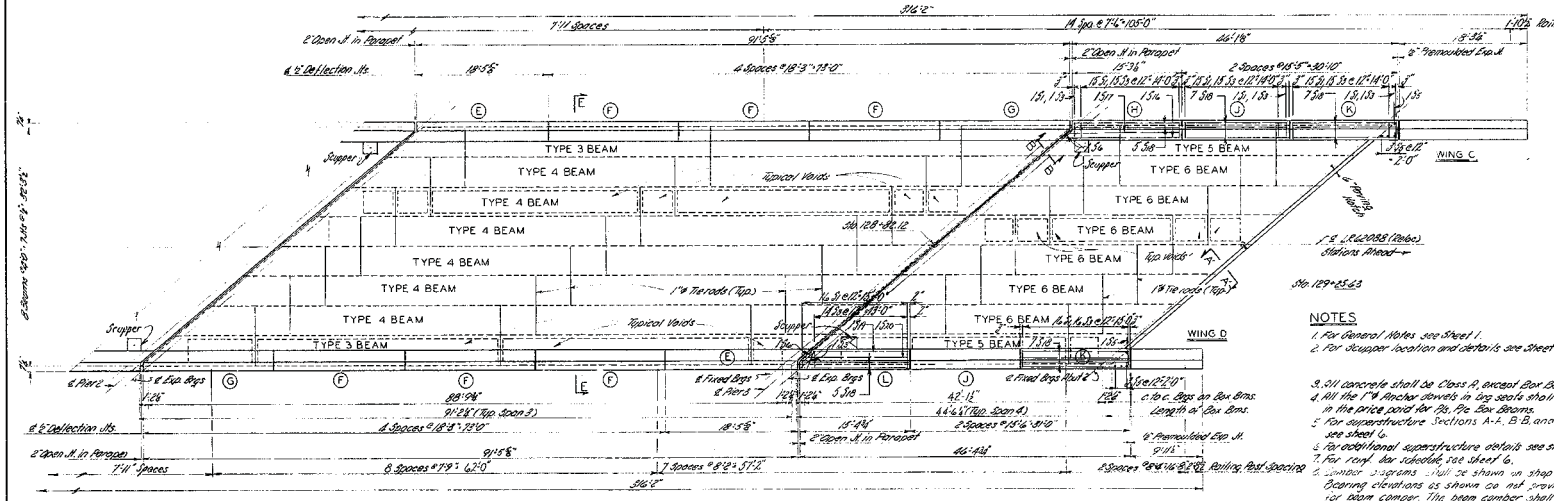

PLAN - SPANS 3 & 4

Scale: 1/8"=1'-0"

Approved: JAN 13 1961

R H Jensen
Bridge Engineer

NOTES

1. For General Notes see Sheet 1.
2. For Scupper location and details see sheet 7.
3. All concrete shall be Class A, except Box Beams.
4. All the 1"ø Anchor dowels in big seats shall be included in the price paid for Rs, Rc Box Beams.
5. For superstructure Sections A-A, B-B, and E-E see sheet 6.
6. For additional superstructure details see sheet 6.
7. For roof. bar schedule, see sheet 6.
8. Lumber diagrams shall be shown on shop drawings. Bearing elevations as shown do not provide for beam camber. The beam camber shall be checked by the contractor. If the beam camber exceeds the vertical curve ordinate for its span, the bearing elevations or slab thickness shall be adjusted accordingly at no additional cost to P.D.H.

1	Revised Detail 'A' to Clarify.	H.M.U.	H.E.L.	8-15-60
NO.	REVISION	BY	CH'KD	DATE

Commonwealth of Pennsylvania

Department of Highways

BRIDGE UNIT

WASHINGTON COUNTY

L.R. 798 SECTION 1

L.R.798 UNDER L.R.62088(RELOC)

SLAB PLAN

STA 1205+50.00

SCALE AS NOTED

SHEET 5 OF 8

S-3661-A

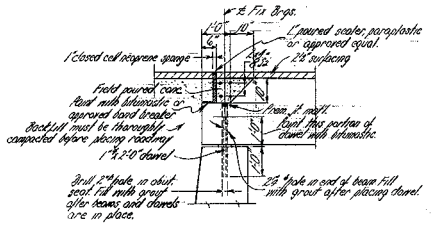

SECTION A - A
SECTION A'-A' SIMILAR
Scale: ½"=1'-0"

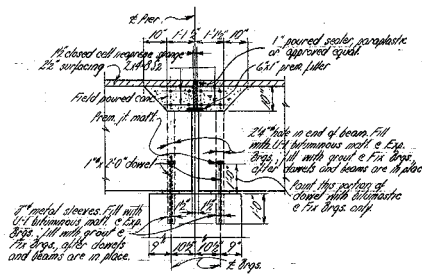

Note: Dowels, dowel holes and sleeves occur in all beams at Fix Brgs. and in fascia beams only at Exp. Brgs.

SECTION B - B
Scale: ½"=1'-0"

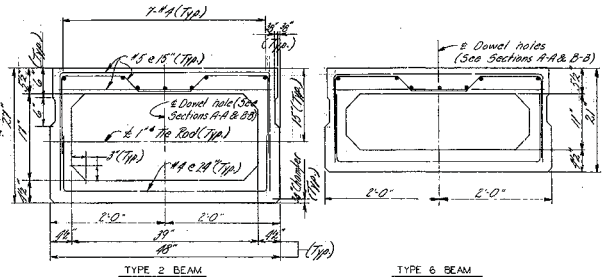

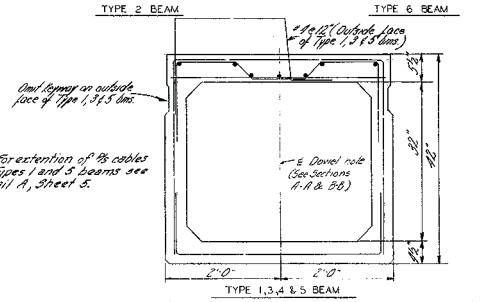

Note: For extention of Ps cables on Types 1 and 5 beams see Detail A, Sheet 5.

Number and size of strands, location of c.g. and concrete stress of release of prestress to be shown on shop detail drawings.

TYPICAL SECTIONS - PRESTRESSED MEMBERS
Scale: 1"=1'-0"

REINF BAR SCHEDULE									
MK	NUMBER	SIZE	LENGTH	TYPE	A	B	C	D	REMARKS
S1	594	4	6'-3"	1	1'-6"	11"	3"		
S2	64	6	27'-3"	Str.					
S3	590	4	2'-6"	Str.					
S4	28	4	19'-0"	Str.					
S5	16	4	3'-9"	Str.					
S6	12	4	3'-0"	Str.					
S7	1	4	17'-3"	Str.					
S8	21	4	19'-0"	Str.					
S9	4	4	19'-6"	Str.					
S10	4	4	18'-9"	Str.					
S11	104	4	17'-9"	Str.					
S12	4	4	16'-0"	Str.					
S13	4	4	16'-9"	Str.					
S14	1	4	20'-6"	Str.					
S15	1	4	19'-9"	Str.					
S16	1	4	16'-6"	Str.					
S17	1	4	15'-9"	Str.					
S18	83	4	15'-0"	Str.					
S19	1	4	14'-3"	Str.					
S20	1	4	14'-0"	Str.					

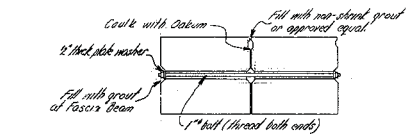

INTERBEAM CONNECTION
Not to Scale

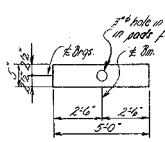

Neoprene bearing pads to be durometer hardness = 60
Spans 1 & 4 - 1" thick pads:
Spans 2 & 3 - 1¼" thick pads:
72 pads 3"x 1"x 5'-0" without holes.
80 pads 3"x 1"x 5'-0" with holes
16 pads 5"x 1¼"x 5'-0" without holes:
20 pads 5"x 1¼"x 5'-0" with holes.

BEARING PADS
Not to Scale

FOR NOTES SEE SHEETS 1 & 5.

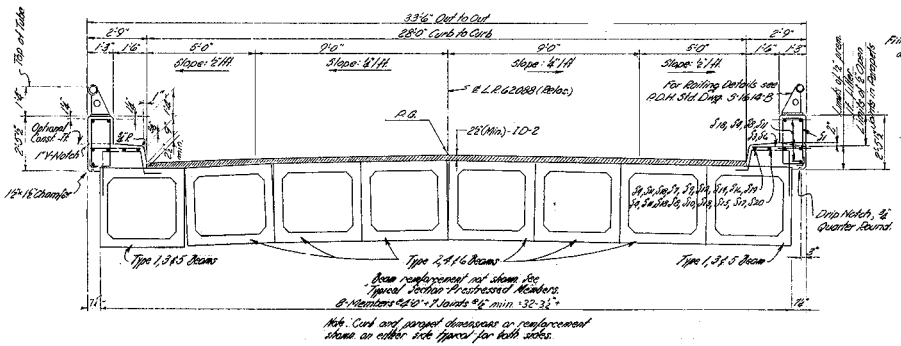

SECTION E-E
Scale: ⅜"=1'-0"

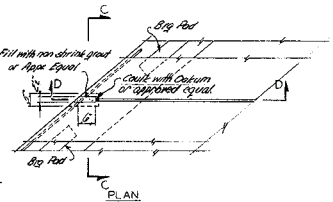

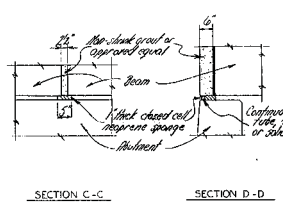

WATERPROOFING DETAIL
Scale: ½"=1'-0"

Approved: JUN 13 1980
Bridge Engineer

Commonwealth of Pennsylvania
Department of Highways
BRIDGE UNIT

WASHINGTON COUNTY
L.R.798 SECTION 1
L.R.798 UNDER L.R.62088 (RELOC)

SUPERSTRUCTURE DETAILS
STA. 1205 +50.00

SCALE: AS NOTED
SHEET 6 OF 8

S-3661-A

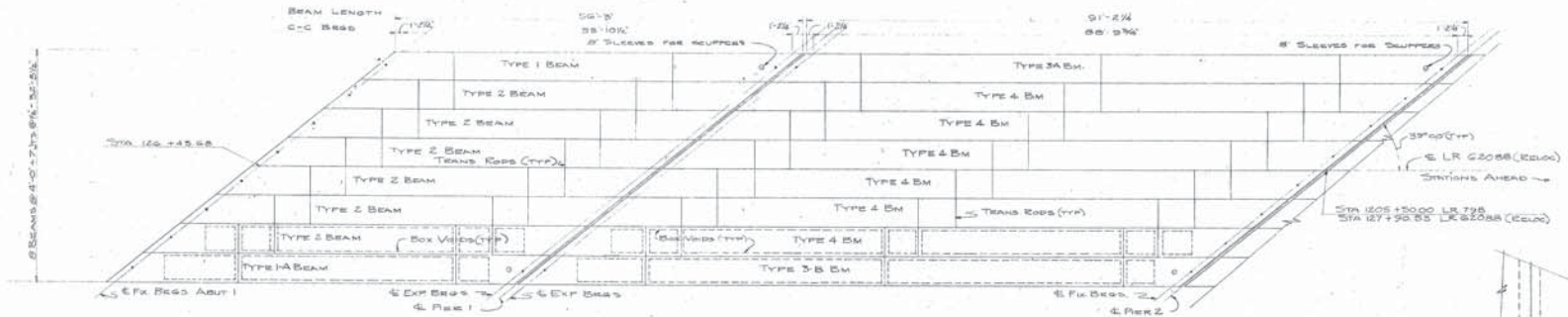

BEAM LAYOUT - SPANS 1 & 2

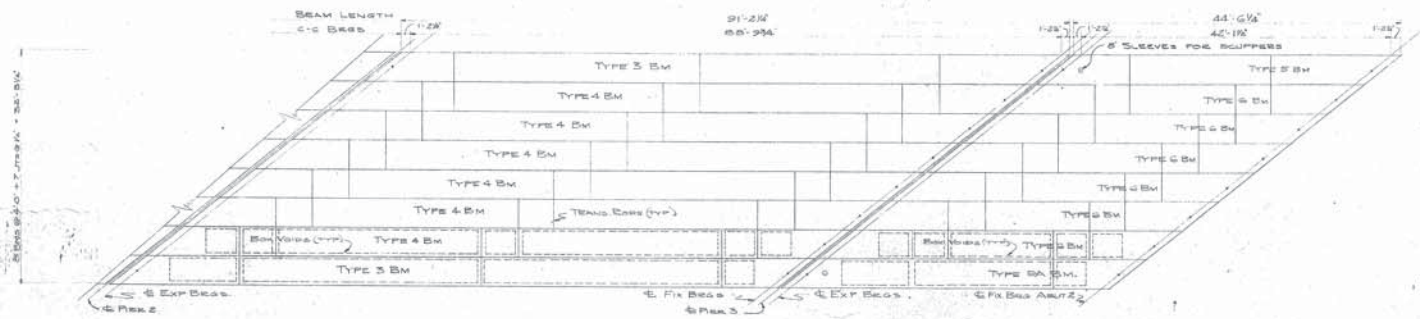

BEAM LAYOUT - SPANS 3 & 4

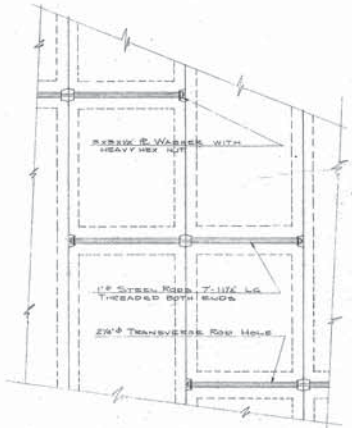

BEARING PADS

DETAIL SHOWING TRANSVERSE ROD CONNECTIONS AT DIAPHRAM

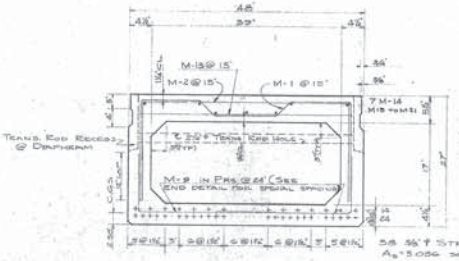

TYPE 2 BEAM

NOTE:
BUEN STRAND OFF FLUSH EXCEPT WHERE INDENTED AND PAINT WITH TWO COATS OF BITUMASTIC PAINT.

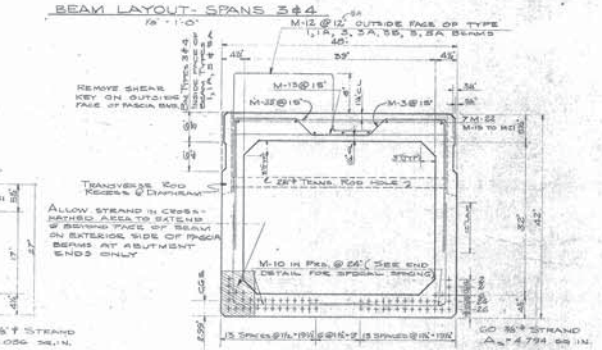

TYPE 1, 1A, 3, 3A, 3B, 4, 5, 5A BEAMS

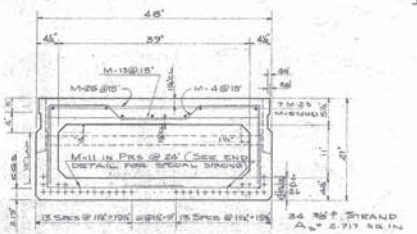

TYPE 6 BEAM

TYPICAL BEAM SECTIONS

PRESTRESS NOTES:
MINIMUM STRAND STRENGTH = 250,000 PSI
MINIMUM CONCRETE STRENGTH @ 28 DAYS
TYPE 1, 1A, 3, 3A, 3B, 4, 5, 5A BMS 5900 PSI
TYPE 2 & 6 BEAMS 6000
MINIMUM CONCRETE STRENGTH AT RELEASE
TYPE 1, 1A, 3, 3A, 3B, 4, 5, 5A BMS 4600 PSI
TYPE 2 & 6 BEAMS 4800
INITIAL PRESTRESS ON EACH ⅝" ϕ STRAND 19000 #

DICKERSON STRUCTURAL CONCRETE

SPANCRETE

JOB: WASHINGTON BRIDGE @ S
FOR: MARSOLINO PA. DEPT.
DATE: 6-28-60

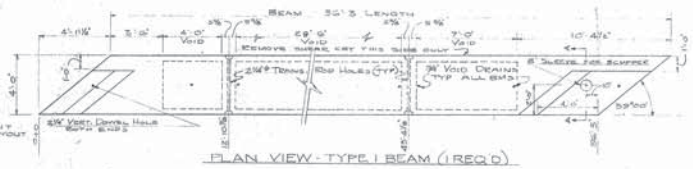

PLAN VIEW - TYPE 1 BEAM (1 REQ'D)

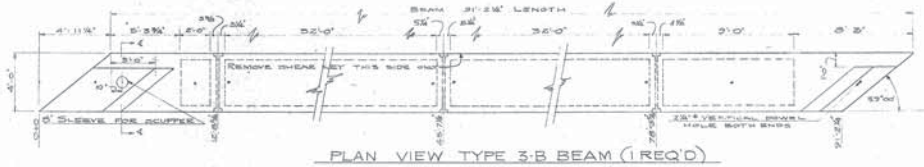

PLAN VIEW TYPE 3-B BEAM (1 REQ'D)

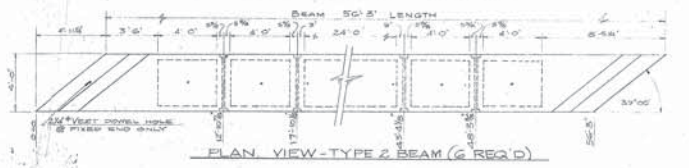

PLAN VIEW - TYPE 2 BEAM (6 REQ'D)

PLAN VIEW TYPE 5 BEAM (1 REQ'D)

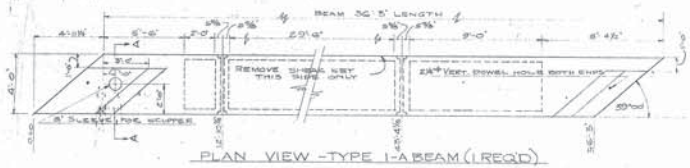

PLAN VIEW - TYPE 1-A BEAM (1 REQ'D)

PLAN VIEW - TYPE 6 BEAM (6 REQ'D)

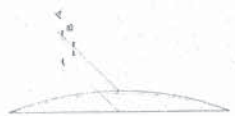

A ESTIMATED CAMBER TO BE CHECKED BY CONTRACTOR IN FIELD
B DEFLECTION DUE TO PRIMARY & WEARING SURFACE

SPANS	1	2 & 3	4
A	0.89	1.33	0.85
B	0.21	0.56	0.16

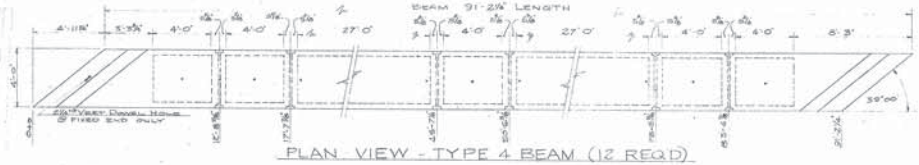

PLAN VIEW - TYPE 4 BEAM (12 REQ'D)

PLAN VIEW - TYPE 5A BEAM (1 REQ'D)

PLAN VIEW - TYPE 3 BEAM (2 REQ'D)

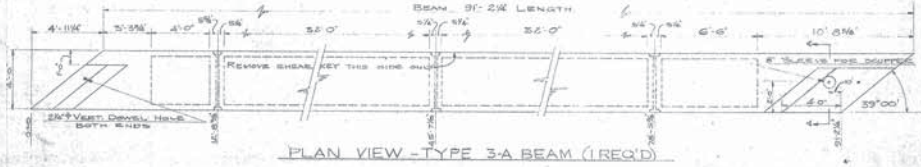

PLAN VIEW - TYPE 3-A BEAM (1 REQ'D)

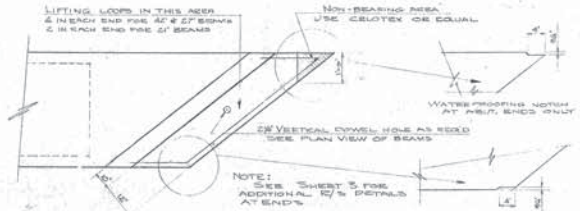

PLAN VIEW - ENDS OF BEAMS

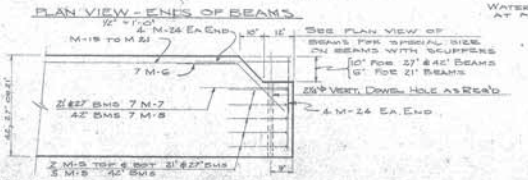

ELEVATION - PARALLEL TO SKEW

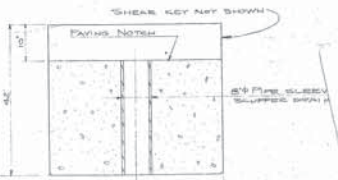

SECTION A-A

PENNA. DEPT. OF HWYS. APPROVED AS TO DESIGN AUG 10 1960

DICKERSON STRUCTURAL CONCRETE CORPORATION

SPANCRETE

JOB: WASHINGTON CO. LR. 798-1 BRIDGE @ STA 1205+50.00
FOR: MARSOLINO CONST. CO PA. DEPT. OF HIGHWAYS
DATE: 7-1-60 DRWN.: C.G.B. APPROVED:
SHEET 5 OF 5 SHTS
JOB NO. 6014

REF. DWG. S-3661 A
P-3661

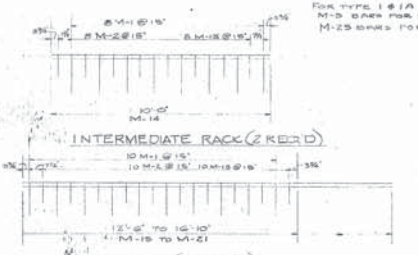

INTERMEDIATE RACK (2 REQ'D)

END RACK (2 REQ'D)

REINFORCING RACK LAYOUT
BEAM TYPES 1 & 2

INTERMEDIATE RACK (1 REQ'D)

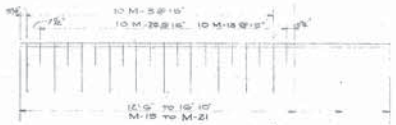

END RACK (2 REQ'D)

REINFORCING RACK LAYOUT
BEAM TYPES 3 & 4

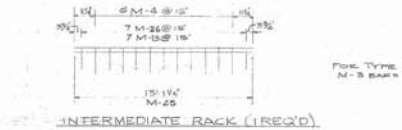

INTERMEDIATE RACK (1 REQ'D)

END RACK (2 REQ'D)

REINFORCING RACK LAYOUT
BEAM TYPES 5 & 6

FOR TYPE 1 & 1A BMS. SUBSTITUTE M-3 BARS FOR M-1 BARS & M-23 BARS FOR M-2 BARS

BAR LIST

MARK	NUMBER	SIZE	LENGTH	DESCRIPTION
M-1	216	5	7'-4"	BENT
M-2	216	5	7'-2"	"
M-3	1086	5	8'-2"	"
M-4	180	5	6'-2"	"
M-5	224	6	9'-10"	"
M-6	448	6	4'-0"	"
M-7	224	6	2'-9"	"
M-8	224	6	4'-0"	"
M-9	300	4	3'-6"	"
M-10	1576	4	4'-8"	"
M-11	234	4	3'-2"	"
M-12	320	4	5'-1"	BENT
M-13	1464	5	5'-3"	STRAIGHT
M-14	112	4	10'-0"	"
M-15	54	4	12'-6"	"
M-16	64	4	15'-7"	"
M-17	64	4	13'-11"	"
M-18	64	4	14'-8"	"
M-19	64	4	15'-5"	"
M-20	64	4	16'-3"	"
M-21	64	4	16'-10"	"
M-22	448	4	15'-9"	"
M-23	56	4	8'-11½"	"
M-24	1352	4	2'-0"	STRAIGHT (SPL)
M-25	1064	5	8'-2"	BENT
M-26	182	5	6'-0"	"
M-9A	360	4	4'-6"	"
M-10A	3200	4	5'-5"	"
M-11A	360	4	4'-2"	BENT

LIST OF MATERIALS

NUMBER	UNITS	DESCRIPTION
118,200	L.F.	3/8" Prestressing Strand
24	Pcs.	39"x17" Box Voids 4'-0" LG
6	Pcs	39"x17" " " 24'-0" LG
68	Pcs	39"x32" " " 4'-0" LG
8	Pcs	39"x32" " " 21'-0" LG
1	Pcs	39"x32" " " 71'-0" LG
5	Pcs	39"x32" " " 31'-0" LG
2	Pcs	39"x32" " " 29'-6" LG
2	Pcs	39"x32" " " 18'-0" LG
2	Pcs.	39"x32" " " 6'-6" LG
24	Pcs	39"x32" " " 27'-0" LG
8	Pcs	39"x32" " " 52'-0" LG
24	Pcs	39"x11" " " 4'-0" LG
6	Pcs	39"x11" Box Voids 31'-0" LG
712	L.F.	2¼" Type 'A' Sandvoid
70	Pcs	1" Transverse Rods 7'-11½" LG
140	Pcs	5"x5"x½" ℄ Washers
140	Pcs	1" Heavy Hex Nuts
190	Pcs	¾" Fascia Forming Inserts
36	Sq.Ft.	¾" Thick Celotex or Equal

BEAM CONCRETE QUANTITIES AND WEIGHTS

BEAM TYPE	CONCRETE PER BEAM (CU YDS)	SHIPPING WEIGHT (TONS)
1 & 1A	10.1	55.8
2	11.9	24.9
3	22.6	47.4
3A & 3B	23.4	49.0
4	23.9	50.0
5 & 5A	12.4	25.9
6	8.2	17.2

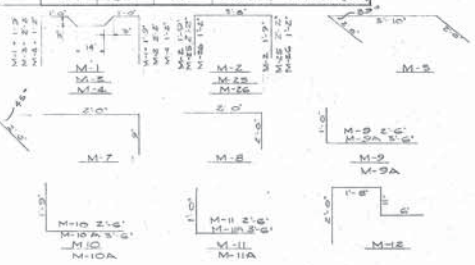

NOTE:
CUT STEEL TO FIT IN BEAMS WITH LARGE PAVING NOTCHES

FOR TYPE 5 & 5A BMS. SUBSTITUTE M-3 BARS FOR M-4 BARS

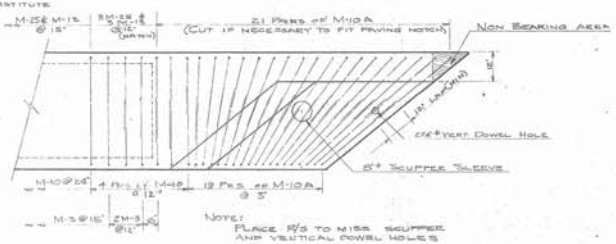

REINFORCING DETAILS ON
BEAM ENDS WITH SCUPPERS
½" = 1'-0"

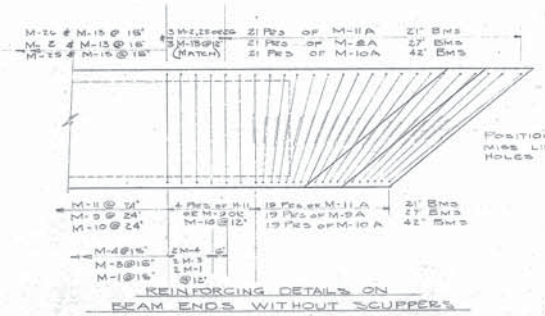

REINFORCING DETAILS ON
BEAM ENDS WITHOUT SCUPPERS

PENNA. DEPT. OF HWYS.
APPROVED AS TO DESIGN
AUG 10 1960

DICKERSON STRUCTURAL CONCRETE CORPORATION

SPANCRETE

WASHINGTON CO. LR 798-1
BRIDGE @ STA. 1205+80.00

MARSOLINO CONST. CO.
PA. DEPT. OF HIGHWAYS

DATE: 5-5-60 DRWN.: C.G.B. APPROVED:

SHEET 3 / 3

JOB NO. 6014

REF. DWG. S-3661A

P-3661

A.2 BRIDGE A

Structural drawings for bridge A (PADoH 1960c).

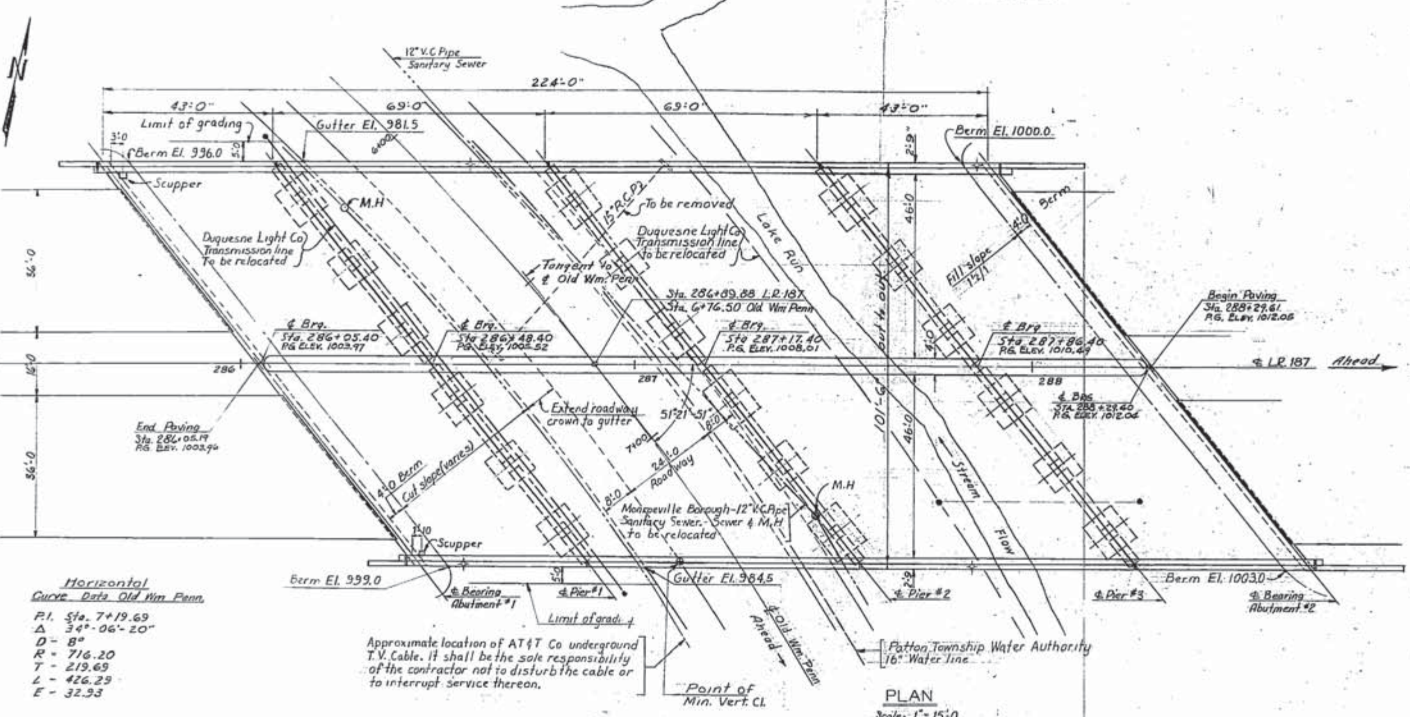

Horizontal Curve Data Old Wm Penn

P.I. Sta. 7+19.69
Δ 34°-06'-20"
D - 8°
R - 716.20
T - 219.69
L - 426.29
E - 32.93

PLAN

Scale: 1" = 15'-0

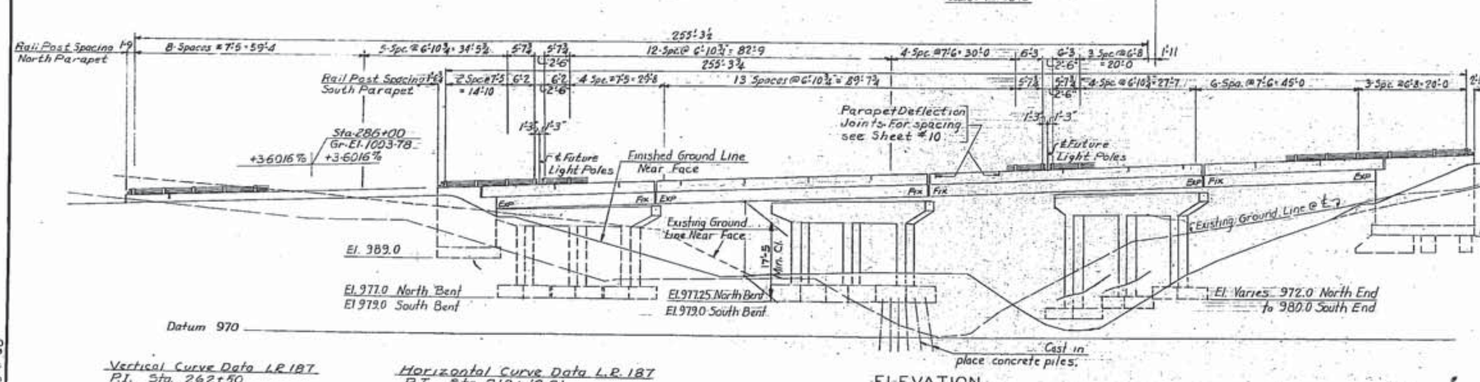

ELEVATION

Scale: 1" = 15'-0

Vertical Curve Data L.R. 187

P.I. Sta. 262+50
Elev. 919.14
V.C. 900'
M.O. 9.59'

-4.920% +3.6016%

Horizontal Curve Data L.R. 187

P.I. Sta. 318+12.21
Δ 55° 49' 35" Rt.
D 1° 30' 00"
R 3919.72'
T 2023.56'
L 3721.76'
S.E. 1/4" Per ft.

GENERAL NOTES

All materials and workmanship shall be in accordance with P.D.H. Forms 408/54 and 409/49, and Section 6.24 "Supplement for Prestressed Conc. Br. Superstructures", Dated Jan. 10, 1958

Design Spec's: Division I of 1957 "Standard Specs. for Highway Bridges of AASHO except roadway slab which is designed for 16,000 lbs wheel load and fc = 1000 p.s.i.

Live Load: H-20-S-16/44 and Modified Interstate Loading (2 axles of 24 kips each @ 4 ft. c/c, 2 wheels of 12 kips @ 6 ft c/c)

Dead Loads: Includes 30 lbs. p. sq. ft. for future wearing surface on the roadway slab.

Steel Reinforcement Bars designed for fs = 18,000 psi. and detailed as per A.C.I. Code. Bars to be lapped min. 40 diameters except as noted.

2" ⌀ Conduits (Galvanized Steel) shall be placed in accordance with details shown on P.D.H. Standard Dwg. SD-20

All piles are to be Cast-in-place Concrete.

Class A Concrete shall be used in curbs, parapets, pier caps, pier cols., deck slab, & backwalls above bridge seats. All other concrete shall be Class B unless otherwise noted.

The base of the footings may be ordered by the Engineer to be at any elevation or of any dimensions to provide a proper foundation.

Neoprene bearing pads, tubing and closed cellular sponge shall conform to specifications dated May 17, 1960.

Two-coat painted waterproofing shall be applied to rear faces of the walls within limits shown or as directed by the Engineer

Parapet, parapet railing, conduits, pull wire, scuppers and wing parapets and curbs are considered part of the superstructure.

Provide 2" cover on reinforcement bars unless otherwise noted.

See P.D.H. Std. Dwg. S-1614B or S-3361 for parapet railing details.

Surface of roadway divisor shall be treated as shown on P.D.H. Std Dwg SD-13

Exposed concrete edges shall be chamfered 1"x1" unless specified or directed by the Engineer otherwise.

Use 3/8" ⌀ prestressing cables with min. tendon strength = 250,000 p.s.i. ULT.

Piles shall be driven to refusal or to practical refusal as directed by the Engineer but in no case to a bearing value less than 72 tons for test piles and 60 tons for bearing piles.

SUMMARY OF QUANTITIES

ITEM	UNIT	ABUT-1	PIER-1	PIER-2	PIER-3	ABUT-2	SUPERSTR.	TOTAL
Class 1 Excavation	C.Y.	—	835	—	—	—	—	835
Class 3 Excavation	C.Y.	472	258	204	228	346	—	1508
		—	—	—	—	—		
Class A Concrete	C.Y.	—	105	98	118	—	714	1035
Class B Concrete	C.Y.	144	58	86	58	283	—	629
Reinforcement Bars	LBS	10,635	37,667	42,590	38,315	16,725	120,651	263,693
		—	—	—	—	—		
Parapet Railing	Lin. Ft.	—	—	—	—	—	510	510
Cast-in-place Conc. Piles	Lin. Ft.	—	—	719	—	—	—	719
Test Piles (Cast-in-place)	Lump Sum	—	—	2 @ 20'	—	—	—	Lump Sum
Prestressed Conc. Beams	Lin. Ft.	—	—	—	—	—	1651 ([illegible]) 1050 ([illegible])	1651 ([illegible]) 1050 ([illegible])
2" ⌀ Galv. Steel Conduit	Lin. Ft.	—	—	—	—	—	527	527
#14 Gal. Steel Pull Wire	Lin. Ft.						548	548

Quantities shown are approximate

THESE DRAWINGS SUPERSEDE DRAWINGS S-3736 DATED JUNE 30, 1959, PREPARED BY MICHAEL BAKER JR. INC., HARRISBURG, PA.

PRESTRESS DESIGN AND REVISION PREPARED BY AMERICAN-MARIETTA CO., PITTSBURGH, PA.

JOHN R. GROVER — John R. Grover, June 20, 1960

APPROVED AUG - 9 1960 K.H. Jensen BRIDGE ENGINEER

Commonwealth of Pennsylvania

Department of Highways

BRIDGE UNIT

FOUR SIMPLE SPANS - PRESTRESS CONCRETE BRIDGE
CARRYING L.R. 187 OVER OLD WILLIAM PENN HIGHWAY
STATION 286+89.88

L.R. 187 0002289 SECTION 12

MONROEVILLE BOROUGH

DISTRICT NO. 11 ALLEGHENY COUNTY

GENERAL PLAN AND ELEVATION

SCALE AS SHOWN
SHEET 1 OF 12

SD 13
SD-20
S-3361
S-1614-B

DWG. NO. S-3736A

DR.	CMC	TR.		CHD.	JRG

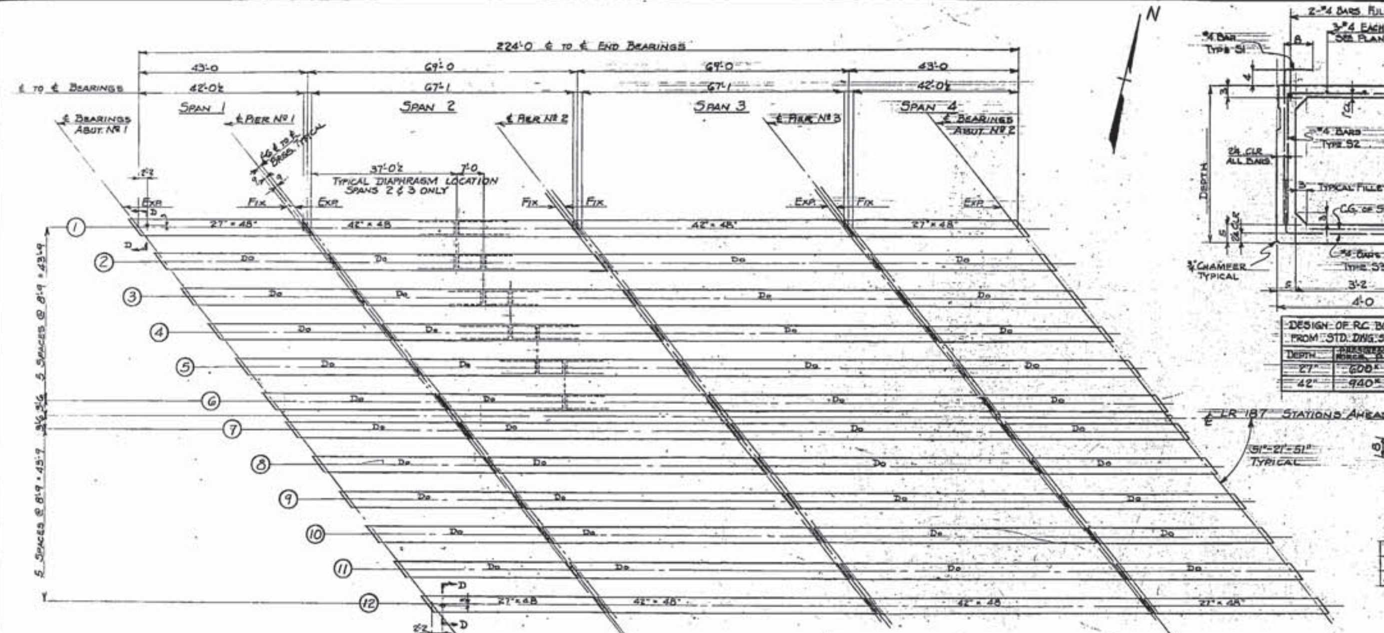

FRAMING PLAN
SCALE: 1" = 15'-0

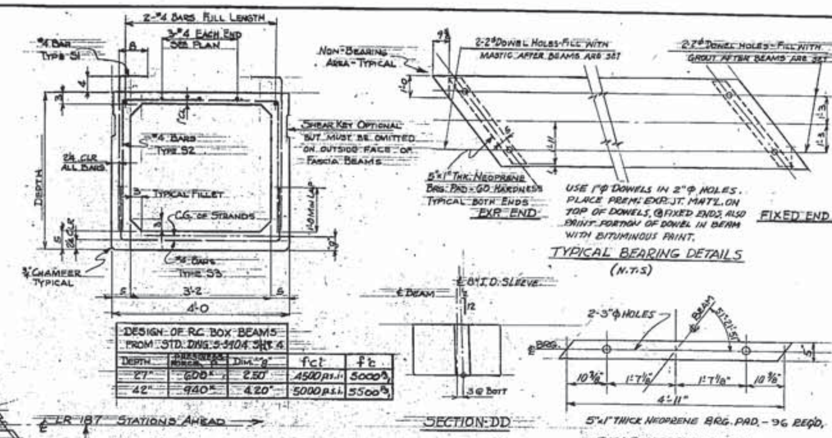

TYPICAL BEARING DETAILS
(N.T.S)

5"×1" THICK NEOPRENE BRG. PAD, - 96 REQ'D.

BEARING PAD DETAIL
SCALE: 3/4" = 1'-0"

DESIGN OF R.C. BOX BEAMS FROM STD. DWG. S-3404 SHT. 4				
Depth	Prestress Force	Dim. "g"	f'ci	f'c
27"	600k	2.50"	4500 p.s.i.	5000 p.s.i.
42"	940k	4.20"	5000 p.s.i.	5500 p.s.i.

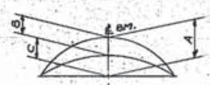

BEAM	A	B	C
27"×48"	0.706"	0.337"	0.369"
42"×48"	1.269"	0.714"	0.555"

CAMBER DIAGRAM

CAMBER NOTES

"A" = Estimated prestress camber less deflection due to dead load of beam. (To be checked in field)
"B" = Deflection due to dead load of slab, curb, parapet, railing & divisor.
"C" = "A" − "B" = Net final camber.
Bearing seat elevations are to be calculated considering net final camber or as otherwise specified on the design plans.
Prestress camber & dead load deflection data given are theoretical and may vary with concrete strength variable prestressing conditions & prestress losses.

- Concrete Strength @ Detensioning;
  27" Beams, f'ci = 4500 p.s.i.
  42" Beams, f'ci = 5000 p.s.i.
- Minimum Strand Strength - 250,000 p.s.i. ULT.
- Locate strands and mild reinforcement to miss dowels, inserts, etc.
- Omit shear keys and threaded inserts from outside face of fascia beams

Ultimate Strength (f'c) = 5000 psi (27" Beam)
= 5500 psi (42" Beam)

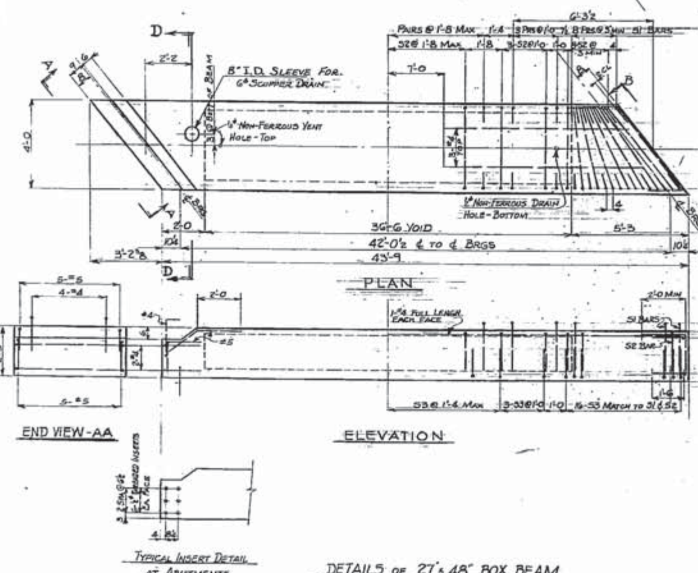

DETAILS OF 27" × 48" BOX BEAM
(NTS)

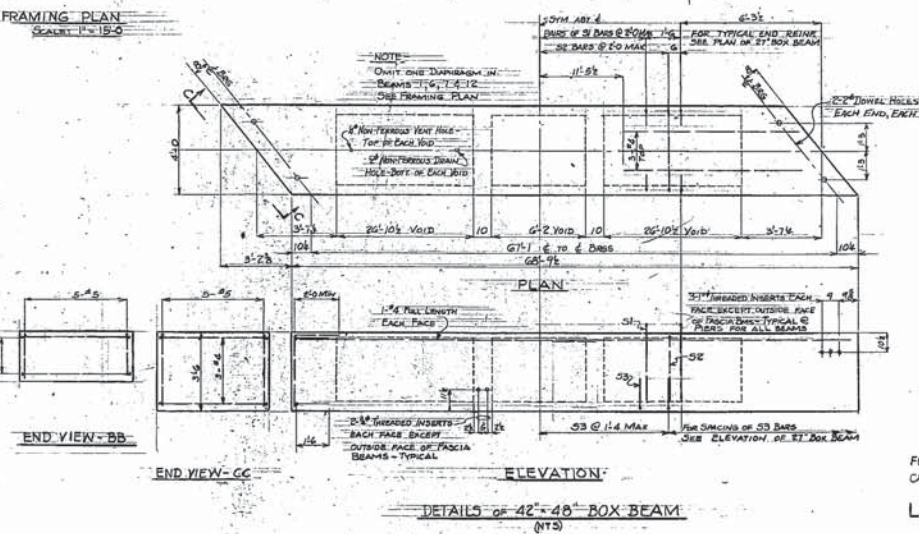

DETAILS OF 42" × 48" BOX BEAM
(NTS)

Approved: AUG 24 1960
K H Jensen
Bridge Engineer

Commonwealth of Pennsylvania
Department of Highways
BRIDGE UNIT

FOUR SIMPLE SPANS - PRESTRESS CONCRETE BRIDGE
CARRYING L.R. 187 OVER OLD WILLIAM PENN HIGHWAY
STATION 286+89.88

L.R. 187 SECTION 12
DISTRICT NO. 11 MONROEVILLE BOROUGH ALLEGHENY COUNTY

FRAMING PLAN AND DETAILS

SCALE AS SHOWN
SHEET 9 OF 12 0002297 S-3736A

DWN EMC
CHD. JRG

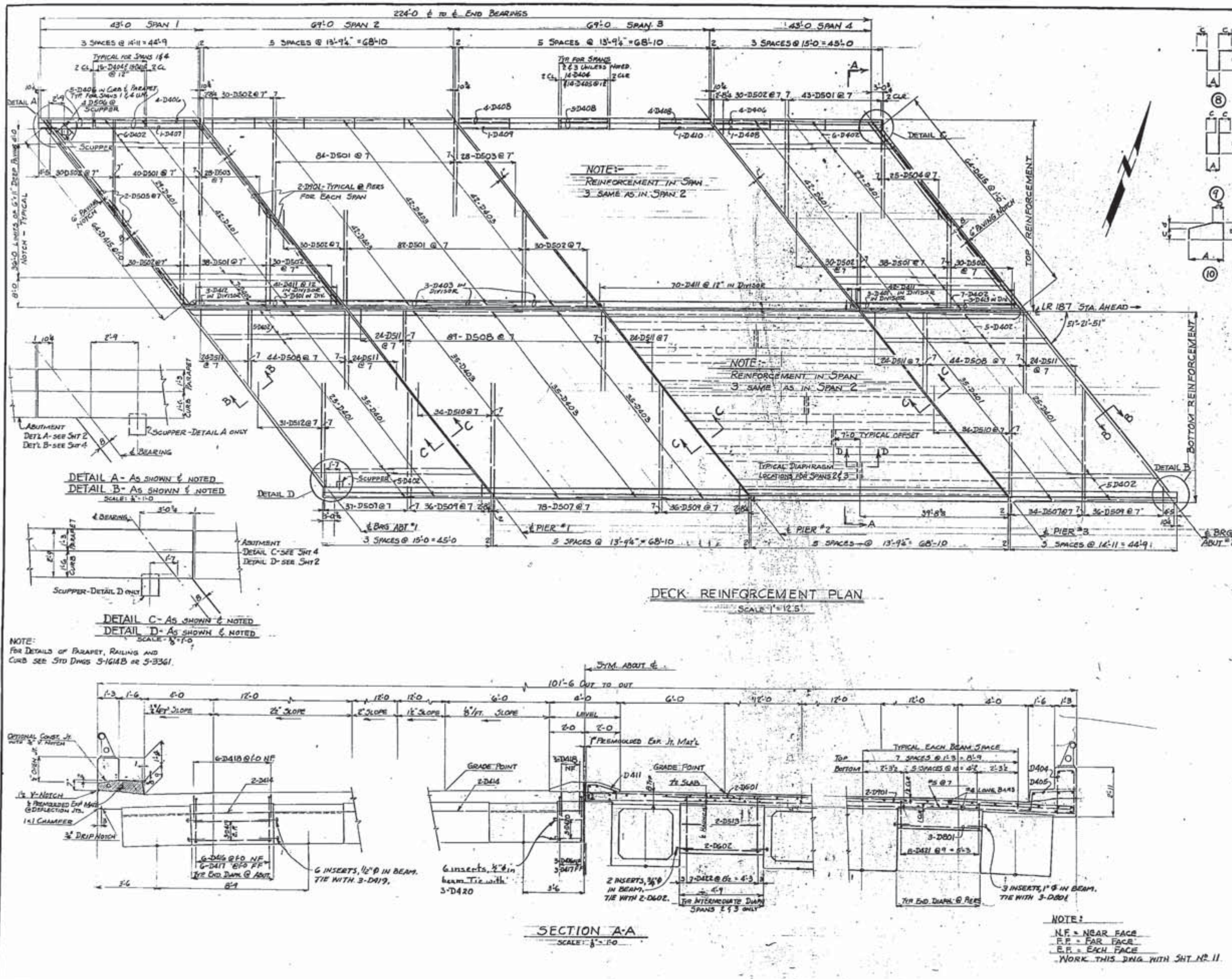

BAR SCHEDULE

MARK	NO. REQ'D	SIZE	TYPE	LENGTH	A	B	C	D	REMARKS
D901	48	9	1	35'-5	34'-2	1'-3			
D801	180	8	STR	6'-0					
D601	40	6	STR	8'-9					
D602	40	6	STR	4'-6					
D501	982	5	1	26'-10	26'-3	7			
D502	[illegible]	5	1	6'-10 to 26'-0	6'-3 to 25'-5	7			VARY EA. BAR BY 8⅞
D503	[illegible]	5	1	5'-3 to 25'-0	4'-8 to 24'-5	7			VARY EA. BAR BY 8⅞
D504	[illegible]	5	1	5'-3 to 22'-10	4'-8 to 22'-3	7			DITTO
D505	16	5	L	33'-10	33'-3	7			
D506	8	5	STR	4'-0					
D507	454	5	STR	30'-7					
D508	532	5	STR	21'-10					
D509	[illegible]	5	STR	6'-3 to 29'-10					VARY EA. BAR BY 8⅞
D510	[illegible]	5	STR	4'-8 to 28'-9					DITTO
D511	[illegible]	5	STR	6'-3 to 21'-0					DITTO
D512	[illegible]	5	STR	4'-8 to 26'-7					DITTO
D513	40	5	STR	4'-6					
D401	536	4	STR	22'-1					
D402	92	4	STR	22'-9					
D403	320	4	STR	23'-10					
D404	460	4	2	6'-3	11	2'-8			
D405	460	4	3	4'-6	2'-4	1'-1	1'-1		
D406	56	4	STR	14'-8					
D407	2	4	STR	15'-8					
D408	94	4	STR	13'-5					
D409	4	4	STR	12'-5					
D410	4	4	STR	14'-5					
D411	456	4	10	2'-11	1'-9	10	6	6	
D412	6	4	STR	19'-7					
D413	6	4	STR	21'-1					
D414	16	4	STR	31'-1					
D415	256	4	4	2'-8	1'-9	11			
D416	132	4	6	3'-11	2'-7	8			
D417	132	4	5	3'-1	1'-9	8			
D418	132	4	STR	2'-0					
D419	120	4	STR	6'-0					
D420	12	4	7	4'-2	7½	1'-8	10		
D421	480	4	9	4'-8	9	1'-5½	6		
D422	140	4	8	7'-10	7	3'-1½	6		

Approved: AUG - 9 1960
[signature]
Bridge Engineer

Commonwealth of Pennsylvania
Department of Highways
BRIDGE UNIT

FOUR SIMPLE SPANS- PRESTRESS CONCRETE BRIDGE
CARRYING L.R. 187 OVER OLD WILLIAM PENN HIGHWAY
STATION 286+ 89.88

L.R. 187 SECTION 12
DISTRICT NO. 11 MONROEVILLE BOROUGH ALLEGHENY COUNTY

DECK PLAN
SCALE AS SHOWN

SHEET 10 OF 12 S-3736 A

0002298

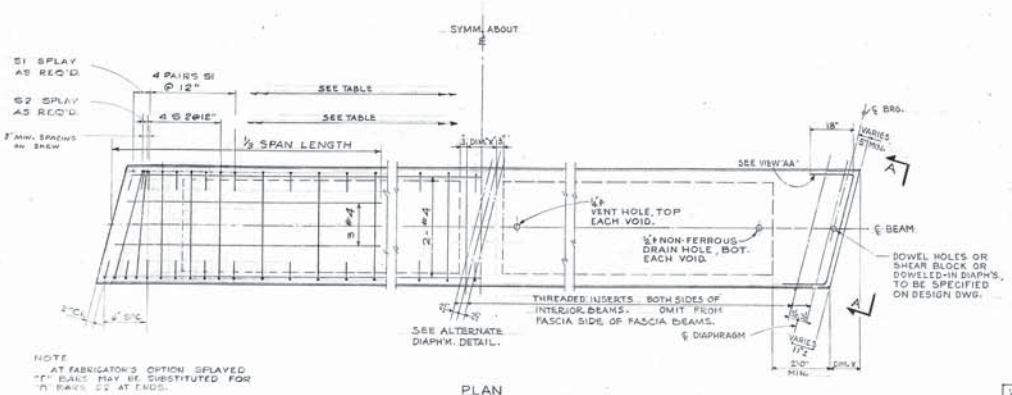

PLAN

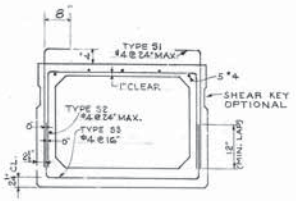

TYPICAL REINFORCMENT

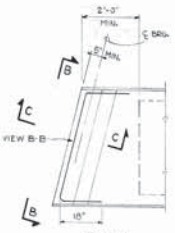

PLAN

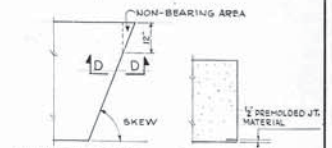

FOR SKEWS 85° OR LESS

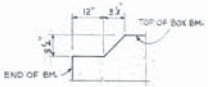

SECTION "CC"

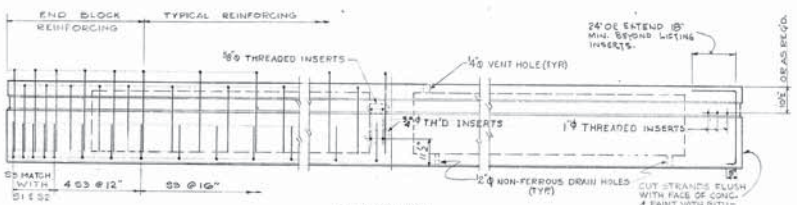

ELEVATION

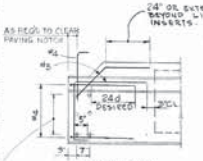

ELEVATION

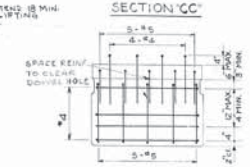

VIEW "BB"

TYPICAL DETAIL AT ABUTMENT

VERTICAL STIRRUP REQUIREMENTS, MAXIMUM SPACING IN INCHES													
SPAN FT.	21" BOX			27" BOX			33" BOX			36" BOX			42" BOX		
	7'0"	8'0"	9'0"	7'0"	8'0"	9'0"	7'0"	8'0"	9'0"	7'0"	8'0"	9'0"	7'0"	8'0"	9'0"
30	16"	13"	11"	15"	14"	14"	16"	16"	16"	16"	16"	16"	16"	16"	16"
35	14"	11"	10"	16"	15"	12"	16"	16"	15"	16"	16"	16"	16"	16"	16"
40	12"	10"	9"	15"	13"	11"	16"	16"	13"	16"	16"	15"	16"	16"	16"
45	11"	9"	8"	14"	12"	10"	16"	15"	12"	16"	16"	14"	16"	16"	16"
50				13"	11"	9"	16"	15"	11"	16"	16"	13"	16"	16"	16"
55				12"	10"	8"	15"	12"	10"	16"	15"	13"	16"	16"	15"
60				11"	9"		14"	12"	10"	16"	14"	12"	16"	16"	14"
65				11"			13"	11"	9"	15"	13"	11"	16"	16"	13"
70							12"	10"		15"	12"	10"	16"	15"	12"
75							11"			15"	11"		16"	14"	12"
80										14"			16"	14"	
85													15"		

NOTE
VERTICAL STEEL REQUIREMETS TO BE OBTAINED BY ANY COMBINATION OF TYPE S1 & S2 STIRRUPS WITHOUT EXCEEDING MAXIMUM SPACING OF EITHER TYPE.

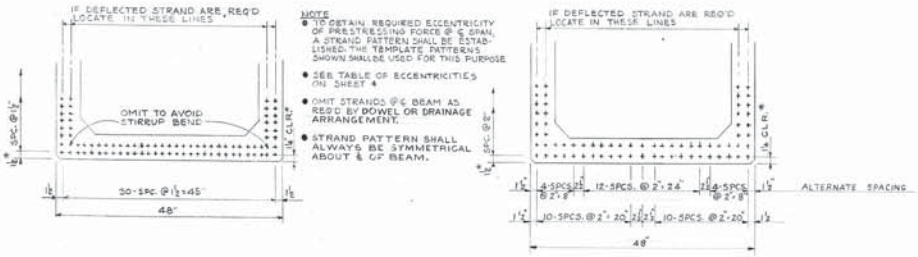

NOTE
- TO OBTAIN REQUIRED ECCENTRICITY OF PRESTRESSING FORCE @ ℄ SPAN, A STRAND PATTERN SHALL BE ESTABLISHED. THE TEMPLATE PATTERNS SHOWN SHALL BE USED FOR THIS PURPOSE
- SEE TABLE OF ECCENTRICITIES ON SHEET 4
- OMIT STRANDS @ ℄ BEAM AS REQ'D BY DOWEL OR DRAINAGE ARRANGEMENT.
- STRAND PATTERN SHALL ALWAYS BE SYMMETRICAL ABOUT ℄ OF BEAM.

TYPICAL STRAND LAYOUT FOR ⅜ϕ STRAND

- 1½" MIN. CLEARANCE SHALL BE MAINTAINED AT ALL TIMES.

1½" FROM ℄ OF STRANDS TO BOTTOM OF BEAM IS DESIRED. CHAIR WILL BE REQUIRED FOR BEAMS WITH SPANS OVER 104'-0".

1½" FROM ℄ OF STRANDS TO BOTTOM OF BEAM WILL REQUIRE CHAIRS FOR SPANS OVER 50'0" (TO ELIMINATE EXCESSIVE STRAND DRAPE).

CHAIRS SHALL BE DETAILED & SHOWN ON SHOP DWGS.

TYPICAL STRAND LAYOUT FOR ½" ϕ STRAND

½" ϕ STRANDS SHALL NOT BE USED FOR SPANS LESS THAN 30'-0"

ANTICIPATED Δ IN.				
BOX	SPAN			
	30	50	70	90
21"×48"				
27"×48"	1/8	3/8		
33"×48"	0	3/8		
36"×48"	0	¼	½	
42"×48"	0	¼	½	

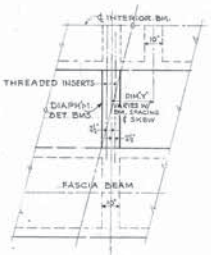

PLAN

ALTERNATE DIAPHRAGM DETAIL

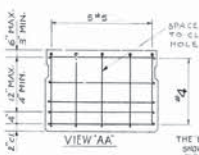

THE END BLOCK REINFORCING SHOWN SHALL BE INCREASED FOR SHARP SKEWS AND FOR HIGHLY CONCENTRATED PRESTRESSING FORCE. REARRANGEMENT OF STRANDS SHALL BE GIVEN CONSIDERATION.

A=ESTIMATED PRESTRESS CAMBER LESS DEFLECTION DUE TO DEAD LOAD OF BEAM (TO BE CHECKED IN FIELD)
B=DEFLECTION DUE TO DEAD LOAD OF SLAB, CURB OR SIDEWALK AND PARAPET.
C=A-B=NET FINAL CAMBER.

- BEARING SEAT ELEVATION AND SLAB THICKNESS SHALL BE CALCULATED CONSIDERING A VALUE "C"
- THE THICKNESS OF THE HAUNCH ON BEAMS SHALL BE VARIED TO COMPENSATE FOR ANY INACCURACIES IN THE CAMBER OF BEAMS.

INSTRUCTION FOR CAMBER COMPUTATION

- THE CAMBER DUE TO PRESTRESS AND THE DEFLECTION DUE TO BEAM DEAD LOAD MAY BE CALCULATED USING A 5% TO 15% LOSS IN PRESTRESS FORCE, Fci IN CALCULATING Eci AND A CREEP FACTOR OF 1.5 TO 2.0 (IN CASE EXACT VALUES ARE NOT AVAILABLE, 5% & A FACTOR OF 2.0 IS ACCEPTABLE)
- THE DEFLECTION DUE TO SUPERIMPOSED DEAD LOADS SHALL BE CALCULATED USING, Fc IN CALCULATING Ec AND NO CREEP FACTOR.
- PRESTRESS CAMBER AND DEAD LOAD DEFLECTION DATA SHOWN IS THEORETICAL AND MAY VARY WITH CONCRETE STRENGTH, VARIABLE PRESTRESSING CONDITIONS AND PRESTRESS LOSSES.

TYPICAL CAMBER DIAGRAM & NOTES
(TO BE SHOWN ON SHOP DWG. & DESIGN DWG.)

APPROVED SEP 19 1960

BRIDGE ENGINEER

INSTRUCTIONS

1. APPLICABLE DETAILS SHOWN ON THIS SHEET ARE TO BE INCLUDED IN FABRICATORS SHOP DWGS.
2. TOPS OF ALL BEAMS SHALL BE STRUCK OFF AND SCORED AS DIRECTED BY THE ENGINEER (SHALL BE SPECIFIED ON SHOP DRWGS).
3. ALL REINFORCING SHOWN ON THIS SHEET IS FOR INTERMEDIATE GRADE STEEL @ f_y = 20,000 P.S.I. IF STRUCTURAL GRADE STEEL IS USED, INCREASE STEEL REQUIREMENTS OF STIRRUPS BY 10%. SPECIFY ON SHOP DRAWING STEEL TO BE USED.
4. THIS SHEET TO BE WORKED WITH SHEETS 3 & 4.
5. PRESTRESS CAMBER & DEAD LOAD DEFLECTIONS SHALL BE SHOWN ON THE SHOP DWGS. & DESIGN PLANS.
6. SHOW TYPICAL CROSS SECTION & FRAMING PLAN OF BRIDGE ON FABRICATORS SHOP DWG.
7. SHOW BEARING PAD DETAILS ON FABRICATORS SHOP DWG.
8. DESIGN LENGTHS SHALL BE SHOWN ON SHOP DWGS., CASTING LENGTH MAY BE GIVEN IN ( ).
9. ALL INSERTS MAY BE CAST IN BEAM OR SELF-DRILLING ANCHORS. TYPE OF ANCHOR SHALL BE SPECIFIED ON SHOP DWGS.
10. FOR BEAM FABRICATION TOLERANCE, SEE SHEET 1.

REVISIONS				
NO.	DESCRIPTION	BY	CHK'D.	DATE

Commonwealth of Pennsylvania

Department of Highways
BRIDGE UNIT

PRESTRESSED CONCRETE BRIDGE STANDARDS

4 FT. SPREAD BOX BEAMS

COMPOSITE

BEAM DETAILS

SCALE: No Scale
SHEET 5 of 6

S-3904

PREPARED BY SCHUPACK AND ZOLLMAN, NEWTOWN SQUARE, IN COOPERATION WITH THE PRESTRESSED CONCRETE ASSOCIATION OF PENNSYLVANIA FOR THE PENNSYLVANIA DEPARTMENT OF HIGHWAYS.

A.3 BRIDGE K

Structural drawings for bridge K (PADoH 1960a and 1960b).

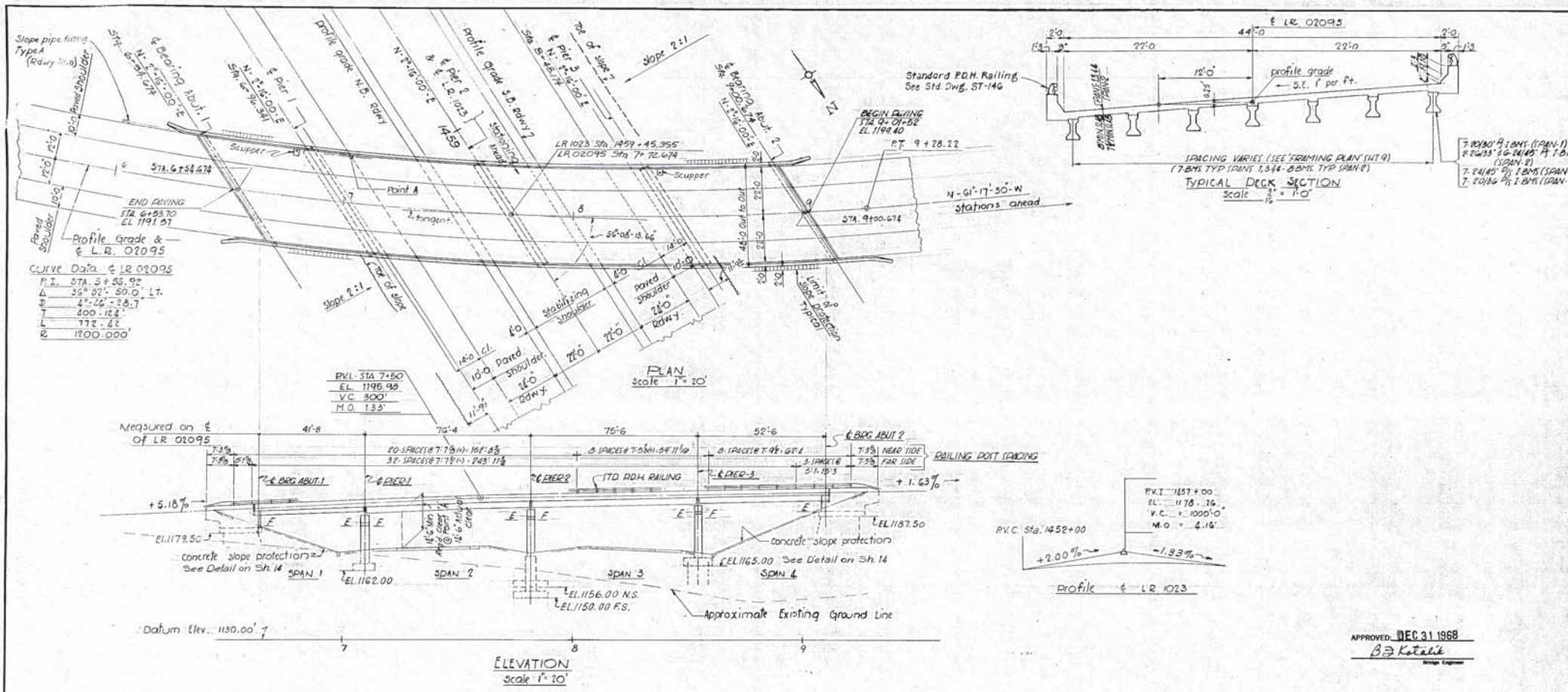

APPROVED: DEC 31 1968
B J Kotalik
Bridge Engineer

Commonwealth of Pennsylvania

DEPARTMENT OF HIGHWAYS
BRIDGE DIVISION
ALLEGHENY COUNTY
BEAVER VALLEY EXPRESSWAY
L.R. 1023, SEC. 1A, STA. 1459+45.355
UNDER L.R. 02095
4-SPAN PS CONCRETE I-BEAM BRIDGE
SUPERSTRUCTURE & SUBSTRUCTURE
GENERAL PLAN

SCALE: AS NOTED

0004057

SHEET 2 OF 16

S-7894A

41288 PEL-X

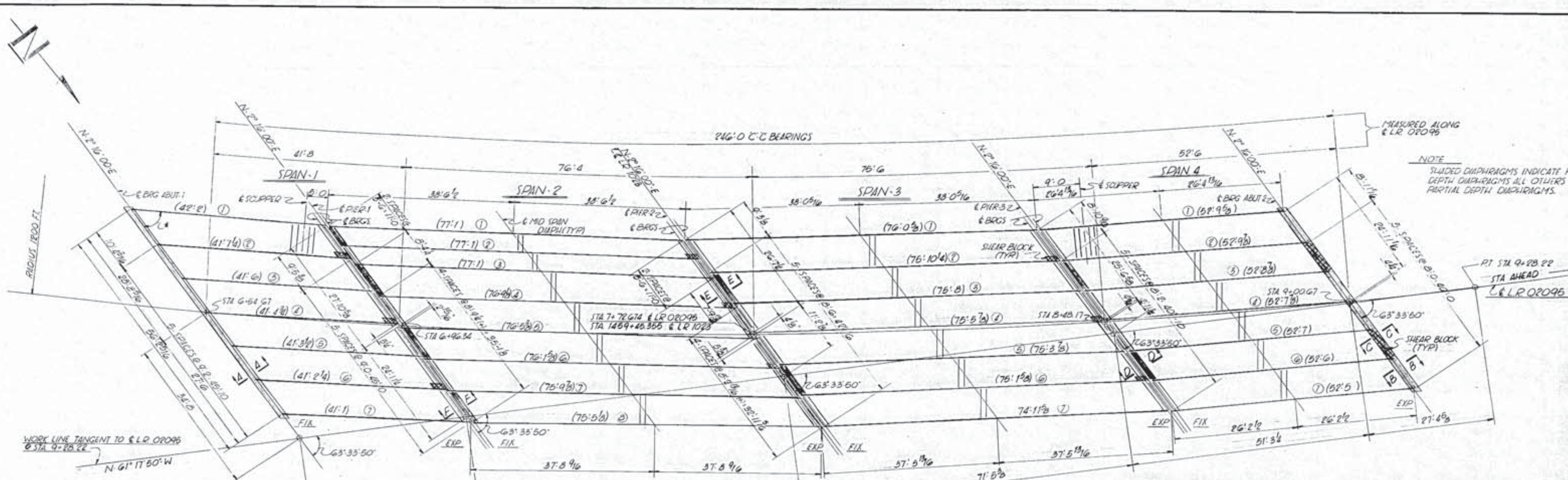

NOTE
SHADED DIAPHRAGMS INDICATE FULL DEPTH DIAPHRAGMS ALL OTHERS ARE PARTIAL DEPTH DIAPHRAGMS.

* FOR SKEW ANGLES AND BEAM DIMENSIONS SEE TABLE BELOW.

NOTES
- LENGTHS FROM ℄ ABUT–℄ PIER OR ℄ PIER–℄ PIER MEASURED ALONG ℄ BEAM ARE GIVEN IN ( ) OPPOSITE THE BM. MARK.
- MID·SPAN DIAPHRAGM LOCATIONS ARE MEASURED ALONG ℄ OF FACISA BEAMS.
- FOR SECTIONS A-A, B-B, C-C, D-D, E-E & F-F SEE SHT. 13.
- FOR DETAILS OF BEAMS @ ABUTS & PIERS & TYP INTERMEDIATE DIAPH. SECTIONS SEE SHT. 10
- FOR SCUPPER & DRAINAGE DETAILS SEE SHT. 14.

FRAMING PLAN & STAKE OUT PLAN

SCALE 1"·10'·0

BEAM DIMENSIONS

SPAN	BM. Nº	BM. SIZE	C-C BEARINGS	TOTAL BM LENGTH	SKEW ANGLE
1	①	20/30	41'·1⅛	42'·6½	50° 38' 27"
	②	↓	40'·6½	41'·11¾	51° 36' 42"
	③		40'·5¼	41'·10½	51° 47' 35"
	④		40'·4	41'·9¼	51° 58' 33"
	⑤		40'·2⅞	41'·8	52° 09' 29"
	⑥	↓	40'·1⅝	41'·6¾	52° 20' 32"
	⑦	20/30	40'·0⅜	41'·5½	52° 31' 37"
2	①	26/33	75'·0⅛	76'·9	53° 32' 15"
	②	26/33	75'·0⅛	76'·7	53° 32' 15"
	③	24/45	75'·0⅛	76'·7	53° 32' 15"
	④	↓	74'·8⅜	76'·3⅞	53° 51' 35"
	⑤		74'·4¾	75'·11⅜	54° 11' 10"
	⑥		74'·1⅛	75'·7⅝	54° 30' 52"
	⑦	↓	73'·9½	75'·3⅞	54° 50' 44"
	⑧	24/45	73'·5⅞	75'·1⅛	55° 10' 46"
3	①	24/45	74'·0⅛	75'·8⅝	57° 16' 00"
	②	↓	73'·10⅝	75'·4¼	57° 30' 33"
	③		73'·8⅜	75'·2	57° 43' 19"
	④		73'·6⅛	74'·11⅞	57° 56' 08"
	⑤		73'·4⅜	74'·9⅞	58° 09' 01"
	⑥	↓	73'·2⅛	74'·7⅞	58° 21' 58"
	⑦	24/45	73'·0¼	74'·7⅝	58° 34' 58"
4	①	20/36	51'·10⅛	53'·2⅛	60° 23' 52"
	②	↓	51'·10⅛	53'·2⅛	60° 21' 30"
	③		51'·9⅛	53'·1⅛	60° 30' 57"
	④		51'·8⅜	53'·0⅜	60° 40' 26"
	⑤		51'·7⅝	52'·11½	60° 49' 58"
	⑥	↓	51'·6⅝	52'·10½	60° 59' 31"
	⑦	20/36	51'·5⅜	52'·9½	61° 09' 05"

V.C. CORRECTION
.025' SPAN-1
.086' SPAN-2
.084' SPAN-3
.041' SPAN-4

S.E. CORRECTION
.063' SPAN-1
.119' SPAN-2 (26/33")
.112' SPAN-2 (24/45")
.111' SPAN-3
.072' SPAN-4

A - ESTIMATED PRESTRESS CAMBER LESS DEFLECTION DUE TO DEAD LOAD OF BEAM (TO BE CHECKED IN FIELD)

B - DEFLECTION DUE TO DEAD LOAD OF SLAB, CURB & PARAPET.

C - A-B NET FINAL CAMBER.

- NET FINAL CAMBER, VERT. CURVE & S.E. CORRECTION HAS BEEN INCLUDED IN THE CALCULATIONS FOR BM. SEAT ELEVATIONS AND HAUNCH THICKNESS @ ℄ BRG.
- THE THICKNESS OF THE HAUNCH ON THE BEAMS SHALL VARY TO COMPENSATE FOR ANY IRREGULARITIES IN THE CAMBER OF THE BEAMS.
- PRESTRESS CAMBER AND DEAD LOAD DEFLECTION DATA SHOWN IS THEORETICAL AND MAY VARY WITH CONCRETE STRENGTH, VARIABLE PRESTRESSING CONDITIONS, AND PRESTRESS LOSSES.

CAMBER DIAGRAM

STRAND DEF'L DETAIL
(N.T.S.)

PRESTRESS LOAD AND CAMBER TABLE

SPAN	BM SIZE	A	B	C	f'c	f'ci	Fi	g @ ℄	g @ END	X	BEARING PADS FIXED END	BEARING PADS EXP. END
1	20/30	0.848"	0.295"	0.553"	5500	5000	821ᴷ	6.68"	6.68	~	9" x 5/8" x 18"	9" x 5/8" x 18"
2	26/33	2.710"	0.983"	1.727"	6000	5150	1172ᴷ	7.02"	11.10"	11'·2½	9" x ½" x 22"	9" x 1¼" x 22"
	24/45	2.602"	0.729"	1.873"	5500	5000	934ᴷ	5.24"	11.40	12'·6 ±	10" x ½" x 22"	10" x 1¼" x 22"
3	24/45	2.115"	0.726	1.389"	5500	5000	955ᴷ	5.58	11.38	12'·6 ±	11" x ¾" x 22"	11" x 1⅛" x 22"
4	20/36	0.785"	0.342	0.443"	5500	5000	716ᴷ	8.41	8.41	~	10" x ½" x 18"	10" x ¾" x 18"

f'c = 28 DAY CLY. STRENGTH & DESIGN STRENGTH OF CONCRETE.
f'ci = CONCRETE STRENGTH @ RELEASE OF PRESTRESS.
Fi = TOTAL INITAIL PRESTRESSING FORCE PER BEAM.
g = DISTANCE FROM BEAM SOFFIT TO C.G. OF STRANDS.
X = DISTANCE FROM ℄ SPAN TO STRAND DEF'L PT. (SEE DETAIL).
- ALL BEARING PADS SHALL BE 60 DUROMETER NEOPRENE.

PRESTRESS NOTES

- ALL MATERIAL AND WORKMANSHIP SHALL BE IN ACCORDANCE WITH SECT. 6.14 SUPPLEMENT FOR "PRESTRESS CONC. BRIDGE SUPERSTRUCTURE" DATED JUNE 22, 1966 OF P.D.H. FORM 408-60.
- PRESTRESS BEAM REINF. AND DETAILS SHALL BE SHOWN ON FABRICATORS SHOP DWGS. AND WILL CONFORM TO THE LATEST P.D.H. REQUIRMENTS.

REFER TO P.D.H. PRESTRESS CONC. BRIDGE STDS. ST-208 (APPR. AUG 17, 1964.)

- REFER TO SHEETS 5, 6 & 8 FOR: DESIGN NOTES AND TYP SECTIONS FOR 20/30", 26/33", 24/45" & 20/36" I-BMS.
- REFER TO SHEET 9 FOR: TYPICAL CAMBER DIAGRAM AND NOTES EXCEPT AS SUPPLEMENTED ON THIS DWG. BEAM FABRICATION DETAILS, AND DETAILS OF MILD STEEL REINF. (MAX STIRRUP SPA. SHALL BE 12" ALL SPANS).

APPROVED: DEC 31 1968
B.J. Kotalik
Bridge Engineer

Commonwealth of Pennsylvania
DEPARTMENT OF HIGHWAYS
BRIDGE DIVISION
ALLEGHENY COUNTY
BEAVER VALLEY EXPRESSWAY
L.R. 1023 SEC. 1A STA. 1459+45.355
UNDER L.R. 02095
4 SPAN P/S CONCRETE I-BEAM BRIDGE
SUPERSTRUCTURE
FRAMING PLAN

SCALE: 1"·10'·0
SHEET 9 OF 16
0004064
S-7894-A

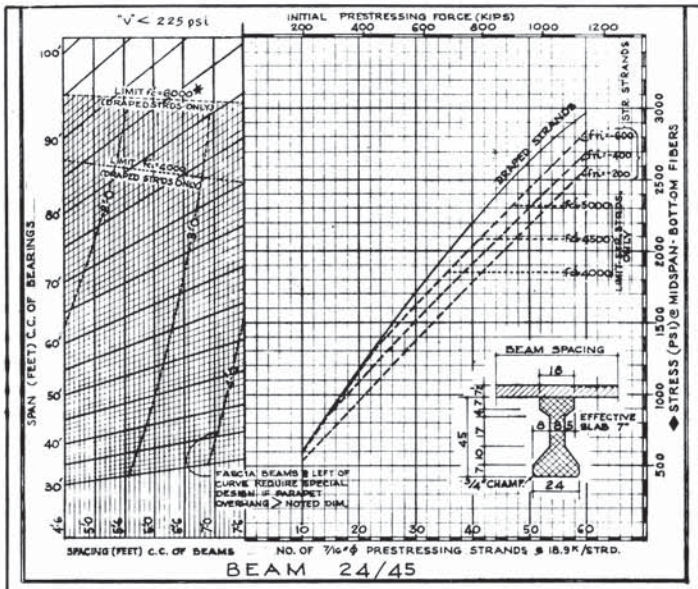

BEAM 24/45

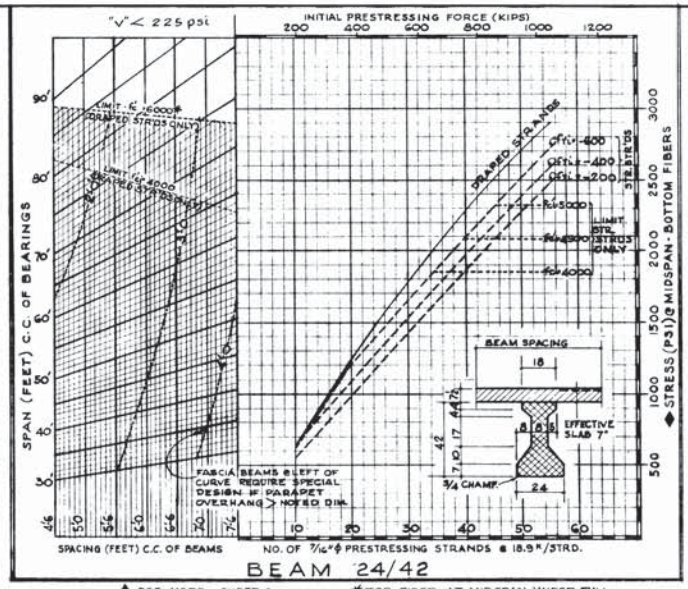

BEAM 24/42

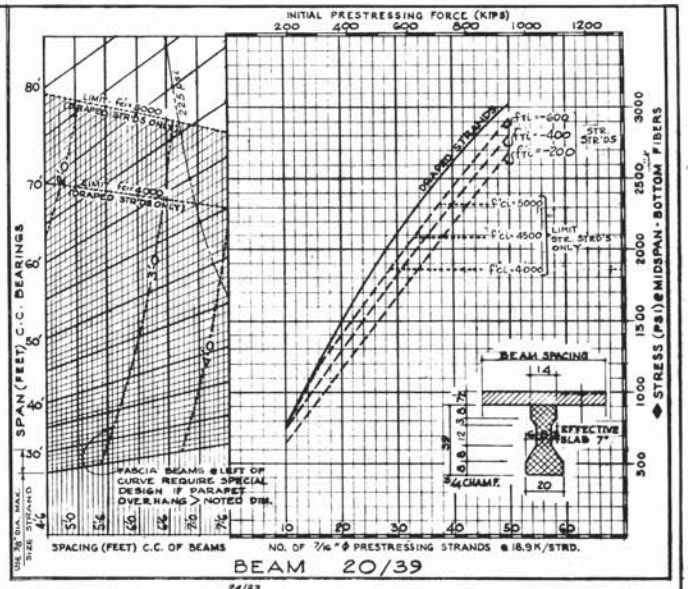

BEAM 20/39

◆ SEE NOTE - SHEET 4

*TOP FIBER AT MIDSPAN UNDER FULL LOAD CONTROLS TO ESTABLISH LIMIT OF 28 DAY CYL. STRENGTH (f'c) USE f'c1 = 5000 PSI

SECTION PROPERTIES

BEAM SIZE	BASIC SECTION						COMPOSITE SECTION											
							4'-0 C.C.		5'-0 C.C.		5'-6 C.C.		6'-0 C.C.		6'-6 C.C.		7'-0 C.C.		7'-6 C.C.	
	CONC.	A	y_b	I	Z_t	Z_b	y_b	I	y_b	I	y_b	I	y_b	I	y_b	I	y_b	I	y_b	I
UNIT	yd³/ft	IN²	IN	IN⁴	IN³	IN³	IN	IN⁴	IN	IN⁴	IN	IN⁴	IN	IN⁴	IN	IN⁴	IN	IN⁴	IN	IN⁴
24/45	0.165	642	20.18	140,129	5,646	6,944	30.65	332,424	31.38	345,475	32.03	357,597	32.64	368,178	33.20	378,607	33.72	388,636	34.21	397,353
24/42	0.151	588	18.04	107,986	4,507	5,986	28.80	282,931	29.48	294,445	30.12	305,157	30.72	314,147	31.26	323,830	31.77	332,077	32.24	340,240
20/39	0.132	513	17.41	77,514	3,590	4,452	28.10	216,059	28.70	224,603	29.30	232,327	29.84	239,951	30.35	245,879	30.81	252,343	31.24	257,999

DIMENSION "B" (INCHES)

FOR 7/16"ϕ STRANDS

NO. OF 7/16" STRANDS	BEAM 24/45				BEAM 24/42				BEAM 20/39			
	DRAPED STR'DS	STRAIGHT STR'DS: f'ci = -600	-400	-200	DRAPED STR'DS	STRAIGHT STR'DS: f'ci = -600	-400	-200	DRAPED STR'DS	STRAIGHT STR'DS: f'ci = -600	-400	-200
10	2.00	2.00	2.00	5.40	2.00	2.00	2.00	5.62	2.40	2.40	2.81	6.62
15	2.67	2.67	3.46	7.42	2.67	2.67	4.04	7.14	2.93	2.93	5.31	7.89
20	3.00	3.00	5.38	8.65	3.00	3.23	5.64	7.99	3.50	4.67	6.61	8.51
25	3.52	4.16	6.68	9.00	3.52	4.61	6.54	8.45	4.00	5.85	7.31	8.87
30	3.93	5.40	7.38	9.36	3.93	5.62	7.14	8.75	4.60	6.62	7.89	9.14
35	4.40	6.28	7.98	9.71	4.40	6.31	7.64	8.99	5.20	7.11	8.23	9.29
40	4.85	6.89	8.38	9.88	4.85	6.82	8.04	9.16	5.90	7.53	8.51	9.42
45	5.38	7.42	8.78	10.07	5.38	7.22	8.27	9.30	6.67	7.88	8.72	9.54
50	5.92	7.79	8.98	10.22	5.92	7.53	8.45	9.44	7.60	8.10	8.86	9.63
55	6.55	8.15	9.18	10.33	6.55	—	—	—	—	—	—	—
60	7.35	8.39	9.38	10.42	—	—	—	—	—	—	—	—

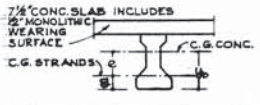

INSTRUCTIONS:

1. FOR CONSTRUCTION PURPOSES SOME STRANDS MAY BE LOCATED IN UPPER FLANGE OR WEB OF BEAM. SUCH STR'DS SHALL BE INCLUDED IN COMPUTING THE CENTER OF GRAVITY OF STRANDS IF PRESTRESSED

2. VALUE "B" FOR Nº OF STRANDS OTHER THAN THAT GIVEN IN TABLE TO BE INTERPOLATED AND NEAREST PRACTICAL VALUE TO BE USED.

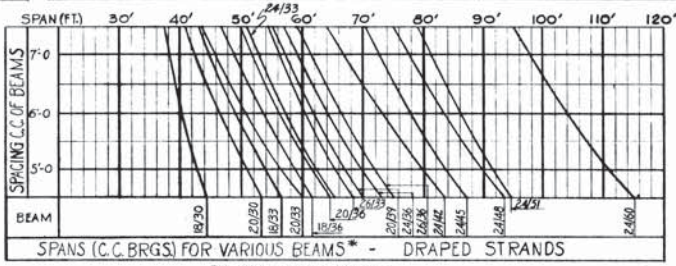

SPANS (C.C. BRGS) FOR VARIOUS BEAMS* - DRAPED STRANDS

FOR DESIGN NOTES SEE SHEET 4

*USE CURVES FOR PRELIMINARY SELECTION OF BEAM SIZE ONLY.

APPROVED AUG 17 1964
R. H. Jensen
BRIDGE ENGINEER

Commonwealth of Pennsylvania
Department of Highways
BRIDGE UNIT

PRESTRESSED CONCRETE BRIDGE - STANDARDS

"I" BEAMS

COMPOSITE DESIGN CURVES
24/45 24/42 20/39

SHEET 5 OF 11

ST-208

PREPARED BY SCHUPACK & ZOLLMAN, NEWTOWN SQUARE, PA. FOR PENNSYLVANIA DEPARTMENT OF HIGHWAYS - CENTRAL OFFICE BRIDGE UNIT

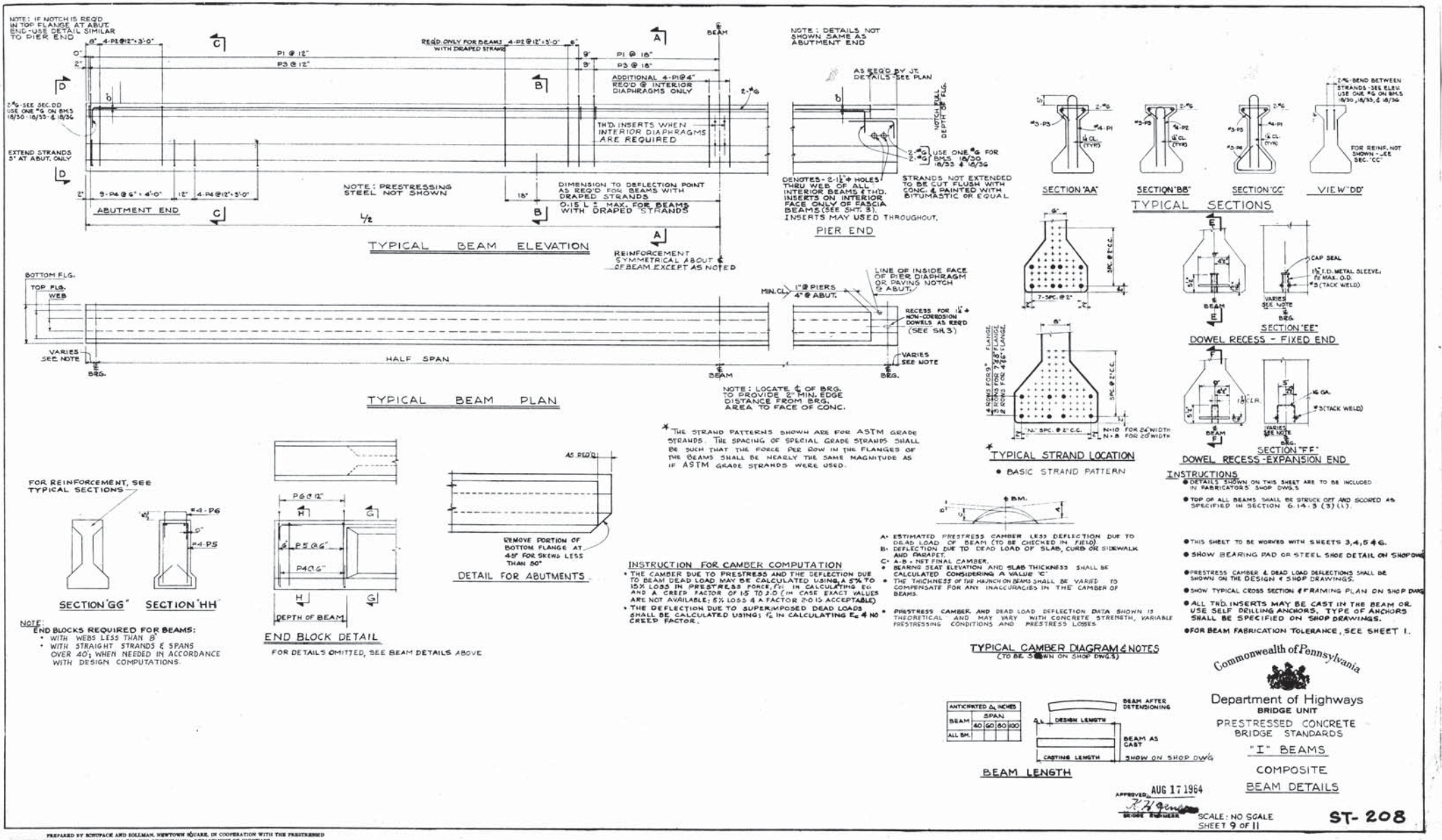

PREPARED BY SCHUPACK AND SOLIMAN, NEWTOWN SQUARE, IN COOPERATION WITH THE PRESTRESSED CONCRETE ASSOCIATION OF PENNSYLVANIA FOR THE PENNSYLVANIA DEPARTMENT OF HIGHWAYS.

BIBLIOGRAPHY

Aidoo, J. (2004). "Flexural Retrofit of Reinforced Concrete Bridge Girders Using Three CFRP Systems." Doctoral Dissertation, University of South Carolina, Columbia, South Carolina.

Aidoo, J., Harries, K.A. and Petrou, M.F. (2006). "Full-scale Experimental Investigation of Repair of Reinforced Concrete Interstate Bridge using CFRP Materials", *ASCE Journal of Bridge Engineering*, 11(3), 350-358.

American Association of State Highway and Transportation Officials (AASHTO). (2007). *LRFD Bridge Design Specifications, 4th Edition*. With Interims, Washington, D.C.

American Association of State Highway Officials (AASHO) (1960). "*Standard Specifications for Highway Bridges*", 286pp.

American Concrete Institute (ACI) 318-08 (2008).*"Building Code Requirements for Structural Concrete and Commentary",* 467pp.

American Concrete Institute (ACI) Committee 440 (2008). *ACI 440.2R-08 "Guide for the Design and Construction of Externally Bonded FRP Systems for Strengthening Concrete Structures"*, 76pp.

Aram, M-R., Czaderki, C. and Motavalli, M. (2008). "Effects of Gradually Anchored Prestressed CFRP Strips Bonded on Prestressed Concrete Beams", *Journal of Composites for Construction*, 12(1), 25-34.

Broomfield, J.P. and Tinnea, J.S., (1992). "Cathodic Protection of Reinforced Concrete Bridge Components", Report No. SHRP-C/UWP-92-618,Strategic Highway Research Program, National Research Council, Washington, D.C.

Cadei, J.M.C., Stratford, T.J., Hollaway, L.C. and Duckett, W.G. (2004). "Strengthening Metallic Structures Using Externally Bonded Fibre-Reinforced Polymers", *CIRIA Pub. No. C595*. 233 pp.

Casadei, P., Galati, N., Boschetto, G., Tan, K.Y., Nanni, A. and Galeki, G. (2006). "Strengthening of Impacted Prestressed Concrete Bridge I-Girder Using Prestressed Near Surface Mounted C-FRP Bars", *Proceedings of the 2nd International Congress*, Federation Internationale du Beton, Naples, Italy.

Chadwell, C.B.and Imbsen, R.A. (2002). *XTRACT: A Tool for Axial Force - Ultimate Curvature Interactions*.

Collins, M.P. and Mitchell, D. (1997). "Prestressed Concrete Structures." Response Publications, Toronto, Canada.

El-Hacha, R. and Elbadry, M. (2006). "Strengthening Concrete Beams with Externally Prestressed Carbon Fiber Composite Cables: Experimental Investigation", *PTI Journal*, 4(2). 53-70.

El-Hacha, R., Wight, R.G. and Green, M.F. (2003), "Innovative System for Prestressing Fiber-Reinforced Polymer Sheets", *ACI Structural Journal*, ACI, 100(3): 305-313.

Feldman, L.R., Jirsa, J.O., Fowler, D.W. and Carrasquillo, R.L. (1993). "Current Practice in the Repair of Prestressed Bridge Girders", Report No. FHWA/TX-96/1370-1, The University of Texas at Austin, Austin, TX.

Grabb-it. (2008). Cable Splice Product Information Sheet, Prestress Supply, Inc.

Green P.S., Boyd, A.J., Lammert, K. and Ansley, M. (2004). "CFRP Repair of Impact-Damaged Bridge Girders Volume 1 – Structural Evaluation of Impact Damaged Prestressed Concrete I Girders Repaired with FRP Materials", UF Project No. 4504-922-12, University of Florida, Gainesville, FL.

Harries, K.A. (2006). "Full-scale Testing Program on De-commissioned Girders from the Lake View Drive Bridge", Report No. FHWA-PA-2006-008-EMG001, University of Pittsburgh, Pittsburgh, PA.

Harries, K.A., Zorn, A. ,Aidoo, J. and Quattlebaum, J. (2006). "Deterioration of FRP-to-Concrete Bond Under Fatigue Loading", *Advances in Structural Engineering - Special Issue on Bond Behaviour of FRP in Structure,* 9(6), 779-789.

Herman, T. (2005). "A Tale of Two Bridges", *Bridges*, Nov/Dec. 2005, 14-16.

Kim, Y.J., Green, M.F. and Fallis, G.J. (2008c). "Repair of Bridge Girder Damaged by Impact Loads with Prestressed CFRP Sheets", *Journal of Bridge Engineering*, 13(1), 15-23.

Kim, Y.J., Wight, R.G. and Green, M.F. (2008a). "Flexural Strengthening of RC Beams with Prestressed CFRP Sheets: Development of Nonmetallic Anchor Systems", *Journal of Composites for Construction*, 12(1), 35-43.

Kim, Y.J., Wight, R.G. and Green, M.F. (2008b). "Flexural Strengthening of RC Beams with Prestressed CFRP Sheets: Using Nonmetallic Anchor Systems", *Journal of Composites for Construction*, 12(1), 44-52.

Klaiber, F.W, Wipf, T.J. and Kempers, B.J. (2003). "Repair of Damaged Prestressed Concrete Bridges using CFRP", *Mid-Continent Transportation Symposium Proceedings*, Center for Transportation Research and Education, Ames, IA.

Klaiber, F.W., Wipf, T.J., and Kash, E.J. (2004). "Effective Structural Concrete Repair – Volume 2 of 3: Use of FRP to Prevent Chloride Penetration in Bridge Columns", Iowa DOT Project TR-428, Iowa Department of Transportation, Ames, IA.

Labia, Y., Saiidi, M. & Douglas. (1996). "Evaluation and Repair of Full-Scale Prestressed Concrete Box Girders", Report No. CCEER-96-2, University of Nevada, Reno, NV.

Law Engineering, Geotechnical, Environmental and Construction Materials Consultants (1990), "Load Testing of Anchoring Assemblies (Grabb-it Cable Splice), Job No. 1460014400 Lab Number: E0429," Testing Report, March 20, 1990.

Naito, C., Sause, R., Hodgson, I., Pessiki, S. & Desai, C. (2006). "Forensic Evaluation of Prestressed Box Beams from the Lake View Drive over I-70 Bridge", ATLSS Report No. 06-13, Lehigh University, Bethlehem, PA.

Nordin, H. and Taljsten, B. (2006). "Concrete Beams Strengthened with Prestressed Near Surface Mounted CFRP", *Journal of Composites for Construction*, 10(1), 60-68.

Nordin, H., Taljsten, B., and Carolin, A. (2002). "CFRP Near Surface Mounted Reinforcement (NSMR) For Pre-Stressing Concrete Beams", *Proceedings of Third International Conference on Composites in Infrastructure*, San Francisco, June 2002.

Oehlers, D.J. and Seracino, R. (2004) *"*Design of FRP and Steel Plated RC Structures*"*, Elsevier, 228pp.

Olson, S.A., French, C.W. & Leon, R.T. (1992). "Reusability and Impact Damage Repair of Twenty-Year-Old AASHTO Type III Girders", Minnesota Department of Transportation Research Report No. 93-04, University of Minnesota, Minneapolis, MN.

PADoH (1960a). District 11 prestressed concrete bridge standards – "I" beams. Approved by PADoH August 17, 1964.

PADoH (1960b). District 11 bridge drawings. January 11, 1968. Approved by PADoH October 25, 1968.

PADoH (1960c). District 11 bridge drawings. June 20, 1959. Approved by PADoH August 9, 1960.

.

Preston, H.K., Osborn, A. E. N. & Roach, C. E. (1987). "Restoration of Strength in Adjacent Prestressed Concrete Box Beams", Report No. FHWA-PA-86-044+84-21, Pennsylvania Department of Transportation, Harrisburg, PA.

Quattlebaum, J., Harries, K.A. and Petrou, M.F. (2005). "Comparison of Three CFRP Flexural Retrofit Systems Under Monotonic and Fatigue Loads", *ASCE Journal of Bridge Engineering*. 10(6), 731-740.

Ramanathan, K. and Harries, K.A. (2008). "Influence of FRP Width-To-Concrete Substrate Width (b_f/b) on Bond Performance of Externally Bonded FRP Systems", *Proceedings of the 12th International Conference on Structural Faults and Repair*, Edinburgh, Scotland.

Reed C.E. and Peterman, R.J. (2005). "Evaluating FRP Repair Method for Cracked Prestressed Concrete Bridge Members Subjected to Repeated Loadings Phase 1", Report No. KTRAN: KSU-01-2, Kansas Department of Transportation, KS.

Reed, C.E. and Peterman, R.J. (2004) "Evaluation of Prestressed Concrete Girders Strengthened with Carbon Fiber reinforced Polymer Sheets", *Journal of Bridge Engineering*, 9(2), 60-68.

Reed, C.E., Peterman, R.J., Rasheed, H. and Meggers, D. (2007). "Adhesive Applications Used During Repair and Strengthening of 30-Year-Old Prestressed Concrete Girders", *Transportation Research Record: Journal of the Transportation Research Board*, 1827/2003, 36-43.

Russell, G. (2009). "Biaxial bending of prestressed concrete box girders subject to longitudinally eccentric loading." MSCE thesis, University of Pittsburgh, Pittsburgh, Pennsylvania.

Schiebel, S., Parretti, R. and Nanni, A. (2001). "Repair and Strengthening of Impacted PC Girders on Bridge A4845 Jackson County, Missouri", Report No. RDT01-017, Missouri Department of Transportation, Jackson City, MO.

Shanafelt, G.O. & Horn, W.B. (1980). "Damage Evaluation and Repair Methods for Prestressed Concrete Bridge Members", NCHRP Report 226, Project No. 12-21, Transportation Research Board, Washington, D.C.

Shanafelt, G.O. & Horn, W.B. (1985). "Guidelines for Evaluation and Repair of Prestressed Concrete Bridge Members", NCHRP Report 280, Project No. 12-21(1), Transportation Research Board, Washington, D.C.

Sika (2008a). "CarboDur Product Data Sheet", *Sika Corporation*, <http://www.sikaconstruction.com/con-prod-name.htm#con-prod-SikaCarboDur> (Sep. 30, 2008).

Sika (2008b). "Prestressing System for Structural Strengthening with Sika CarboDur CFRP Plates", Sika Corportion, USA.

Sika (2008c). "SikaWrap Hex 103C Product Data Sheet", *Sika Corporation*, <http://www.sikaconstruction.com/con-prod-name.htm#con-prod-SikaWrapHex103C> (Sep. 30, 2008).

Spancrete (1960). *Washington County L.R. 798-1 Bridge at STA. 1205+50.00 Drawings* (3 sheets). June 28, 1960. Approved by PADoH August 10, 1960.

Tabatabi, H., Ghorbanpoor, A. and Turnquist-Naas, A. (2004). "Rehabilitation Techniques for Concrete Bridges – The Wisconsin DOT Report", Project No. 0092-01-06, University of Wisconsin-Milwaukee, Milwaukee, WI.

Tumialan, J.G., Huang, P., Nanni, A. and Jones, M. (2001). "Strengthening of an Impacted PC Girder on Bridge A10062 St Louis County, Missouri", Report No. RDT01-013, University of Missouri-Rolla, Rolla, MO.

Washington State DOT (2008). Response to Survey conducted as part of present PennDOT-funded project.

Wight, R.G., Green, M.F., and Erki, M-A. (2001). "Prestressed FRP Sheets for Post-strengthening Reinforced Concrete Beams", *Journal of Composites for Construction*, 5(4), 214-220.

Williams Form Engineering Corporation (2008). 150ksi All Thread Bar Information, USA.

Wipf, T.J., Klaiber, F.W., Rhodes, J.D. and Kempers, B.J. (2004). "Effective Structural Concrete Repair – Volume 1 of 3: Repair of Impact Damaged Prestressed Concrete Beams with CFRP", Iowa DOT Project TR-428, Iowa Department of Transportation, Ames, IA.

Yu, P., Silva, P.F. and Nanni, A. (2008a). "Description of a Mechanical Device for Prestressing Carbon Fiber-Reinforced Polymer Sheets-Part I", *ACI Structural Journal*, 105(1), 3-10.

Yu, P., Silva, P.F. and Nanni, A. (2008b). "Flexural Strength of Reinforced Concrete Beams Strengthened with Prestressed Carbon Fiber-Reinforced Polymer Sheets-Part II", *ACI Structural Journal*, 105(1), 11-19.

Zobel, R.S. and Jirsa, J. O. (1998). "Performance of Strand Splice Repairs in Prestressed Concrete Bridges", *PCI Journal*, 43(6), 72-84.